Development of Organic Photovoltaic and Fluorescent Materials Based on Characteristics of Silicon and Tin Elements

(ケイ素およびスズ元素の特長を活かした有機太陽電池および発光材料の開発)

Daiki Tanaka

2014

Hiroshima University

Contents

General introduction

The introduction of heteroatoms to π-conjugation systems are of current interest, since the unique properties based on the characteristics of heteroatoms are often realized. Various main group elements, in particular group 13-16 elements, are introduced to π-conjugation systems, and the resulting systems show interesting functionalities such as ion sensing[1], excellent photoluminescence[2], and hole/electron transporting properties[3]. In particular, an interest is focused on π-conjugation systems bearing group 14 heavy elements, such as silicon and germanium. For group 14 heavy elements, it is known that (1) long σ-bonds provide good solubility of the compounds because of the flexibility, (2) group 14 heavy element σ-electron systems possess the high-lying HOMO and the low-lying LUMO[4], (3) delocalization of σ-electrons along σ-bonds reduces σ-σ* energy gap[5], (4) group 14 heavy element σ-orbital can interact with neighboring carbon π-orbital because of similar energy level of the σ-orbital and π-orbital[6], and (5) low energy σ-σ* transition in the UV range leads to the photoreactivity[5] (Figure 1).

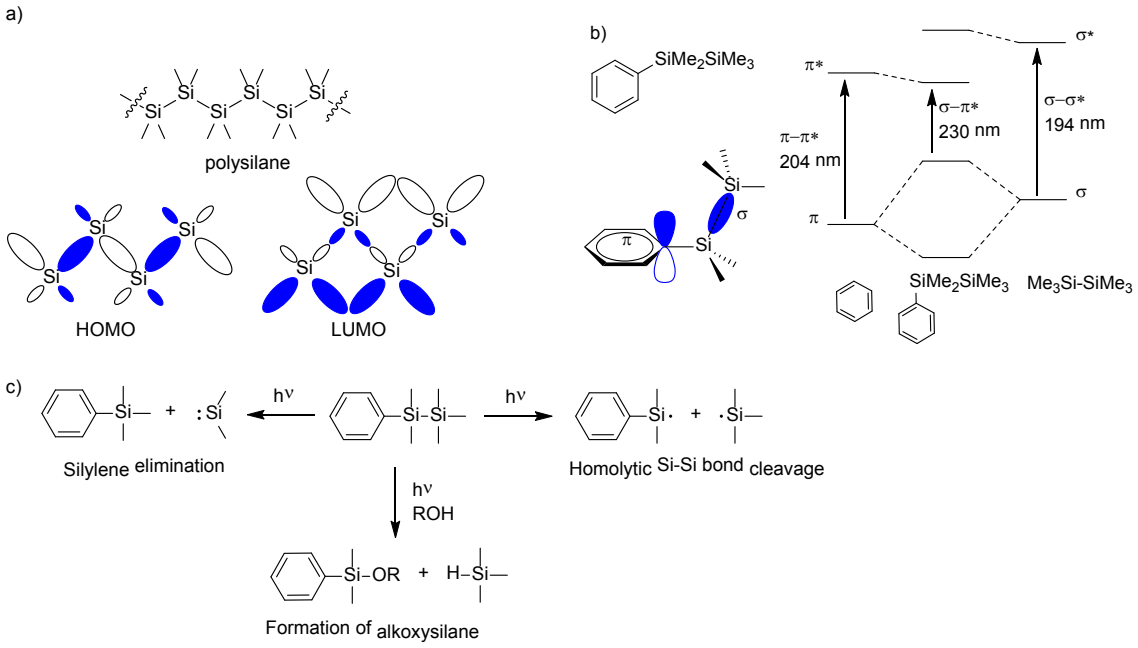

Figure 1. Features of group 14 heavy element-containing compounds. a) Interactions between σ-orbitals (σ conjugation), b) between σ- and π-orbital (σ-π conjugation), and c) photoreactivity of Si-Si bonds.

Furthermore, it is known that the substitution mode of group 14 element on a π-conjugation system affects the electronic states of the compounds. As shown in Figure 1b, generally, silicon-attached π-conjugated system has the high-lying HOMO as a result of σ-π conjugation[6]. In contrast, silicon-bridged cyclic π-conjugation system, silole, shows the low-lying LUMO level originated from bonding interaction between silicon σ*-orbital and π*-orbital (Figure 2) [7]. These electronic effects of group 14 element substitution make it possible to use the group 14 element substituted π-conjugation compounds as organic functional materials (Chart 1)[1-3].

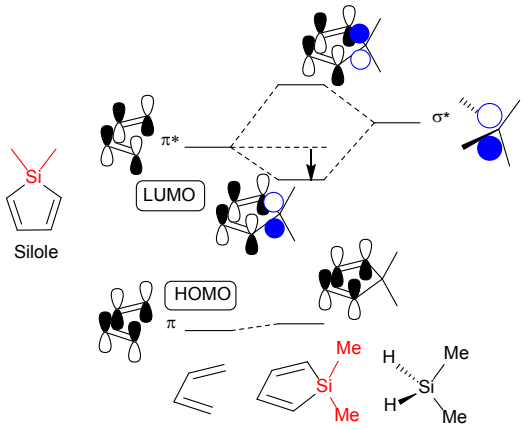

Figure 2. Low-lying LUMO arising from σ*-π* conjugation.

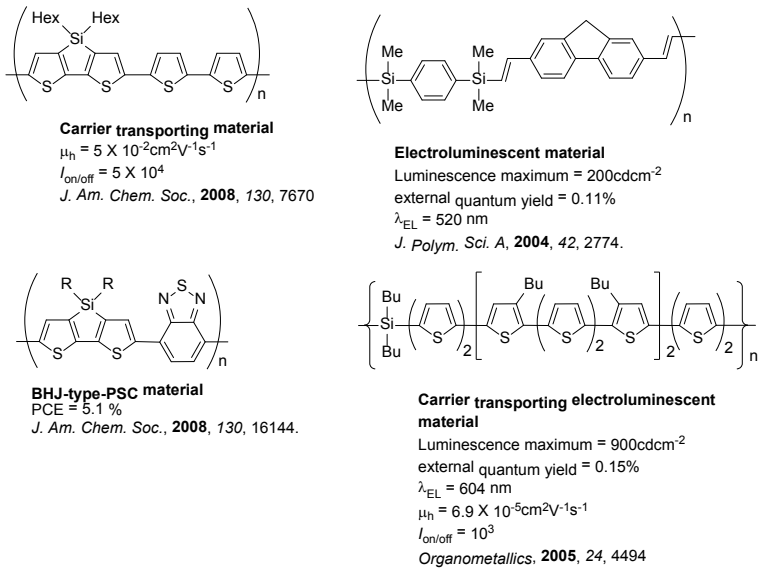

Chart 1. Functional materials containing group 14 heavy element.

On the other hand, dye sensitized solar cells (DSSCs)[8] and bulk hetero junction (BHJ) solar cells[9] attract much attention because of their advantages such as low cost fabrication and flexible light weight devices.

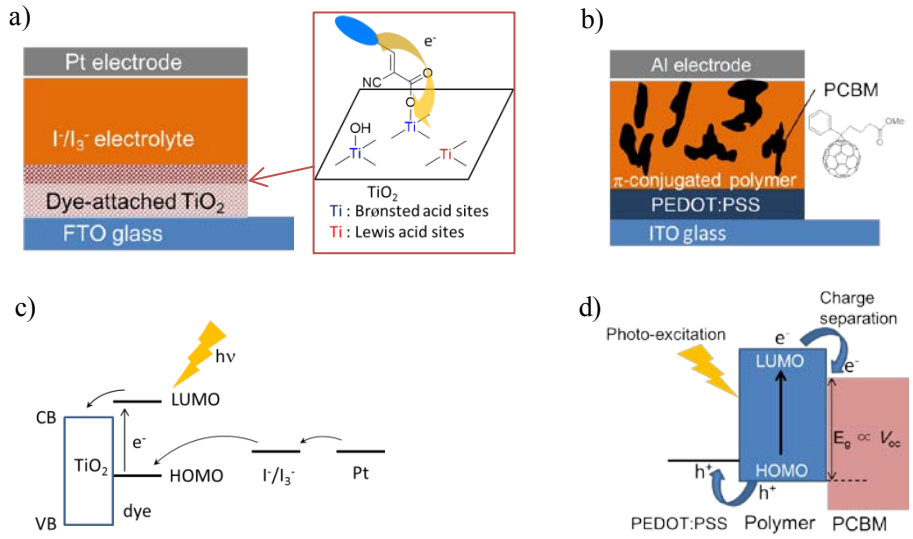

Figure 3. Device structures and energy diagrams of DSSCs (a, c) and BHJ solar cells (b, d).

As shown in Figure 3, π-conjugated monomeric/polymeric compounds are used as the active materials of the devices. In order to realize the high performance of devices, the π-conjugated materials are required to possess broad absorption bands in low energy region to utilize broad range of the sun light wavelength[10]. In addition, it is also required for DSSC materials that they should have an anchor unit to link on the TiO_2 surface. Whereas, for BHJ cells, the π-conjugated compounds should have low-lying HOMO, producing high open circuit voltage (V_{oc})[11]. To achieve these requirements, a variety of molecular design was examined, and introduction of group 14 element substituents is often studied to manipulate the π-conjugated system leading to the desired functionality, including photo conducting properties.

In this thesis, the author describes synthesis, properties, and applications of group 14 element-containing functional materials.

In Chapter 1, preparation of the hybrids of oligothiophene- or diethynylpyrene-disilanylene alternate polymers with single walled carbon nanotube (SWNT) is described (Chart 2). The hybrids of the polymers with SWNT were prepared by ball milling the polymers with SWNT, providing soluble polymer-SWNT hybrids. Previously, Ohshita *et al* found that disilanylene-oligothienylene alternate polymers could be attached on TiO_2 surface by irradiation of TiO_2 in the polymer solution through the formation of Si-O-Ti bonds via photo-excitation of Si-Si bonds followed by reactions with Ti-OH. In particular, poly(disilanylenequinquethienylene) (**DS5T**) exhibited clear sensitizing effects when attached on TiO_2, being usable for DSSCs. The resulting polymer-SWNT hybrids were also attached to TiO_2 surface, photochemically. DSSCs were fabricated using the hybrid-attached TiO_2 and the cell performance is discussed in comparison with that based on **DS5T**-attached TiO_2 without SWNT. Interestingly, the former exhibited higher PCE than the later, primarily due to the higher photo current. However, the PCEs of these DSSCs were rather low and further studies were examined to improve the cell performance by using disilanylene polymers with more red-shifted and broad absorptions (Chapter 2).

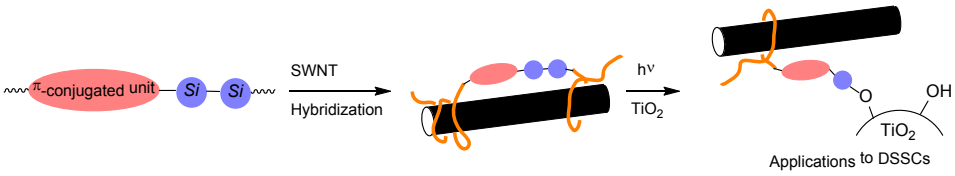

Chart 2. Hybrid formation of SWNT with organsilicon polymer and attachment of organosilicon polymer-SWNT hybrid to inorganic oxide surface, described in Chapter 1.

In Chapter 2, synthesis of polymers with alternating donor-acceptor (D-A) type π-conjugated units and disilanylene bonds and their applications to DSSCs are described (Chart 3). Bis(ethynylthienyl)benzothiadiazole units were introduced to the polymer as the D-A type π-conjugated units to provide low energy absorption of the polymers derived from donor-acceptor

interaction. The D-A type polymers were synthesized by the Sonogashira reactions of bis(iodothienyl)benzothiadiazole with diethynyldisilane in the presence of a palladium catalyst. The polymers were photochemically-attached on TiO_2, and applied to DSSCs, which exhibited PCE of 0.26% higher than that with **DS5T**-modified electrode[12], because of the broad and low energy absorption of D-A type polymers. TiO_2 electrodes thermally modified with the polymers by the reactions of ethynylene-Si bonds with Ti-OH and the hybrid formation of D-A type polymer with SWNT are also studied.

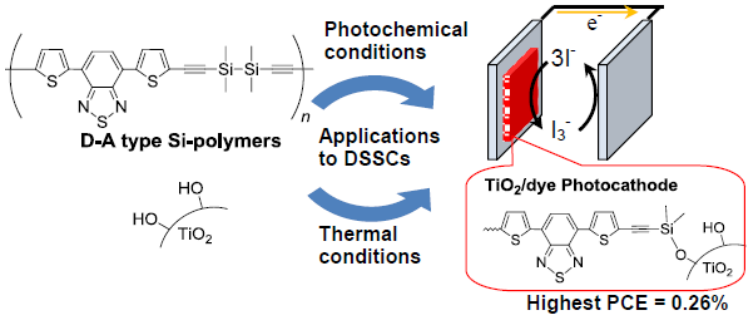

Chart 3. Application of D-A type organosilicon polymer to dye sensitizer of DSSC, described in Chapter 2.

In Chapter 3, synthesis of disilanylene polymers having more expanded D-A type π-conjugated units is described (Chart 4). In this work, D-A units containing bithiophene as the donor and benzochalcogenadiazole or pyridine as the acceptor are employed as π-conjugated units of the polymers. The polymers exhibit lower energy absorptions than those described in Chapter 2, except the pyridine containing polymer. Although the pyridine-containing polymer has a higher energy absorption than those of the rest benzochalcogenadiazole polymers, the DSSC device based on pyridine-containing polymer shows the highest PCE of 0.40% among those examined in this chapter. Since pyridine containing polymer can be attached on TiO_2 surface by both photoreactions of Si-Si bonds with Ti-OH of the Brønsted acid sites of TiO_2 and coordination of pyridine units to

Lewis acid sites on TiO_2, efficient electron injection to TiO_2 is achieved, leading to highest PCE.

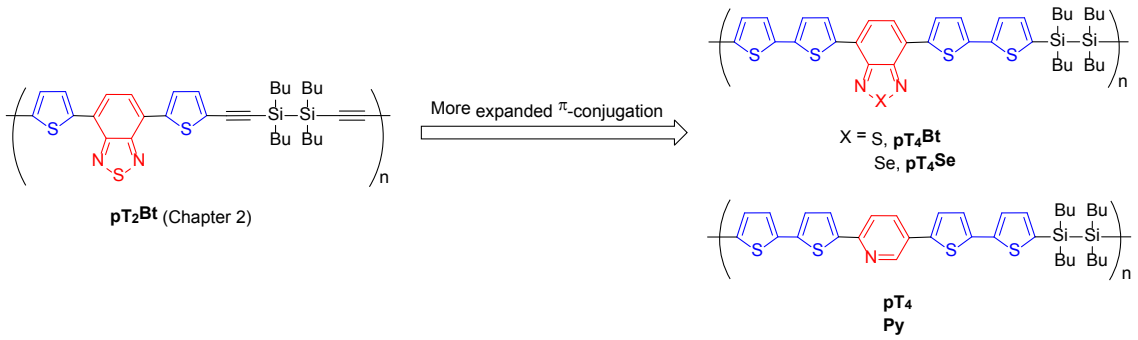

Chart 4. Synthesis of D-A type organosilicon polymers bearing expanded π-conjugated unit, described in Chapter 3.

In Chapter 4, synthesis of dithienosilole-pyridine alternate polymers and the complex formation of the polymers with organoboron compounds are described (Chart 5). The Lewis basic pyridine unit in the polymers formed a stable complex with strong Lewis acid, tris(pentafluorophenyl)borane, which was confirmed by ^{11}B NMR spectra. The polymer-borane complexes have lower bandgaps than those of the pristine polymers, due to enhancement of electron-withdrawing property of pyridine unit by the formation of complex with borane, which enhances the D-A interaction in the polymer backbone. Furthermore, HOMO levels of polymer-borane complexes are lower than those of the pristine polymers. BHJ solar cells were fabricated using the polymers and their complexes, and the performance were evaluated. The polymer-borane complex-based BHJ solar cell exhibited higher V_{oc} than that of corresponding pristine polymer-based cell, reflecting the lower HOMO energy level of polymer-borane complex. DSSCs were also fabricated using the present polymers, whose performance is also discussed.

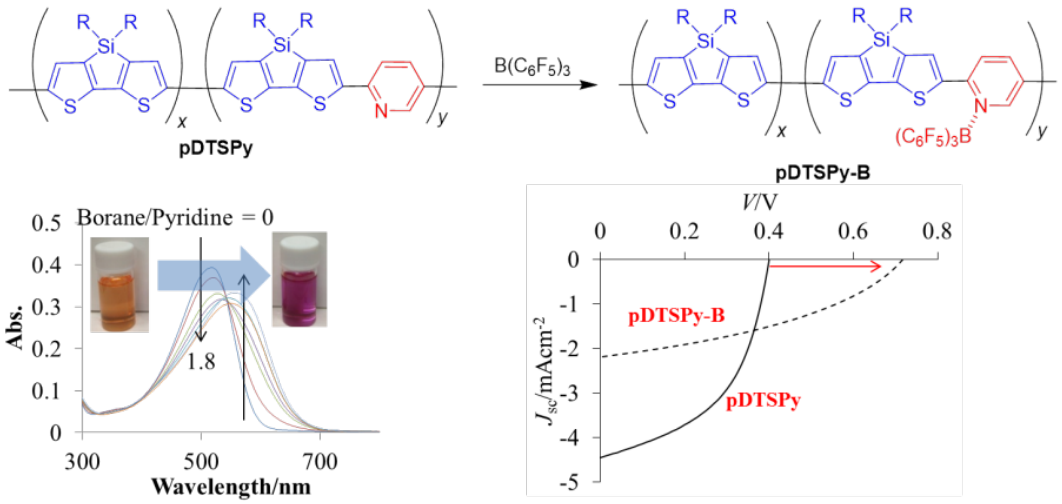

Chart 5. Preparation of pyridine-containing organosilicon polymer-organoboron complex, described in Chapter 4.

In Chapter 5, synthesis of tin-bridged bithiophenes, dithienostannoles (**DTSn**s), and the optical properties are described (Chart 6). **DTSn**s were synthesized by the reactions of dilithiobithiophene or –bibenzothiophene with dichlorodiphenylstannane as the solids that were stable under ambient conditions. Electronic states of **DTSn**s are quite similar to those of the silicon and germanium analogues. One of the present **DTSn**s (**DTSn1**) showed interesting chromic behaviors depending on the states. Thus, **DTSn1** showed strong emission in only the crystal state, in contrast to that the silicon analogues show strong emission in both solutions and as crystals. Furthermore, **DTSn1** in amorphous phase exhibited no emission similar to that in solution. Single-crystal X-ray diffraction analysis was also carried out to understand the crystallization induced emission enhancement (CIEE) properties of **DTSn1**.

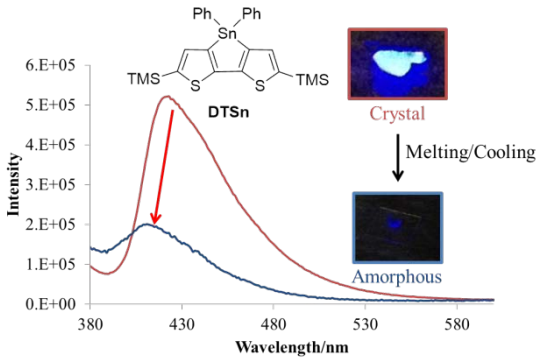

Chart 6. Crystallization induced emission enhancement behavior of dithienostannole, described in Chapter 5.

References

1 (a) S. Yamaguchi, S. Akiyama, K. Tamao, *J. Am. Chem. Soc.*, **2001**, *123*, 11372; (b) S. Yamaguchi, S. Akiyama, K. Tamao, *J. Am. Chem. Soc.*, **2000**, *122*, 6793; (c) R. Gullyev, S. Ozturk, E. Sahin, E. U. Akkaya, *Org. Lett.*, **2012**, *14*, 1528; (d) I.-S. Ke, M. Myahkostupov, F. N. Castellano, F. P. Gabbaï, *J. Am. Chem. Soc.*, **2012**, *134*, 15309; (e) A. Ajayaghosh, P. Carol, S. Sreejith, *J. Am. Chem. Soc.*, **2005**, *127*, 14962; (f) Y. Bao, H. Wang, Q. Li, B. Liu, Q. Li, W. Bai, B. Jin, R. Bai, *Macromolecules*, **2012**, *45*, 3394; (g) K. Tanaka, T. Kumagai, H. Aoki, M. Deguchi, S. Iwata, *J. Org. Chem.*, **2001**, *66*, 7328.

2 (a) J. Ohshita, Y. Kurushima, K.-H. Lee, A. Kunai, Y. Ooyama, Y. Harima, *Organometallics*, **2007**, *26*, 6591; (b) J. Ohshita, Y. Tominaga, D. Tanaka, Y. Ooyama, T. Mizumo, N. Kobayashi, H. Higashimura, *Dalton Trans.*, **2013**, *42*, 3646; (c) S. Kim, K.-H. Song, S. O. Kang, J. Ko, *Chem. Commun.*, **2004**, 68; (d) S. Yamaguchi, T. Shirasaka, S. Akiyama, K. Tamao, *J. Am. Chem. Soc.*, **2002**, *124*, 8816; (e) A. Iida, S. Yamaguchi, *J. Am. Chem. Soc.*, **2011**, *133*, 6952; (f) N. Sakamoto, C. Ikeda, M. Yamamura, T. Nabeshima, *J. Am. Chem. Soc.*, **2011**, *133*, 4762; (g) K. Geramita, J. McBee, T. D. Tilley, *J. Org. Chem.*, **2009**, *74*, 820; (h) Y. Yabusaki, N. Ohshima, H. Kondo, T. Kusamoto, Y. Yamanori, H. Nishihara, *Chem. Eur. J.*, **2010**, *16*, 5548; (i) A. Fukazawa, Y. Ichihashi, Y. Kosaka, S. Yamaguchi, *Chem. Asian J.*, **2009**, *4*, 1729; (j) M. G. Hobbs, T. Baumgartner, *Eur. J. Inorg. Chem.*, **2007**, 3611; (k) D. R. Bai, C. Romero-Nieto, T. Baumgartner, *Dalton Trans.*, **2010**, *39*, 1250; (l) S. Durben, Y. Dienes, T. Baumgartner, *Org. Lett.*, **2006**, *8*, 5893; (m) Y. Matano, H. Imahori, *Org. Biomol. Chem.*, **2009**, *7*, 1258.

3 (a) J. Ohshita, K. Yoshimoto, M. Hashimoto, D. Hamamoto, A. Kunai, Y. Harima, Y. Kunugi, K. Yamashita, M. Kakimoto, M. Ishikawa, *J. Organomet. Chem.*, **2003**, *665*, 29; (b) J. Ohshita, M. Nodono, A. Takata, H. Kai, A. Adachi, K. Sakamaki, K. Okita, A. Kunai, *Macromol Chem. Phys.*, **2000**, *201*, 851; (c) K. Tamao, M. Uchida, T. Izumizawa, K. Furukawa, S. Yamaguchi, *J.*

Am. Chem. Soc., **1996**, *118*, 11974; (d) J. Ohshita, H. Kai, A. Takata, T. Iida, A. Kunai, N. Ohta, K. Komaguchi, M. Shiotani, A. Adachi, K. Sakamaki, K. Okita, *Organometallics*, *2001*, *20*, 4800; (e) H. Usta, G. Lu, A. Facchetti, T. J. Marks, *J. Am. Chem. Soc.*, **2006**, *128*, 9034; (f) J. Ohshita, Y. Hatanaka, S. Matsui, T. Mizumo, Y. Kunugi, Y. Honsho, A. Saeki, S. Seki, J. Tibbelin, H. Ottosson, T. Takeuchi, *Dalton Trans.*, **2010**, *39*, 9314; (g) J. Ohshita, M. Miyazaki, D. Tanaka, Y. Morihara, Y. Fujita, Y. Kunugi, *Polym. Chem.*, **2013**, *4*, 3116; (h) X. He, T. Baumgartner, *RCS Adv.*, **2013**, *3*, 11334.

4 C. G. Pitt, M. M. Bursey, P. F. Rogerson, *J. Am. Chem. Soc.*, **1970**, *92*, 519.

5 (a) R. West, *J. Organomet. Chem.*, **1986**, *300*, 327; (b) R. D. Miller, J. Michl, *Chem. Rev.*, **1989**, *89*, 1359.

6 (a) H. Sakurai, J. Organomet. Chem., 1980, 200, 261; (b) H. Sakurai, *Pure Appl. Chem.*, **1987**, *59*, 1638; (c) H. Tsuji, Y. Shibano, T. Takahashi, M. Kumada, K. Tamao, *Bull. Chem. Soc. Jpn.*, **2005**, *78*, 1334; (d) T. Karatsu, *J. Photochem. Photobiol. C: Photochem. Rev.*, **2008**, *9*, 111.

7 (a) K. Tamao, S. Yamaguchi, M. Shiozaki, Y. Nakagawa, Y. Ito, *J. Am. Chem. Soc.*, **1992**, *114*, 5867; (b) S. Yamaguchi, K. Tamao, *J. Chem. Soc., Dalton Trans.*, **1998**, 3693; (c) S. Yamaguchi, Y. Itami, K. Tamao, *Organometallics*, **1998**, *17*, 4910.

8 (a) B. O'Regan, M. Grätzel, *Nature*, **1991**, *353*, 737; (b) M. Grätzel, *Inorg. Chem.*, **2005**, *2*, 6841.

9 (a) M. Hiramoto, H. Fujikawa, M. Yokoyama, *Appl. Phys. Lett.*, **1991**, *58*, 1062; (b) G. Yu, J. Gao, J. C. Hummelen, F. Wudl, A. J. Heeger, *Science*, **1995**, *270*, 1789.

10 (a) A. Hagfeldt, G. Boschloo, L. Sun, L. Kloo, H. Pettersson, Chem. Rev., 2010, 110, 6595; (b) S. Ardo, G. J. Meyer, *Chem. Soc. Rev.*, **2009**, *38*, 115; (c) Y.-J. Cheng, S.-H. Yang, C.-S. Hsu, *Chem. Rev.*, **2009**, *109*, 5868; (d) B. C. Thompson, J. M. J. Fréchet, *Angew. Chem. Int. Ed.*, **2008**, *47*, 58.

11 S. Günes, H. Neugebauer, N. S. Sariciftci, *Chem. Rev.*, **2007**, *107*, 1324.

12 D. Tanaka, J. Ohshita, Y. Ooyama, T. Mizumo, Y. Harima, *J. Organomet. Chem.*, **2012**, *719*, 30.

Chapter 1

Hybridization of Carbon Nanotubes with Si–π Polymers and Attachment of Resulting Hybrids to TiO_2 Surface

Introduction

Recently, dye sensitized solar cells (DSSCs)[1] attract much attention because of its advantages, such as device flexibility, low production cost, and tunable cell color. In particular, the development of efficient dye sensitizers is a major subject to obtain high performance DSSCs with high power conversion efficiency (PCE), since the photocurrent of DSSCs depends largely on photo absorptions of dye sensitizers. Attachment of dye sensitizers on TiO_2 electrode surface is necessary to inject photo-excited electrons of dye sensitizers to TiO_2 electrode. Typically, a carboxylic acid group is employed as the attachment unit in the dyes, which forms an ester linkage (RCO-O-Ti, R = chromophore) by dehydration with a hydroxyl group on the TiO_2 surface (Ti-OH).[2] However, the ester linkage is rather labile and undergoes hydrolytic decomposition gradually to detach the dye, shortening the DSSC lifetime. To obtain long-term stable DSSCs, the development of the anchor units which lead to long lifetime DSSCs attracts much attention.

As described in General Introduction, photoreactions of Si-Si bonds with hydroxyl groups leading to the formations of chemically stable Si-O bonds are known.[3] It was recently reported that an organosilicon polymer, poly(disilanylenequinquethienylene) (**DS5T**), could be attached on TiO_2 surface by the reactions of photo-excited Si-Si bonds of **DS5T** with Ti-OH groups on the TiO_2 surface leading to the formation of Si-O-Ti anchoring bonds (Scheme 1, a).[4] The resulting polymer-TiO_2 hybrid materials exhibited clear application to DSSCs. Similar utilization of Si-O-Ti bonds as anchoring linkages was recently reported by Hanaya *et al*. They described attachment of

alkoxysilyl- and hydroxysilylazobenzene dyes to TiO_2 surface by the formation of Si-O-Ti bonds, and DSSC performance of the resulting dye-modified TiO_2 electrodes. Those TiO_2 electrodes modified by the dyes through the formation of Si-O-Ti linkage exhibited higher resistance toward hydrolysis in water soaking test than dye-modified TiO_2 electrodes by the ester linkages.[5]

On the other hand, carbon nanotubes (CNTs) are of current interest, because they possess unique electrical, mechanical, and thermal properties. In particular, the applications of high electron conductivity and strong electron accepting nature of CNTs to electronic devices and organic semiconducting devices have been widely studied.[6] However, CNTs are essentially insoluble in common organic solvents due to their strong tendency to form aggregates, and much effort has been made to solubilize them.[7] The introduction of carboxy groups on the surface and edge of CNTs and the conversion of the carboxy groups into amide and ester units are often employed.[8] Other chemical modifications of the CNT surface with organic groups have been reported to enhance solubility and/or dispersibility.[9] However, such chemical modifications may change the properties of the CNTs and therefore, recent attention is focused on the nonbonding interaction of CNTs with solubilizing organic compounds.[10] It is expected that organosilicon polymers with π-conjugated units can disperse CNTs by the hybridization of organosilicon polymers with CNTs through π-π interactions. The organosilicon polymer-CNT hybrids may be further hybridized with inorganic oxides by the reactions of photoexcited organosilicon units.

In this chapter, the author describes the preparations of new hybrid materials composed of single-walled carbon nanotubes (SWNTs) and organosilicon polymers bearing π-conjugated units, as shown in Chart 1, and further hybridization by the photoreactions of the resulting organosilicon polymer-SWNT hybrid materials with TiO_2 leading to the formations of new three component hybrids, composed of polymer/SWNT/TiO_2 (Scheme 1, b), which can be applied to DSSC photoelectrodes.

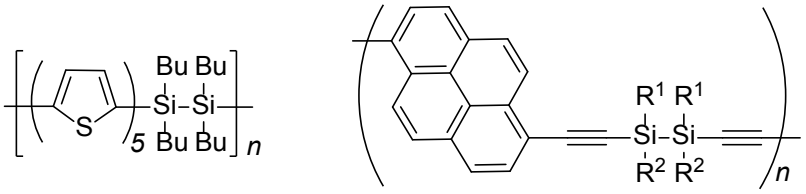

DS5T

DSPB ($R^1 = R^2 =$ Bu)
DSPP ($R^1 =$ Ph, $R^2 =$ Me)

Chart 1. Si-π polymers.

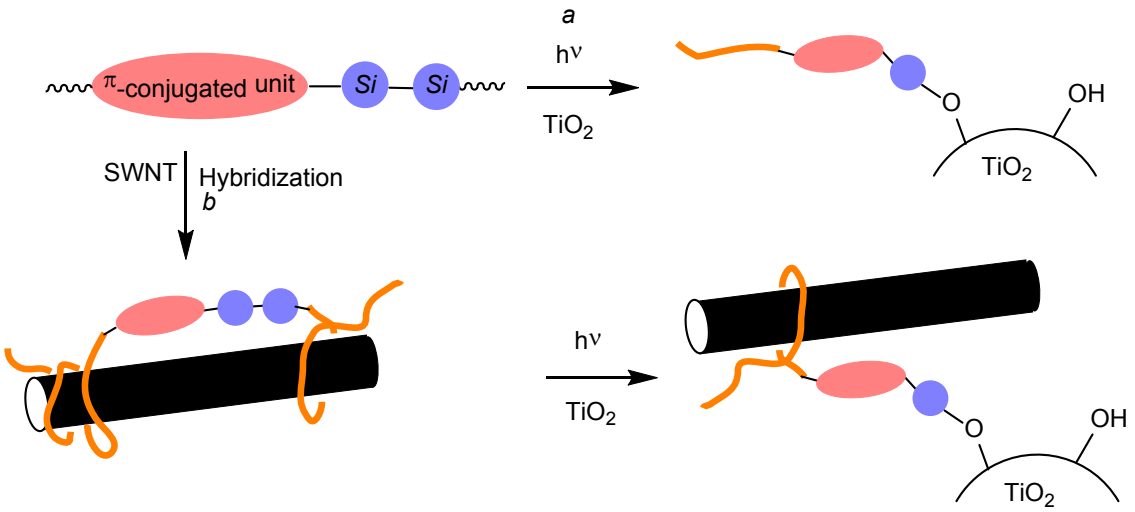

Scheme 1. Preparation of organicinorganic hybrids using Si-π polymers.

Results and discussion

Hybrid preparations by in-situ method

The author synthesized polymer-SWNT hybrids by two ways, i.e.; the in-situ method and the ball-milling method. Polymer-SWNT hybrids were prepared as brownish black solids by the Sonogashira coupling of dibromopyrene with diethynyldisilane in the presence of SWNTs (**SWNT1**: 1.2-1.5 nmϕ and **SWNT2**: 0.7-1.3 nmϕ), followed by reprecipitation of the soluble products from $CHCl_3$/EtOH (in situ method, Table 1). The absorption and emission spectral shapes were not evidently affected by the hybridization, but the emission quantum efficiencies were clearly decreased (cf. Φ = 0.30 and 0.15 for present polymers **DSPB** and **DSPP**, respectively), suggesting quenching of the emission by energy or electron transfer from the photoexcited polymers to SWNTs. The UV absorption and emission spectra of hybrids are shown in Figure 1. In contrast, the introduction of large amounts of SWNTs resulted in increases in the quantum efficiencies to some extent (Runs 3 and 6 in Table 1). It is possible that the aggregation of SWNTs may affect the quenching process. Hybrid **PB2I-10** prepared from **SWNT2** showed weak absorption bands due to SWNTs (Run 7 in Table 1). Figures 2a and 2b illustrate SEM images of the drop-cast films of **PB1I-15** and **PP1I-15**, showing tube and string-like structures with diameters of 50-100 nm, ascribed to bundled SWNTs that are probably covered by the polymer substances. No such structures were observed at all in **DSPB** and **DSPP**, shown in Figure 2c and 2d. The molecular weights of the hybrids were measured by GPC to be approximately M_w = 10,000 (M_w/M_n = 1.4) for **PB1I** and M_w = 3,000 (M_w/M_n = 1.4) for **PP1I**. However, presumably, SWNTs were detached from the polymers by GPC and these values reflect the molecular weights of the SWNT-free Si-π polymers only.

Table 1. Preparation of **DSPB**- and **DSPP**-SWNT hybrids by in situ hybridization.

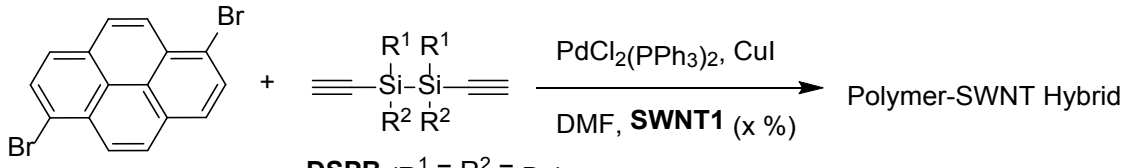

DSPB ($R^1 = R^2 =$ Bu)
DSPP ($R^1 =$ Ph, $R^2 =$ Me)

Run	Polymer / mmol[a]	SWNT / wt%[b]	Hybrid / mg	Emission Φ[c]
1	**DSPB** (0.875)	**SWNT1**[d] (5)	**PB1I-5** (148)	0.22
2	**DSPB** (0.875)	**SWNT1**[d] (10)	**PB1I-10** (152)	0.11
3	**DSPB** (0.875)	**SWNT1**[d] (15)	**PB1I-15** (160)	0.18
4	**DSPP** (0.583)	**SWNT1**[d] (5)	**PP1I-5** (154)	0.15
5	**DSPP** (0.583)	**SWNT1**[d] (10)	**PP1I-10** (211)	0.07
6	**DSPP** (0.583)	**SWNT1**[d] (15)	**PP1I-15** (202)	0.08
7	**DSPB** (0.875)	**SWNT2**[e] (15)	**PB2I-15** (137)	0.24

[a]Each monomer amount used for the preparation. [b]% of SWNT based on dibromopyrene.

[c]Absolute emission quantum efficiency in $CHCl_3$ as determined by an integral sphere.

[d]**SWNT1**: 1.2-1.5 nmϕ. [e]**SWNT2**: 0.7-1.3 nmϕ.

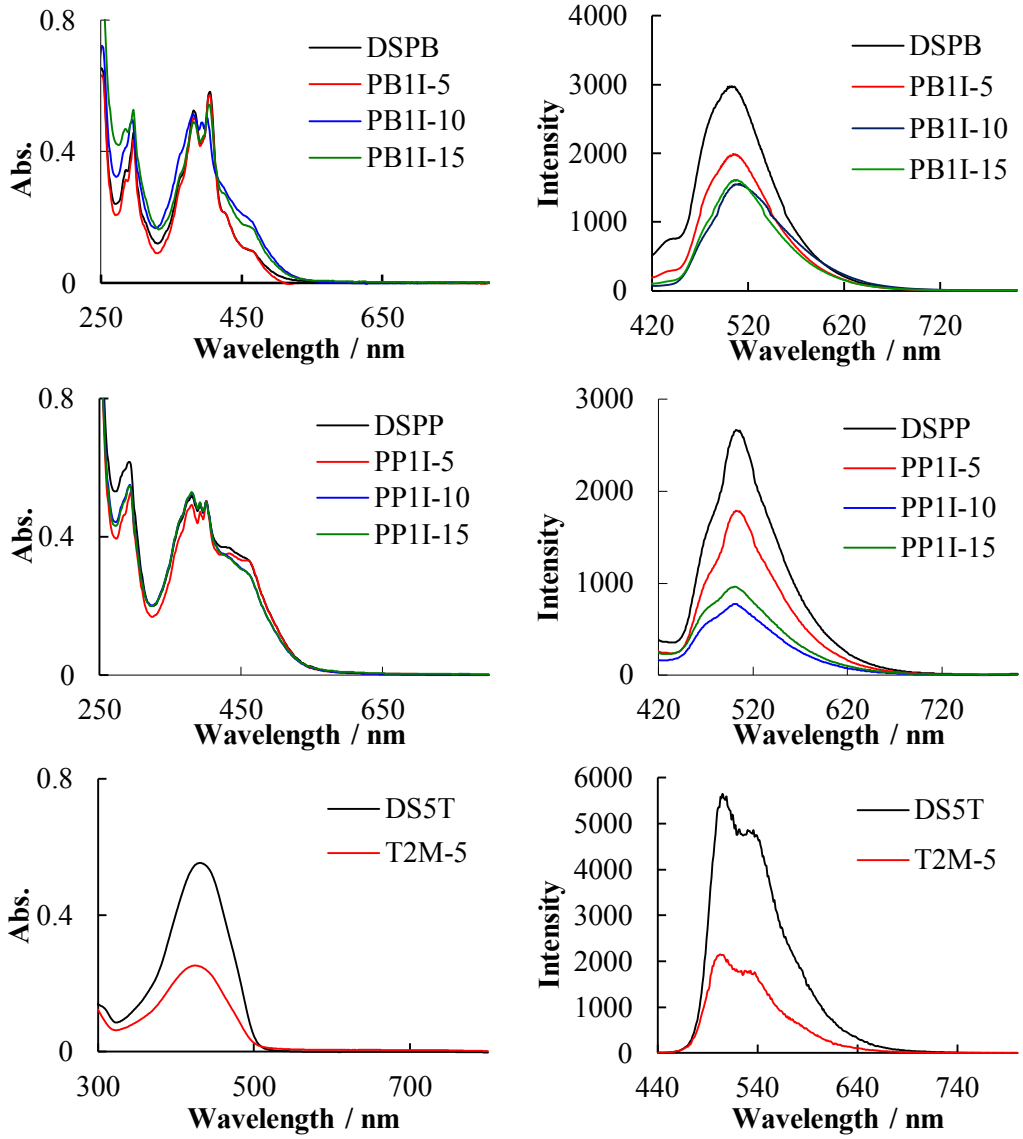

Figure 1. UV-vis absorption (left) and emission (right) spectra of the polymers and the hybrids in chloroform with the concentration of 8.0×10^{-3} g/L and 2.7×10^{-3} g/L for UV-vis and emission spectroscopy, respectively.

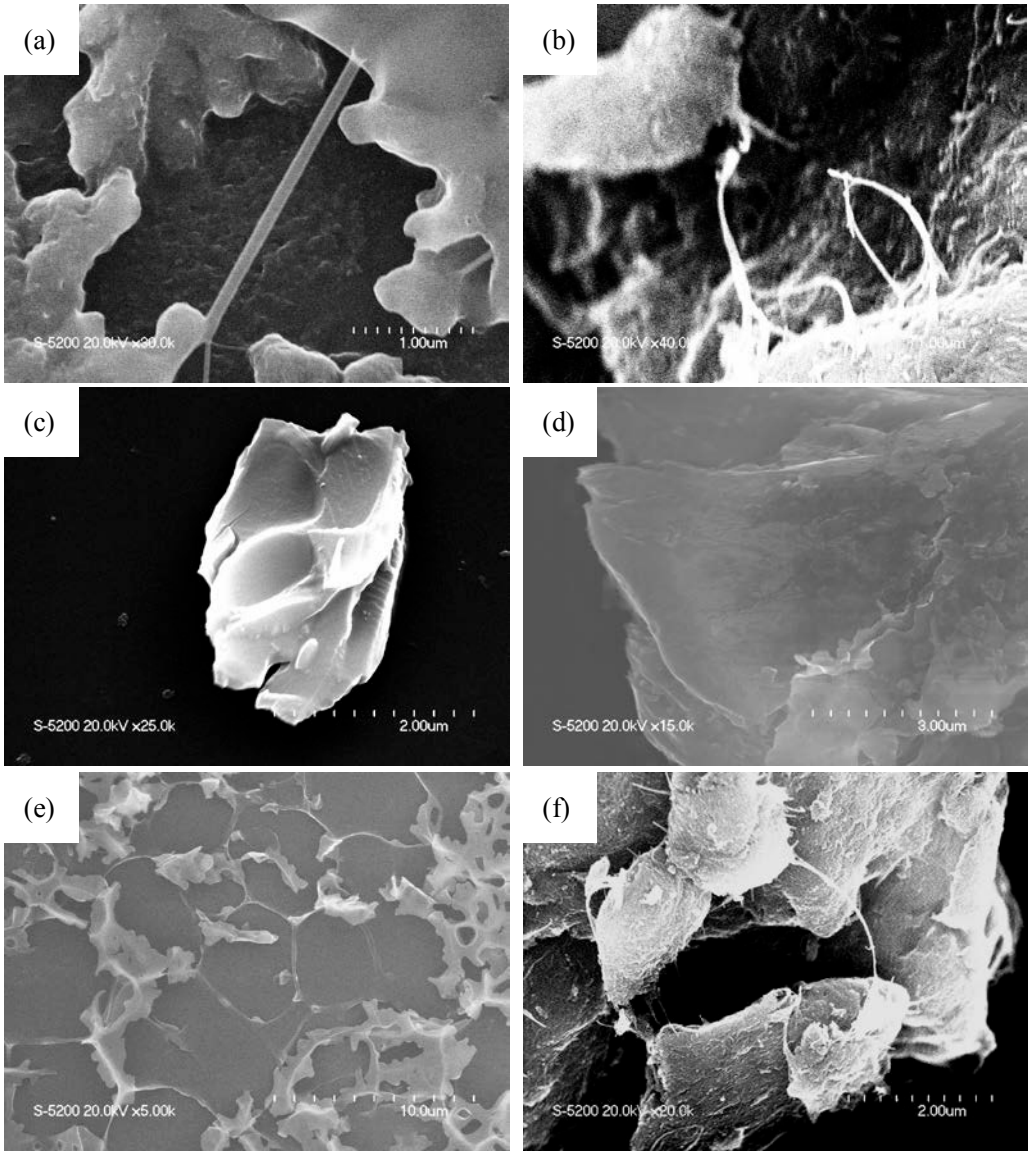

Figure 2. SEM images of drop-cast films of (a) **PB1I-15**, (b) **PP1I-15**, (c) **DSPB**, (d) **DSPP**, (e) **PB2M-10**, (f) TiO_2 attached to **PB1I-15**.

Hybrid preparations by ball-milling method

Similar hybrid materials were prepared also by ball milling the polymers with SWNTs in the solid state.[11] The milled mixtures were dissolved in chloroform and filtered (Table 2, Figure 2e). The hybrids prepared by ball milling became insoluble when evaporated and thus they could not be purified by reprecipitation and must be stored in solution. This is probably due to the higher contents of SWNT in the hybrids prepared by ball milling than those by the in situ method. The absorption spectra of the hybrids with **SWNT2** clearly showed multiple bands in the NIR region, which are characteristic of nonaggregated SWNTs (Figure 3),[12] in contrast to the hybrids with **SWNT1** that showed no clear bands in the NIR region, probably due to the low concentration of SWNTs and/or band broadening by aggregation. A hybrid material of **DS5T** with **SWNT2** (Run 4) could be also prepared by this method.

Table 2. Preparation of polymer-SWNT hybrids by ball milling.

Si-π polymer —(Ball Milling; **SWNT1** or **2** (x %))→ Polymer-SWNT Hybrid

Run	Polymer / mg	SWNT / wt%[a]	Hybrid / mg	Emission Φ[b]
1	**DSPB** (22)	**SWNT1**[c] (5)	**PB1M-5** (19)[d]	0.20
2	**DSPB** (26)	**SWNT2**[c] (5)	**PB2M-5** (21)[d]	0.23
3	**DSPB** (25)	**SWNT2**[c] (10)	**PB2M-10** (14)[d]	0.18
4	**DS5T**[e] (26)	**SWNT2**[c] (5)	**TB2M-5** (17)[d]	0.15

[a]% of SWNT based on polymer weight. [b]Absolute emission quantum efficiency in $CHCl_3$ as determined by an integral sphere. [c]**SWNT1**: 1.2-1.5 nmϕ, **SWNT2**: 0.7-1.3 nmϕ.

[d]Yield was determined by evaporation of a portion of the hybrid solution. [e]Φ in $CHCl_3$ = 0.21.

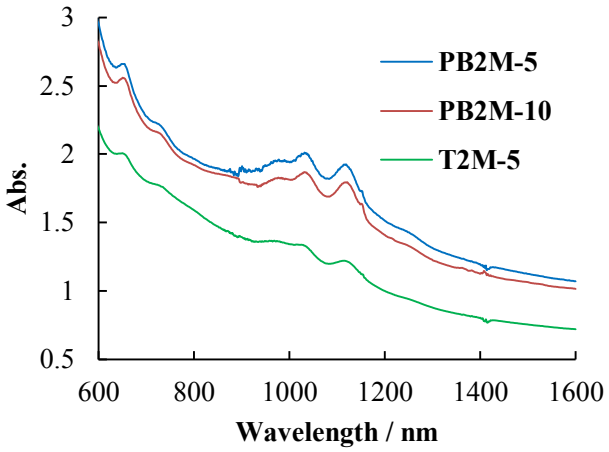

Figure 3. NIR spectra of the polymer-SWNT hybrids.

Preparation of polymer/SWNT/TiO_2 three component hybrids and their applications to DSSCs

When TiO_2 electrodes were irradiated with a UV lamp through a filter (>400 nm) in chloroform solutions containing the polymer-SWNT hybrids in an argon atmosphere and the resulting electrodes were washed with chloroform, dark brown hybrid-attached TiO_2 electrodes were obtained (Figure 2f). The author then fabricated a DSSC with the structure of FTO (fluorine-doped SnO_2)/**TB2M-5**-attached TiO_2/I_3^-·I^-/Pt and examined its performance (Figure 4). The maximum IPCE (incident photon-to-current conversion efficiency) was found at 417 nm, nearly consistent with the absorption maximum of **DS5T** (436 nm), indicating that the photoexcitation occurred in **DS5T**. As can be seen in Table 3, the cell with **TB2M-5**-modified TiO_2 electrode showed power conversion efficiency PCE of 0.39%, which was approximately 3.5 times higher than that with the **DS5T**-attached TiO_2 electrode reported previously.[4] The increased current (J_{sc}) is primarily responsible for the improved efficiency of the present device,[13] and it is likely that the introduction of SWNTs facilitated the carrier transport from photoexcited **DS5T**. The author examined also applications of **DSPB** and **PB2M-5** to DSSCs. However, both the DSSCs based on these materials showed only very low activity with PCE = 0.06-0.07%.

Table 3. Performance of DSSCs based on modified TiO_2.

Electrode	J_{sc} / $mAcm^{-2}$	V_{oc} / mV	FF	PCE / %
DS5T-TiO_2[a]	0.76	-292	0.52	0.11
TB2M-5-TiO_2	1.84	-340	0.62	0.39

[a]See ref. 4.

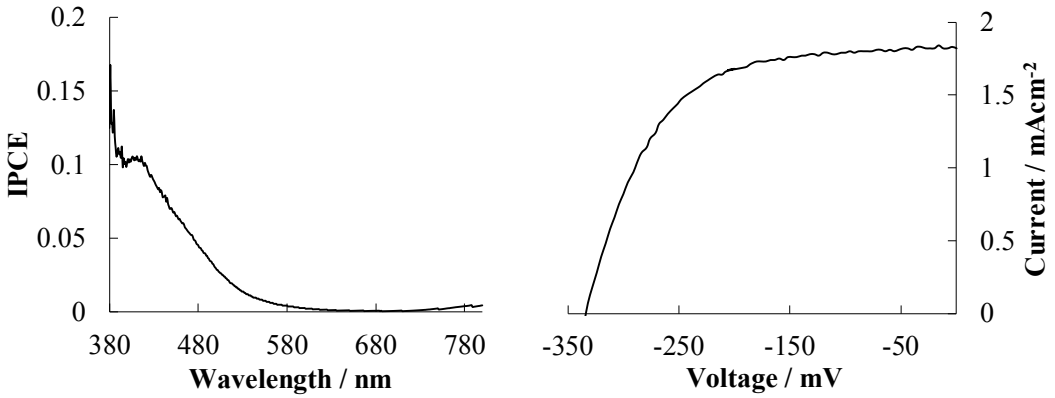

Figure 4. IPCE spectrum (left) and *J*-*V* plots (right) of the DSSC based on **TB2M-5**-TiO_2.

Conclusions

In conclusion, the author demonstrated the hybrid formation between Si-π alternate polymers and SWNTs. The attachment of the hybrids to the TiO_2 surface was also studied. Although methods to attach CNTs to silicon metal surfaces have been reported,[14] the present work provides a unique and convenient methodology to attach SWNTs to the TiO_2 surface by a solution process with π-conjugated chromophores, using readily accessible organosilicon polymers.[15] This seems applicable to a variety of new SWNT-containing organic devices.

Experimental

General

All reactions were carried out in dry nitrogen. Triethylamine and DMF were dried over KOH and CaH_2, respectively, and distilled immediately before use. NMR spectra were measured on a JEOL model LA-400 spectrometer. UV and emission spectra were measured on Shimadzu UV-3150 UV-vis-NIR and Hitachi F-4500 spectrophotometers, respectively. Emission quantum yields were determined using an integral sphere attached by a Hamamatsu-Photonics C9920-01 spectrophotometer. IR spectra were obtained on a Shimadzu FT-IR 8700 spectrometer. Polymer **DS5T** was prepared as reported in the literature[16]. **SWNT1** and **SWNT2** were purchased from Sigma-Aldrich Co., and purified according to the literature method[17].

*Preparation of **DSPB***

A mixture of 0.292 mg (0.875 mmol) of tetrabutyldiethynyldisilane, 0.315 g (0.875 mmol) of dibromopyrene, 5 mL of triethylamine, 50 mg of $PdCl_2(PPh_3)_2$, 15 mg of CuI, and 30 mL of DMF was heated at 80°C for 72 h. The resulting mixture was filtered to remove the precipitate and the solvent was removed from the filtrate under reduced pressure. Reprecipitation of the residue from chloroform/ethanol gave 0.219 g (47% yield) of **DSPB** as dark brown solids: M_w = 10,000 (M_w/M_n = 1.3); ^{1}H NMR (δ in $CDCl_3$) 0.95-1.09 (m, 12H, Bu), 1.36-1.86 (m, 24H, Bu), 7.89-8.76 (m, 8H, aromatic proton); ^{13}C NMR (δ in $CDCl_3$) 13.2, 13.9, 26.6, 27.3, 97.9, 107.5, 118.6, 124.0, 124.9, 126.3, 128.0, 130.2, 131.1, 132.3; IR 2133 cm^{-1} ν(C≡C).

*Preparation of **DSPP***

Polymer **DSPP** was prepared as dark brown solids in a fashion similar to that above: M_w = 3,400 (M_w/M_n = 1.5); ^{1}H NMR (δ in $CDCl_3$) 0.61 (br s, 6H), 7.30-8.25 (m, 24H); IR 2133 cm^{-1} ν(C≡C).

Preparation of the polymer-SWNT hybrids by in-situ hybridization

Polymer synthesis was performed in the presence of SWNT in a fashion similar to that above. The reaction mixture was filtered by a paper filter (5μm) and the solvent was evaporated from the filtrate then the residue was reprecipitated from chloroform/ethanol to give the hybrid materials as dark red solids: ^{1}H NMR and IR spectra of the hybrids were almost the same as those of the SWNT-free polymers **DSPB** and **DSPP**.

Preparation of the polymer-SWNT hybrids by ball-milling

The polymer and SWNT was ball-milled at 300 rpm for 3h at ambient temperature. To the milled mixture was added 5-10 mL of chloroform and the mixture was filtered through a paper filter (5 μm), then the insoluble substances were washed thoroughly with chloroform (40-60 mL), until the chloroform solution became colorless. The filtrate and the extract were combined and concentrated to 5 mL. Further concentration resulted in precipitation of insoluble black materials. A portion of the concentrated solution was taken and evaporated to determine the concentration.

Fabrication and evaluation of DSSCs

In a ball-milling apparatus was placed 1.3 g of TiO_2 (Degussa P-25, 80% anatase + 20% rutile). To this was added deionized water (1.86 mL) in 6 portions and the mixture was ground and mixed at ambient temperature at 300 rpm for 10 min every after the addition. Then the mixture was further mixed with 80 mg of PEG and 3-5 drops of nitric acid by ball-milling at 300 rpm for 2-3 h to give TiO_2 slurry. The TiO_2 (5×5 mm^2) layer was prepared on a FTO glass plate by casting the slurry, and the plate was sintered at 500 °C for 30 min. The TiO_2-coated FTO glass plate was immersed in a chloroform solution of a hybrid (0.5 g/L) under an argon atmosphere and irradiated with a UV

lamp through filters that cut lights <400 nm and those in IR region, for 40 min. The plate was washed thoroughly with chloroform, and was air-dried at room temperature. Finally, a DSSC was fabricated with a thin liquid layer of an acetonitrile solution containing LiI (0.5 M)/I_2 (0.05M), which was sandwiched between the TiO_2/FTO and Pt counter electrodes. The DSSC thus prepared was irradiated with a monochromatic light from the FTO side and the photocurrent was monitored as a function of wavelength by a digital electrometer (Advantest TR-8652).

References

1 (a) B. O'Regan, M. Grätzel, *Nature*, **1991**, *353*, 737; (b) M. Grätzel, *Inorg. Chem*., **2005**, *2* 6841.

2 (a) G. Zhang, H. Bala, Y. Cheng, D. Shi, X. Lv, Q. Yu, P. Wang, *Chem. Commun*., **2009**, 2198; (b) W. Zeng, Y. Cao, Y. Bai, Y. Wang, Y. Shi, M. Zhang, F. Wang, C. Pan, P. Wang, *Chem. Mater*., **2010**, 22 1915; (c) P. Bonhôte, J.-E. Moser, R. Humphry-Baker, N. Vlachopoulos, S.M. Zakeeruddin, L. Walder, M. Grätzel, *J. Am. Chem. Soc*., **1999** *121* 1324.

3 A. Kunai, T. Ueda, K. Horata, E. Toyoda, I. Nagamoto, J. Ohshita, M. Ishikawa, K. Tanaka, *Organometallics*, **1996**, *15*, 2000.

4 J. Ohshita, J. Matsukawa, M. Hara, A. Kunai, S. Kajiwara, Y. Ooyama, Y. Harima, M. Kakimoto, *Chem. Lett.*, **2008**, *37*, 316.

5 (a) K. Kakiage, M. Yamamura, E. Fujimura, T. Kyomen, M. Unno, M. Hanaya, *Chem. Lett.*, **2010**, *39*, 260; (b) M. Unno, K. Kakiage, M. Yamamura, T. Kogure, T. Kyomen, M. Hanaya, *Appl. Organometal. Chem.*, **2010**, *24*, 247.

6 (a) J. van de Lagemaat, T. M. Barnes, G. Rumbles, S. E. Shaheen, T. J. Coutts, C. Weeks, I. Levisky, J. Peltora, P. Glatkowsky, *Appl. Phys. Lett.*, **2006**, *88*, 233503; (b) A. Kongkanand, R. M. Dominguez, P. V. Kamat, *Nano Lett.*, **2007**, *7*, 676; (c) M. S. Arnold, J. D. Zimmerman, C. K. Renshaw, X. Xu, R. R. Lunt, C. M. Austin, S. R. Forrest, *Nano Lett.*, **2009**, *9*, 3354.

7 For reviews, see: (a) B. I. Kharisov, O. V. Kharissova, H. L. Gutierrez, U. O. Méndez, *Ind. Eng. Chem. Res.*, **2009**, *48*, 572; (b) N. Nakashima, T. Fujigaya, *Chem. Lett.*, **2007**, *36*, 692.

8 (a) J. Liu, A. G. Rinzler, H. Dai, J. H. Hafner, R. K. Bradley, P. J. Boul, A. Lu, T. Iverson, K. Shelimov, C. B. Huffman, F. Rodriguez-Macias, Y.-S. Shon, T. R. Lee, D. T. Colbert, R. E. Smalley, *Science*, **1998**, *282*, 95; (b) J. Chen, M. A. Hamon, H. Hu, Y. Chen, A. M. Rao, P. C. Eklund, R. C. Haddon, *Science*, **1998**, *282*, 1253; (c) J. E. Riggs, Z. Guo, D. L. Carroll, Y.-P. Sun, *J. Am. Chem. Soc.*, **2000**, *122*, 5879; (d) T. Umeyama, N. Tezuka, M. Fujita, Y. Matano, N.

Takeda, K. Murakoshi, K. Yoshida, S. Isoda, H. Imahori, *J. Phys. Chem. C*, **2007**, *111*, 9734.

9 (a) Z. Yao, N. Braidy, G. A. Botton, A. Adronov, *J. Am. Chem. Soc.*, **2003**, *125*, 16015; (b) Y. Liu, Z. Yao, A. Adronov, *Macromolecules*, **2005**, *38*, 1172; (c) Z. Li, Y. Dong, M. Häussler, J. W. Y. Lam, Y. Dong, L. Wu, K. S. Wong, B. Z. Tang, *J. Phys. Chem. B*, **2006**, *110*, 2302; (d) G.-J. Wang, S.-Z. Huang, Y. Wang, L. Liu, J. Qiu, Y. Li, *Polymer*, **2007**, *48*, 728.

10 (a) H. Murakami, T. Nomura, N. Nakashima, *Chem. Phys. Lett.*, **2003**, *378*, 481; (b) Y. Tomonari, H. Murakami, N. Nakashima, *Chem.-Eur. J.*, **2006**, *12*, 4027; (c) A. Ikeda, Y. Tanaka, K. Nobusawa, J. Kikuchi, *Langmuir*, **2007**, *23*, 10913; (d) S. Woo, Y. Lee, V. Sunkara, R. K. Cheedarala, H. S. Shin, H. C. Choi, J. W. Park, *Langmuir*, **2007**, *23*, 11373; (e) A. Ikeda, T. Hamano, K. Hayashi, J. Kikuchi, *Org. Lett.*, **2006**, *8*, 1153; (f) Y. Ji, Y. Y. Huang, A. R. Tajbakhsh, E. M. Terentjev, *Langmuir*, **2009**, *25*, 12325; (g) C. Backes, C. D. Schmidt, F. Hauke, C. Böttcher, A. Hirsch, *J. Am. Chem. Soc.*, **2009**, *131*, 2172; (h) T. Ogoshi, T. Saito, T. Yamaguchi, Y. Nakamoto, *Carbon*, **2009**, *47*, 117; (i) C. Backes, C. D. Schmidt, K. Rosenlehner, F. Hauke, J. N. Coleman, A. Hirsch, *Adv. Mater.*, **2010**, *22*, 788.

11 A. Ikeda, K. Hayashi, T. Konishi, J. Kikuchi, *Chem. Commun.*, **2004**, 1334.

12 M. J. O'Connell, S. M. Bachilo, C. B. Huffman, V. C. Moore, M. S. Strano, E. H. Haroz, K. L. Rialon, P. J. Boul, W. H. Noon, C. Kittrell, J. Ma, R. H. Hauge, R. B. Weisman, R. E. Smalley, *Science*, **2002**, *297*, 593.

13 Applications of SWNTs to DSSCs have been reported. See, for example: H. Imahori, T. Umeyama, *J. Phys. Chem. C*, **2009**, *113*, 9029.

14 K. T. Constantopoulos, C. J. Shearer, A. V. Ellis, N. H. Voelcker, J. G. Shapter, *Adv. Mater.*, **2010**, *22*, 557.

15 For reviews, see: a) J. Ohshita, A. Kunai, *Acta Polym.*, **1998**, *49*, 379. b) W. Uhlig, *Prog. Polym. Sci.*, **2002**, *27*, 255. c) T.-Y. Luh, Y.-J. Cheng, *Chem. Commun.*, **2006**, 4669.

16 J. Ohshita, K. Yoshimoto, M. Hashimoto, D. Hamamoto, A. Kunai, Y. Harima, Y. Kunugi, K. Yamashita, M. Kakimoto, M. Ishikawa, *J. Organomet. Chem.*, **2003**, *665*, 29.

17 Y. Liu, Z. Yao, A. Adronov, *Macromolecules*, **2005**, *38*, 1172.

Chapter 2

Synthesis of Disilanylene Polymers with Donor-Acceptor-Type π-Conjugated Units and Applications to Dye-Sensitized Solar Cells

Introduction

Recently, dye sensitized solar cells (DSSCs) with dye-attached TiO_2 electrodes as the photoactive anodes, have attracted much attention[1], because of their advantages, such as device flexibility, low production cost, and tunable cell color. The development of efficient sensitizing dyes is a major subject to obtain high performance DSSCs with high power conversion efficiency (PCE). Generally, sensitizing dyes consist of a donor-acceptor (D-A) unit and an attachment group[2]. The D-A interaction is known to provide broad and red-shifted absorption bands, which provide the use of wide range of the sun light wavelength, enhancing the photocurrent. Typically, a carboxylic acid group is employed as the attachment unit in the dyes, which forms an ester linkage by dehydration with a hydroxyl group on the TiO_2 surface (Ti-OH)[3]. However, the ester linkage is rather labile and undergoes hydrolytic decomposition gradually to detach the dye, shortening the DSSC lifetime.

As described in General Introduction and Chapter 1, polymers with Si-Si bonds are photoactive and can be photolyzed in the presence of TiO_2 to form Si-O-Ti bonds. This was recently applied to attach organosilicon polymers on TiO_2 surface. In this process, direct reactions of Ti-OH surface with the photo-excited Si-Si bonds, forming chemically stable Si-O-Ti linkages, would be involved as shown in Scheme 1[4].

Interestingly, the TiO_2 electrode modified by photolysis with quinquethiophene-disilanylene polymer **DS5T** (Chart 1) showed DSSC activity with the structure of FTO/polymer-attached TiO_2/I^-

I_3^-/Pt. However, the power conversion efficiencies (PCEs) of the cell was only as high as 0.1%. This is probably due to that the polymers had no D-A type structures. In Chapter 1, the author described effects to improve the PCE by using the hybrids of **DS5T** with SWNT. The PCE was successfully increased up to 0.39% but still the value was low in comparison to the DSSCs with conventional organic dyes. In this chapter, the author describes the synthesis of D-A type organosilicon polymers bearing photoreactive Si-Si bonds and their applications to DSSCs[5]. Thermal attachment of the polymers with ethynylene-Si units on TiO_2 surface was also examined.

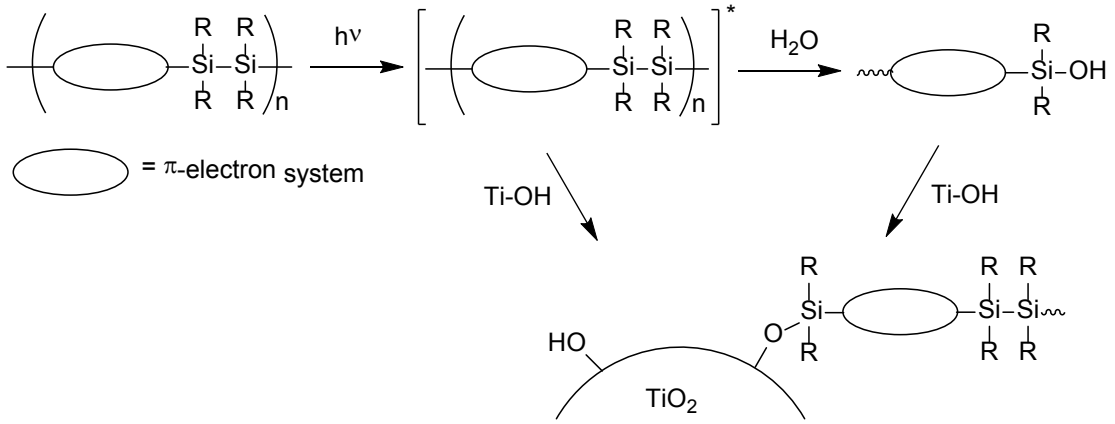

Scheme 1. Photochemical attachment of organosilicon polymers on the TiO_2 surface.

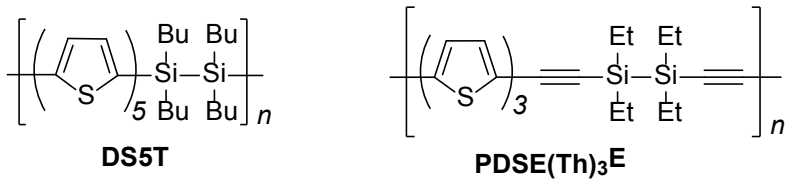

DS5T **PDSE(Th)$_3$E**

Chart 1. Organosilicon polymers with oligothiophene units.

Results and discussion

Polymer synthesis

For the preparation of D-A type organosilicon polymers containing thiophene as the donor and benzothiadiazole as the acceptor, the author first examined model reactions to optimize the polymerization conditions (Eq. (1) and Table 1). The Sonogashira-coupling reactions of (triethylsilyl)acetylene with bis(iodothienyl)benzothiadiazole in Et_3N gave the coupling product (**T_2Bt**) in 79% yield (run 1). Changing the solvent to *i*Pr_2NH led to a slight increase of the yield but required a longer reaction time (run 2). In the catalytic cycle of the Sonogashira-coupling, the Pd(II) catalyst is first reduced to Pd(0),[6] and in the present reactions, (triethylsilyl)acetylene seems to work as the reducing agent. To compensate for the consumption of (triethylsilyl) acetylene to reduce Pd(II), a slight excess (2.2 equiv) of the acetylene was used for the reaction in run 3 to increase the yield to 87%. Using microwave irradiation did not affect the yield, although the reaction time could be drastically shortened (run 4). Finally, the author examined the reaction with Pd(0), to permit the use of exactly 2 equiv of (triethylsilyl)acetylene (run 5). Since the control of exact stoichiometry is essential to obtain high molecular weight polymers from copolymerization of two or more monomer compounds, the author employed the reaction conditions of run 5 for the following polymerization.

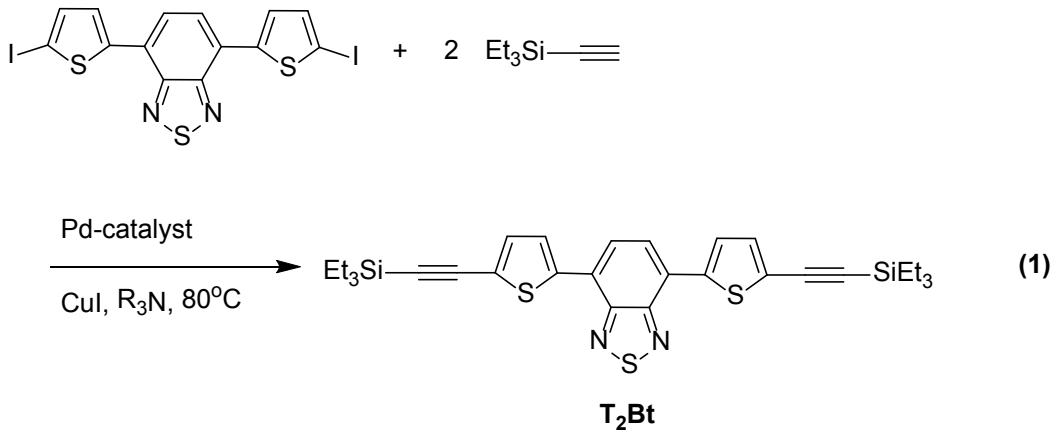

(1)

Table 1. Conditions of model reaction

Run	Catalyst	Solvent	Time/days	Yield/%[a)]
1	$PdCl_2(PPh_3)_2$	Et_3N	2	79
2	$PdCl_2(PPh_3)_2$	iPr_2NH	5	86
3 [b)]	$PdCl_2(PPh_3)_2$	Et_3N	2	87
4[b,c)]	$PdCl_2(PPh_3)_2$	Et_3N	1 h	88
5	$Pd_2(dba)_3$, $4PPh_3$	Et_3N	2	88

[a)] NMR yield. [b)] A slight excess (2.2 equiv) of triethylsilylacetylene was used. [c)] Under microwave irradiation.

The copolymerization of tetrabutyldiethynyldisilane and bis(iodothienyl)benzothiadiazoles was performed under the same conditions as those of the model reaction run 5 (Eq. (2)). Tetrabutyl-substituted diethynyldisilane was used as the monomer to give sufficient polymer solubility. Removal of the resulting insoluble precipitates from the reaction mixtures by filtration, followed by reprecipitation of the soluble fractions from chloroform/2-propanol or hexane afforded the corresponding polymers in 11-68% yields (Table 2). Polymer **pT$_2$Bt** was obtained only in low

yield with a low molecular weight, because of its low solubility. The author also examined the preparation of **pT$_2$Bt** under microwave-irradiation. However, the molecular weight was M_n = 3,600 (M_w/M_n = 1.6), which was lower than that prepared under normal heating. Polymers **pT$_2$Bt-in** and **pT$_2$Bt-out** with solubilizing n-butyl-substituents exhibited the high molecular weights and yields than those of **pT$_2$Bt**, respectively. Polymer **pT$_2$Bt-out** was purified by reprecipitation from chloroform/hexane, but **pT$_2$Bt-in** was soluble in hexane and reprecipitated from chloroform/2-propanol.

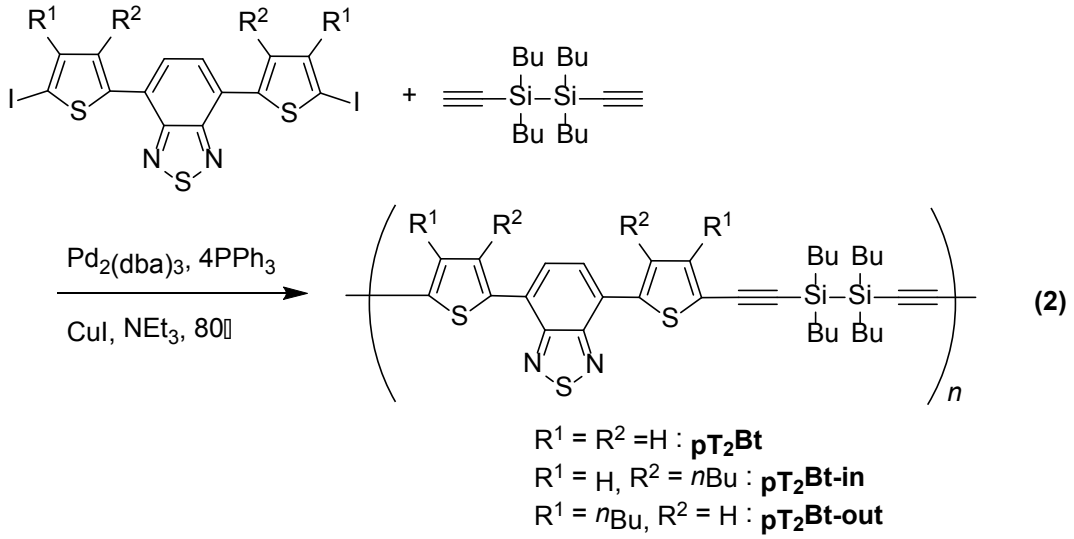

(2)

Table 2. Optical and electrochemical properties of the polymers

Polymer	M_n	M_w/M_n	Yield /%	λ_{max} /nm[a)]	λ_{em} /nm[b)]	HOMO /eV[c)]	LUMO /eV[d)]
pT$_2$Bt	7300	1.7	11	487, 330	583	-5.43	-3.16
pT$_2$Bt-in	8000	1.9	68	430, 331	583	-5.62	-3.14
pT$_2$Bt-out	15000	1.6	32	504, 349	616	-5.40	-3.23

[a)] In chloroform. [b)] Irradiated at absorption λ_{max}. [c)] Estimated from edge potential of CV recorded in TBAP/AN. [d)] Estimated by the formula of LUMO = HOMO + $E_{0\text{-}0}$.

Optical and electrochemical properties of D-A type organosilicon polymer

The UV-vis absorption and emission spectra of the present polymers are shown in Figure 1a and 1b, respectively. Absorption and emission maxima (λ_{max} and λ_{em}) of the polymers in chloroform are summarized in Table 2, which are red shifted from those of poly [(tetraethyldisilanylene)ethynylene(terthiophenylene)ethynylene] **PDSE(Th)$_3$E** (Chart 1), reported previously (λ_{max} = 395 nm),[7] indicative of the effects of the D-A structure enhancing the conjugation in the present polymers. The absorption bands of the polymers shifted to shorter wavelengths in the order of **pT$_2$Bt-out** > **pT$_2$Bt** > **pT$_2$Bt-in**. Absorption maxima of **pT$_2$Bt-out** and **pT$_2$Bt** are at 504 nm and 487 nm, respectively, which are red shifted than that of model compound **T$_2$Bt** (λ_{max} = 480 nm), suggesting σ-π conjugation in the polymer main chain to an extent. For polymer **pT$_2$Bt-in**, it is likely that the introduction of the *n*-butyl groups hindered the thienyl-benzothiadiazole unit from being planar, to suppress the conjugation[8], as compared to **pT$_2$Bt-out** and **pT$_2$Bt**. On the other hand, electronic effects of the electrondonating *n*-butyl groups that elevate the HOMO energy level would be responsible for the red shifted absorption and emission maxima of **pT$_2$Bt-out** from those of **pT$_2$Bt**, respectively. To estimate HOMO and LUMO energy levels, the author measured cyclic voltammograms (CVs) of the polymer films coated on Pt electrodes, in acetonitrile (AN) containing 100 mM tetrabutylammonium perchlorate (TBAP) as the supporting electrolyte, using Ag/Ag^+ as the reference electrode and Fc/Fc^+ as the external standard. All polymers exhibited irreversible anodic profiles, as often observed for the previously reported organosilicon polymers.[4, 9, 10] The HOMO levels of the polymers determined by the CV anodic onsets are lower than the I^-/I_3^- redox potential (-4.84 eV) and the LUMO levels estimated by the HOMO level and the optical band gaps are higher than the TiO_2 conduction level (-3.94 eV). This clearly indicates the potential of these polymers as the dye sensitizers for DSSCs in the structure of anode/polymer-attached $TiO_2/I^-{\cdot}I_3^-$/cathode (Table 2).

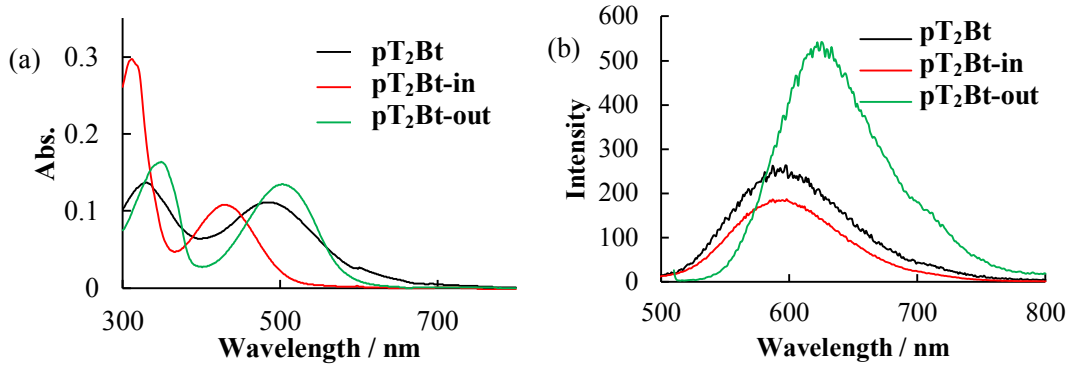

Figure 1. UV absorption (a) and emission (b) spectra of the polymers in chloroform at 2.7 × 10^{-3} mg/mL.

Applications of D-A type organosilicon polymers as dye sensitizers of DSSCs

The polymers were photochemically attached to the TiO_2 surface. Thus, TiO_2 electrodes prepared on FTO plates were immersed in argon-saturated solutions of the polymers in $CHCl_3$ (2 mg/mL) and irradiated (>400 nm) for 40 min. The resulting red-colored TiO_2 electrodes were rinsed thoroughly with $CHCl_3$. The UV spectra of the polymer-attached TiO_2 electrodes showed absorption bands ascribed to the polymers, although the absorption maxima were shifted to shorter region than those of the pristine polymers, suggesting that photodegradation of π-conjugated systems in the polymer main chains had occurred to an extent. For example, **pT$_2$Bt**-attached TiO_2 showed the blue-shifted absorption maximum approximately by 20 nm from that of **pT$_2$Bt** in chloroform as shown in Figure 2a and 2c. In the IR spectra of the polymer-attached TiO_2, intense bands due to the C≡C stretching were observed as illustrated for the **pT$_2$Bt**-attached TiO_2 in Figure 2d that shows the signal at 2162 cm^{-1}. DSSCs (FTO/polymer-attached TiO_2/I^-·I_3^-/Pt) were fabricated and the performance was evaluated. The IPCE (incident photon to current efficiency) spectra and the *J-V* curves of the cells are shown in Figure 3 and the DSSC parameters are summarized in Table 3. All polymers exhibited clear sensitizing effects and the highest PCEs (power conversion efficiencies) of the polymer-based cells was 0.26 % for the DSSC based on **pT$_2$Bt-out**, presumably reflecting the

expanded conjugation. The IPCE for **pT$_2$Bt**-based cell was higher than that with **pT$_2$Bt-out** in the whole wavelength range, although the PCE of both the cells were almost the same. Such disagreement is not unusual and probably due to the different solar power for the IPCE measurements (12 mW/cm^2) and the PCE evaluation (100 mW/cm^2).

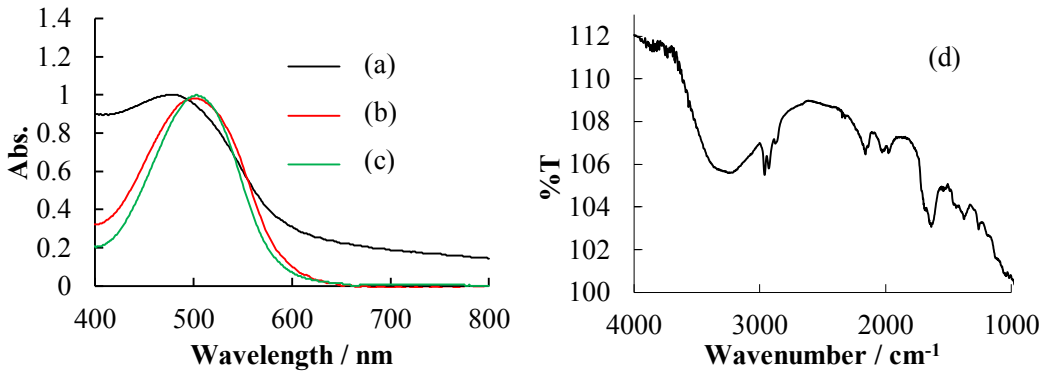

Figure 2. Normalized transmission UV spectra of TiO_2 electrodes photochemically (a) and thermally modified (b) by **pT$_2$Bt**, and **pT$_2$Bt** in chloroform (c), and reflectance FT-IR spectrum of the photochemically modified TiO_2 with **pT$_2$Bt** (d).

Table 3. DSSC performance using polymer-attached TiO_2

	Method[a)]	J_{sc} / mAcm^{-2}	V_{oc} / mV	FF	PCE / %
pT$_2$Bt	A	1.30	-308	0.61	0.25
pT$_2$Bt-in	A	0.29	-228	0.46	0.03
pT$_2$Bt-out	A	1.08	-392	0.60	0.26
pT$_2$Bt	B	0.74	-376	0.61	0.17
pT$_2$Bt-SWNT	A	1.31	-296	0.50	0.20
pT$_2$Bt-SWNT	B	0.78	-372	0.61	0.18

[a)] A : Photochemical modification, B : Thermal modification.

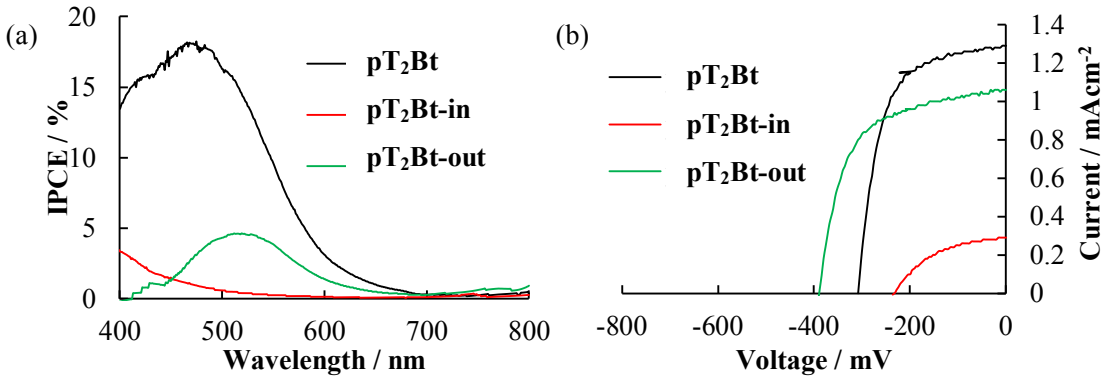

Figure 3. IPCE Spectra (a) and *J–V* curves (b) of DSSCs with photochemically modified TiO_2.

Attempts to improve DSSC performance by non-photochemical attachment of polymers on TiO_2 and by hybridization with SWNT

Since polymer degradation under the photochemical conditions was suggested by the UV spectral analysis, the author examined the polymer attachment by a thermal method in dark. Thus, thermally modified TiO_2 electrode was obtained by immersing a TiO_2 electrode in a **pT$_2$Bt** chloroform solution (2 mg/mL) for 4 h at 40 °C. The transmission UV spectrum of the TiO_2 electrode thermally treated with **pT$_2$Bt** is shown in Figure 2b, which is essentially the same as that of the chloroform solution of **pT$_2$Bt** (Figure 2c), suggesting no considerable degradation of the π-conjugated system was involved during the thermal process. The reflectance FT-IR spectrum of the thermally modified TiO_2 electrode also resembles that of photochemically modified one. The thermal attachment mechanism is not clear yet. However, since similar treatment of TiO_2 with polymer **DS5T** (Chart 1) that can attach on TiO_2 photochemically, afforded no attachment of the polymers in dark[4], it seems likely that the ethynylene-Si bonds reacted with the Ti-OH surface.

As described in Chapter 1, the author found that the DSSC performance with TiO_2 electrode photochemically modified with **DS5T** could be improved by utilizing organosilicon polymer-SWNT (single-walled carbon nanotube) hybrid materials prepared by ball milling of organosilicon polymers with SWNT, as the dye sensitizers.[11] This is probably due to high carrier mobility of SWNT.

Polymer **pT$_2$Bt** was blended with SWNT in a ball milling apparatus at 300 rpm for 3 h, and the resulting mixture was extracted with chloroform to give a chloroform-soluble **pT$_2$Bt**-SWNT hybrid material. The NIR-UV spectrum of the **pT$_2$Bt**-SWNT hybrid exhibited three peaks around 1100 nm which were characteristic to SWNT (Figure 4a). As shown in Figure 4b, the emission intensity was lowered by hybridization with SWNT, suggesting the efficient energy or electron transfer from photo-excited **pT$_2$Bt** to SWNT to quench the emission, as reported previously for the **DS5T**-SWNT hybrid.[11]

DSSC performance using the thermally modified TiO_2 electrodes with **pT$_2$Bt** and **pT$_2$Bt**-SWNT is also summarized in Table 3. The DSSC performance, however, was inferior to that with the photochemically modified ones.

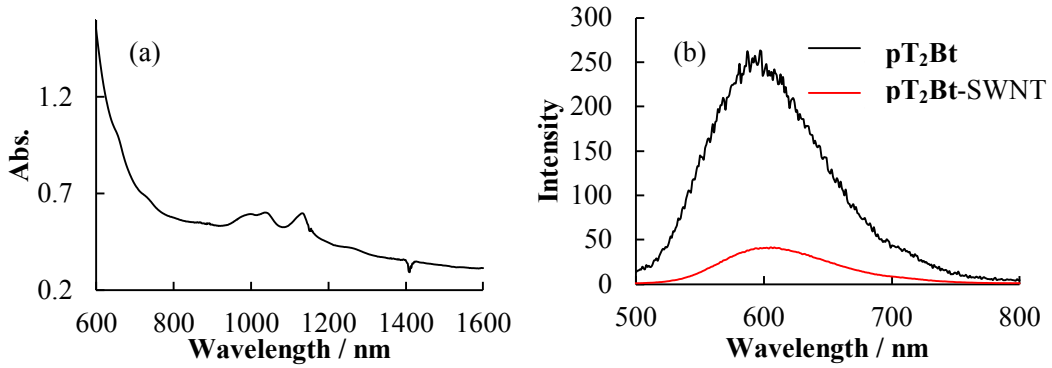

Figure 4. NIR-UV spectrum of **pT$_2$Bt**-SWNT hybrid in chloroform (a) and emission spectra of pristine **pT$_2$Bt** and **pT$_2$Bt**-SWNT in chloroform at both 2.7 $\times$ 10^{-3} mg/mL.

Conclusions

The author synthesized new D-A type organosilicon polymers, by the Sonogashira-coupling reactions, which exhibited red shifted absorption bands reflecting the D-A structures. These polymers were attached to TiO_2 electrodes under photochemical and thermal conditions and the resulting polymer-attached TiO_2 electrodes were applied to DSSC with the maximum PCE of 0.26%. Although PCEs from the present DSSCs were not very high yet, these results clearly indicate the potential utility of the present methodology to prepare the hybrid materials of D-A type organosilicon polymers and inorganic oxides.

Experimental

General

All reactions were carried out under a dry argon atmosphere. THF and ether were dried over sodium/benzophenone and distilled immediately before use. DMF and triethylamine, and chloroform were distilled from calcium hydride and phosphorus (IV) oxide, respectively, and were stored over activated molecular sieves 4A under an argon atmosphere until use. Usual work up described below involves hydrolysis of the reaction mixture with water, separation of the organic layer, extraction of the aqueous layer with chloroform, drying the combined organic layers and the extract over anhydrous magnesium sulfate, and evaporation of the solvent, in that order. Bis(iodothienyl)benzothiadiazole[15,16] and tetrabutyldiethynyldisilane[17] were prepared as reported in the literature. For the preparation of 3- and 4-butyl-2-(tributylstannyl)thiophenes, the corresponding butyl(lithio)thiophenes prepared by the reactions of 2-bromo-3-butylthiophene with *n*-butyllithium and 3-butylthiophene with LDA in THF, respectively, were treated with tributylstannyl chloride. After filtration of the reaction mixtures, the solvents were evaporated and the residues were used for the following coupling reactions without further purification.[18] Fabrication and evaluation of DSSCs were carried out in a fashion similar to Chapter 1.

Measurements

^{1}H and ^{13}C NMR spectra were recorded on Varian System500 and MR400 spectrometers. UV absorption and emission spectra were measured on Hitachi U-3210 and F-4500 spectrophotometers, respectively. IR spectra were obtained on a Shimadzu FT-IR 8700 spectrometer. Measurement of high resolution APCI mass spectroscopy was carried out using Thermo Fisher Scientific LTQ Orbitrap XL at the Natural Science Center for Basic Research and Development (N-BARD), Hiroshima University, while EI-mass spectra were measured on a Shimadzu QP-2020A

spectrometer.

Synthesis of 4,7-bis(3- and 4-butyl-2-thienyl)-2,1,3-benzothiadiazoles

In a 100 mL two necked flask fitted with a reflux condenser was placed a mixture of 4,7-dibromo2,1,3-benzothiadiazole (1.00 g, 3.40 mmol), 3-butyl-2-(tributylstannyl)thiophene (2.92 g, 6.80 mmol), $PdCl_2(PPh_3)_2$ (0.12 g, 0.20 mmol), CuI (0.03 g, 0.2 mmol), and THF (50 mL) and the mixture was stirred at the reflux temperature for 2 days. After usual work up, the residue was subjected to silica gel column chromatographywith hexane/ethyl acetate = 20/1 as an eluent to give 1.15 g (82% yield) of 4,7-bis(3-butyl-2-thienyl)-2,1,3-benzothiadiazole as an orange oil: MS m/z. 412 [M^+]; ^{1}H NMR (δ in $CDCl_3$) 0.83 (t, 6H, *J* = 7 Hz, Bu), 1.28 (m, 4H, Bu), 1.62 (m, 4H, Bu), 2.67 (t, 4H, *J* = 8 Hz, Bu), 7.11 (d, 2H, *J* = 5 Hz, thiophene ring H), 7.44 (d, 2H, J = 5 Hz, thiophene ring H), 7.65 (s, 2H, phenylene ring H); ^{13}C NMR (δ in $CDCl_3$) 13.23, 22.51, 29.04, 32.86, 125.84, 127.39, 129.19, 129.87, 132.13, 141.62, 154.24; High resolution APCI/MS calcd *m/z* = 413.11744 ([M+H]$^+$), found *m/z* = 413.11743.

4,7-Bis(4-butyl-2-thienyl)-2,1,3-benzothiadiazole was prepared in a fashion similar to that above, using 4-butyl-2-(tributylstannyl)thiophene instead of 3-butyl-2-(tributylstannyl)thiophene: 70% yield; red solid; mp 72.4^{o}C; MS m/z = 412 [M^+]; ^{1}H NMR (δ in $CDCl_3$) 0.96 (t, 6H, *J* = 7.2 Hz, Bu), 1.42 (m, 4H, Bu), 1.69 (m, 4H, Bu), 2.70 (t, 4H, *J* = 8.0 Hz, Bu), 7.04 (d, 2H, *J* = 0.8 Hz, thiophene ring H), 7.84 (s, 2H, phenylene ring H), 7.98 (d, 2H, *J* = 1.2 Hz, thiophene ring H); ^{13}C NMR (δ in $CDCl_3$) 13.96, 22.43, 30.33, 32.64, 121.53, 125.53, 125.98, 128.98, 138.98, 144.31, 152.61; High resolution APCI/MS calcd *m/z* = 413.11744 ([M+H]$^+$), found *m/z* = 413.11804.

Synthesis of 4,7-bis(3-butyl-5-iodo-2-thienyl)-2,1,3-benzothiadiazole

In a 100 mL two necked flask fitted with a reflux condenser was placed a mixture of

4,7-bis(3-butyl-2-thienyl)-2,1,3-benzothiadiazole (1.15 g, 2.80 mmol), chloroform (30 mL), and acetic acid (5 mL). The mixture was cooled down to 0°C, and N-iodosuccinimide (1.26 g, 5.60 mmol) was slowly added to the mixture over 10 min at 0°C and further stirred for 6 h at room temperature. After usual work up, the residue was subjected to silica gel column chlomatography with hexane/ethyl acetate = 20/1 as an eluent to give 1.60 g of the title compound (86% yield) as an orange oil: MS *m/z* = 664 [M^+]; ^{1}H NMR (δ in $CDCl_3$) 0.83 (t, 6H, *J* = 7 Hz, Bu), 1.27 (m, 4H, Bu), 1.58 (m, 4H, Bu), 2.63 (t, 4H, *J* = 8 Hz, Bu), 7.24 (s, 2H, thiophene ring proton), 7.59 (s, 2H, phenylene ring proton); ^{13}C NMR (δ in $CDCl_3$) 13.83, 22.49, 28.23, 32.77, 74.71, 126.5d8, 129.58, 138.14, 139.05, 143.60, 153.93; High resolution APCI/MS calculated *m/z* = 664.91072 ([M+H]$^+$), found *m/z* = 664.90967 ([M+H]$^+$).

4,7-Bis(4-butyl-5-iodo-2-thienyl)-2,1,3-benzothiadiazole was prepared from 4,7-bis(4-butyl-2-thienyl)-2,1,3-benzothiadiazole in a fashion similar to that above: 89% yield; red solid; m.p. = 127.3°C; MS *m/z* = 664 [M^+]; ^{1}H NMR (δ in $CDCl_3$) 0.98 (t, 6H, *J* = 7.2 Hz, Bu), 1.43 (m, 4H, Bu), 1.64 (m, 4H, Bu), 2.63 (t, 4H, *J* = 7.6 Hz, Bu), 7.71 (s, 2H, thiophene ring H), 7.77 (s, 2H, phenylene ring H); ^{13}C NMR (δ in $CDCl_3$) 13.98, 22.39, 32.19, 32.21, 77.52, 124.91, 125.28, 127.67, 143.54, 148.16, 152.11; High resolution APCI/MS calcd *m/z* = 664.91072 ([M+H]$^+$), found *m/z* = 664.90961.

Model reaction

In an autoclave was placed a mixture of 4,7-bis(5-iodo-2-thienyl)-2,1,3-benzothiadiazole (0.06 g, 0.1 mmol), triethylsilylacetylene (0.03 g, 0.2 mmol), $Pd_2(dba)_3$ (6 mg), CuI (2 mg), and triethylamine (5 mL) and the mixture was stirred at 80 °C for 2 days. After usual work up, the residue was subjected to silica gel column chromatography with hexane/ethyl acetate = 20/1 as an eluent to give and the model compound **T_2Bt** was given as red solids: m.p. = 93.9 °C; MS *m/z* = 576

[M^+]; ^{1}H NMR (δ in $CDCl_3$) 0.70 (q, 12 H, J = 8 Hz, CH_2), 1.06 (t, 18H, J = 8 Hz, CH_3), 7.30 (d, 2H, J = 4 Hz, thiophene ring proton), 7.85 (s, 2 H, phenylene ring proton), 7.94 (d, 2 H, J = 4 Hz, thiophene ring proton); ^{13}C NMR (δ in $CDCl_3$) 4.32, 7.50, 98.65, 98.84, 124.92, 125.62, 127.06, 133.34, 140.18, 152.39; High resolution APCI/MS calcd m/z = 577.16591 ([M+H]$^+$), found m/z = 577.16595 ([M+H]$^+$).

Synthesis of D-A type polymers

A mixture of 4,7-bis(5-iodo-2-thienyl)-2,1,3-benzothiadiazole (0.15 g, 0.30 mmol), 1,1,2,2-tetrabutyl-1,2-diethynyldisilane (0.09 g, 0.3 mmol), $Pd_2(dba)_3$ (18 mg), triphenylphosphine (14 mg), CuI (5 mg), and triethylamine (10 mL) was placed in an autoclave and was stirred at 80 ^{o}C for 2 days. After usual work up, the residue was reprepicipitated from chloroform/hexane to give **pT_2Bt** in 11% yield (18 mg) as dark red solids: m.p. > 300 ^{o}C; M_n = 7300, M_w/M_n = 1.7; ^{1}H NMR(δ in CD_2Cl_2) 0.90-0.99 (m, 18H, Bu), 1.39-1.55 (m, 18H, Bu), 7.69-7.91 (m, 6H, aromatic ring H); ^{13}C NMR (δ in $CDCl_3$) 12.67,12.84, 13.78, 13.86, 25.81, 25.92, 26.45, 26.55, 26.75, 26.86, 27.00, 98.84, 101.12, 125.08, 125.35, 126.98, 127.12, 127.63, 128.02, 128.43, 128.55, 131.10, 132.10, 133.12, 140.11, 152.17; IR 2134 cm^{-1} ($\nu_{C\equiv C}$). Polymers **pT_2Bt-in** and **pT_2Bt-out** were prepared in a similar fashion to that of **pT_2Bt** (vide supra). Data for **pT_2Bt-in** reprecipitated from chloroform/2-propanol: waxy dark orange solids; m.p. > 300 ^{o}C; M_n = 8000, M_w/M_n = 1.9; ^{1}H NMR (δ in $CDCl_3$) 0.66-0.94 (br m, 25H, Bu), 1.21-1.66 (br m, 25H, Bu), 2.70-2.78 (br m, 4H, Bu), 7.20-7.22 (br m, 2H, aromatic ring H), 7.62-7.63 (br m, 2H, aromatic ring H); IR 2137 cm^{-1} ($\nu_{C\equiv C}$). Data for **pT_2Bt-out** reprecipitated from chloroform/hexane: dark red solid; m.p. >300^{o}C; M_n = 15000, M_w/M_n = 1.6; ^{1}H NMR (δ in $CDCl_3$) 0.86-0.97 (br m, 30H, Bu), 1.39-1.53 (br m, 16H, Bu), 1.67-1.71 (br m, 6H, Bu), 2.76-2.79 (br m, 4H, Bu), 7.74 (br s, 2H, aromatic ring H), 7.86 (br s, 2H, aromatic ring H); ^{13}C NMR (δ in $CDCl_3$) 8.61, 12.88, 13.89, 26.59, 27.05, 46.00, 128.47, 128.59,

132.04, 132.15; IR 2137 cm^{-1} ($\nu_{C\equiv C}$).

*Preparation of **pT$_2$Bt**-SWNT*

A mixture of 25 mg of **pT$_2$Bt** and 1.3 mg of SWNT (Aldrich, 0.7-1.3 nmΦ) was placed in a ball mill and blended for 3 h at 300 rpm. The resulting mixture was extracted with chloroform. The soluble **pT$_2$Bt**-SWNT chloroform solution was concentrated by a rotary evaporator to approximately 10 mL. Since **pT$_2$Bt**-SWNT was insolubilized by drying up, this was stored as the concentrated solution in a freezer at -15 ^{o}C.

References

1 (a) B. O'Regan, M. Grätzel, *Nature*, **1991**, *353*, 737; (b) M. Grätzel, *Inorg. Chem*., **2005**, *2* 6841.

2 Y. Ooyama, Y. Harima, *Eur. J. Org. Chem*., **2009**, *18*, 2903.

3 (a) G. Zhang, H. Bala, Y. Cheng, D. Shi, X. Lv, Q. Yu, P. Wang, *Chem. Commun*., **2009**, 2198; (b) W. Zeng, Y. Cao, Y. Bai, Y. Wang, Y. Shi, M. Zhang, F. Wang, C. Pan, P. Wang, *Chem. Mater*., **2010**, 22 1915; (c) P. Bonhôte, J.-E. Moser, R. Humphry-Baker, N. Vlachopoulos, S.M. Zakeeruddin, L. Walder, M. Grätzel, *J. Am. Chem. Soc*., **1999** *121* 1324.

4 J. Ohshita, J. Matsukawa, M. Hara, A. Kunai, S. Kawajima, Y. Ooyama, Y. Harima, M. Kakimoto, *Chem. Lett.*, **2008**, *37*, 316.

5 Similar D-A type organosilicon polymers with photo-inert monosilanylene bridges were synthesized, previously J. Ohshita, S. Kangai, H. Yoshida, A. Kunai, S. Kajiwara, Y. Ooyama, Y. Harima, *J. Organomet. Chem*., **2007**, *692*, 801.

6 K. Sonogashira, Y. Tohda, N. Hagiwara, *Tetrahedron Lett*., **1975**, *50*, 4467.

7 M. Kakimoto, H. Kashihara, Y. Yamaguchi, T. Takiguchi, *Macromolecules*, **2000**, *33*, 760.

8 H. Zhou, L. Yang, S. Xiao, S. Liu, W. You, *Macromolecules*, **2010**, *43*, 811.

9 J. Ohshita, A. Takata, H. Kai, A. Kunai, K. Komaguchi, M. Shiotani, A. Adachi, K. Sakamaki, K. Okita, Y. Harima, Y. Kunugi, K. Yamashita, M. Ishikawa, *Organometallics*, **2000**, *19*, 4492.

10 J. Ohshita, K. Sugimoto, A. Kunai, Y. Harima, K. Yamashita, *J. Organomet. Chem*., **1999**, *580*, 77.

11 J. Ohshita, D. Tanaka, J. Matsukawa, T. Mizumo, H. Yoshida, Y. Ooyama, Y. Harima, *Chem. Lett*., **2011**, *40*, 87.

12 For the synthetic procedure, see P.F. Xia, J. Lu, C.H. Kwok, H. Fukutani, M.S. Wong, Y. Tao, *J. Polym. Sci. A*, *Polym. Chem*., **2009**, *47*, 137.

13 For the spectral data, see J.-L. Wang, Z.-M. Tang, Q. Xiao, Y. Ma, J. Pei, *Org. Lett*., **2008**, *10*,

4271.

14 M. Ishikawa, T. Horio, T. Hatano, A. Kunai, *Organometallics*, **1993**, *12*, 2078.

15 For a similar reaction to produce 3-butyl-2-(tributhylstannyl)thiophene, see S.C. Ng, L.G. Xu, H.S.O. Chan, *Synth*. *Met*., **1998**, *94*, 185.

Chapter 3

Synthesis of Donor-Acceptor Type New Organosilicon Polymers and Their Applications to Dye-Sensitized Solar Cells

Introduction

In Chapter 2, the author described improvement of DSSCs performance based on organosilicon polymer-modified TiO_2 electrode by the introduction of D-A structures. However, the PCEs of DSSCs based on D-A type organosilicon polymer-modified TiO_2 electrodes are not very high yet. In this Chapter, the development of more efficient organosilicon polymers for DSSCs based on a different strategy is described.

The development of efficient anchoring units for photoexcited electron injection to TiO_2 is necessary to obtain high PCEs of DSSCs and is extensively investigated[1-6]. Generally, cyanoacrylic acid unit which led to efficient photoexcited electron injection to TiO_2 is utilized as electron-withdrawing anchoring unit[7]. However, the use of cyanoacrylic acid as the anchor causes some problems, such as degradation of inorganic oxide electrodes is facilitated by strong acidity of cyanoacrylic acid[8], limitations of solvent to dissolve dyes, and restriction of molecular design. Recently, pyridine unit which could be attached on TiO_2 surface by coordination with Lewis acid sites and/or hydrogen bonding is reported[6c] as a new electron-withdrawing anchoring unit, and pyridine-containing disilanylene polymers can be attached both on the TiO_2 Lewis and Brønsted acid sites. It is also known that electron-injection is facilitated by using pyridine as the anchoring unit, thus enhanced photocurrent may be expected.

In this study, expecting obtaining organosilicon polymers with higher performance as the DSSC dye, the author synthesized pyridine-containing disilanylene polymers. In addition, two new D-A

type organosilicon polymers were synthesized, which consisted of bithiophene units as the donor and benzochalcogenadiazole units as the acceptor, thus more expanded π-conjugation units than the previously reported D-A type polymer **pT$_2$Bt** (Chapter 2). Similar to **DS5T** and **pT$_2$Bt**, the polymers could be photochemically attached on TiO_2 surface, and the resulting polymer-modified TiO_2 electrodes were applied to DSSCs.

Results and discussion

Polymer synthesis and optical properties

New D-A type organosilicon polymers were synthesized by the Stille cross coupling reactions of bis(iodothienyl)benzochalcogenadiazoles or bis(bromothienyl)pyridine with bis(stannylthienyl)-disilane in DMF as shown in Scheme 1. The resulting polymeric substances were purified by reprecipitation from chloroform/hexane or ethanol. The polymers were given as red (**pT$_4$Bt**), purple (**pT$_4$Se**), and orange (**pT$_4$Py**) solids and were soluble in common organic solvents such as chloroform, toluene, and THF. Their melting points were 83.3 ^{o}C, 100.4 ^{o}C, and 107.3 ^{o}C, respectively, and the structures of the polymers were verified by the NMR spectroscopy. In the ^{1}H NMR spectra, the signal integration ratios were consistent with the regular polymer structures, although the signals were rather broad.

Polymers **pT$_4$Bt** and **pT$_4$Se** exhibited longer and broader absorption maxima than that of **DS5T** (λ_{max} = 436 nm, M_n = 30,000, M_w/M_n = 2.5, Chart 1)[9] bearing π-conjugation units with a similar size, likely due to the introduction of the D-A type π-conjugated units. In contrast, absorption maximum of polymer **pT$_4$Py** that had pyridylene as the acceptor was at shorter wavelength than that of **DS5T**, probably due to the lower planarity of the π-conjugated unit by the steric repulsion between the pyridylene protons and the thienylene protons. Shorter conjugation length as the result of the lower molecular weight of the polymer may also responsible for the blue shifted absorption. Polymer **pT$_4$Se** showed the longest absorption wavelength among these polymers, likely because the electropositive selenium atom in the benzoselenadiazole unit elevated the HOMO level. The photoluminescence (PL) maxima of the present polymers were red-shifted in the order of **pT$_4$Py** < **pT$_4$Bt** < **pT$_4$Se**, in accordance with the UV absorption spectra. Polymer **pT$_4$Bt** exhibited longer absorption wavelength than that of **pT$_2$Bt** (Chart 1, Chapter 2),[10] as the result of the expanded π-conjugation (Figure 1) (Table 1).

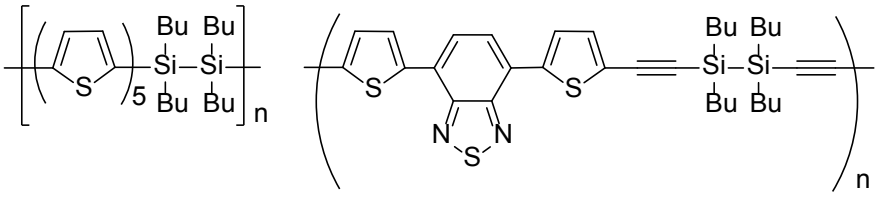

DS5T
λ_{max} = 436 nm
PCE = 0.11%

pT$_2$Bt
λ_{max} = 487 nm
PCE = 0.25%

Chart 1. Previously reported organosilicon polymers.

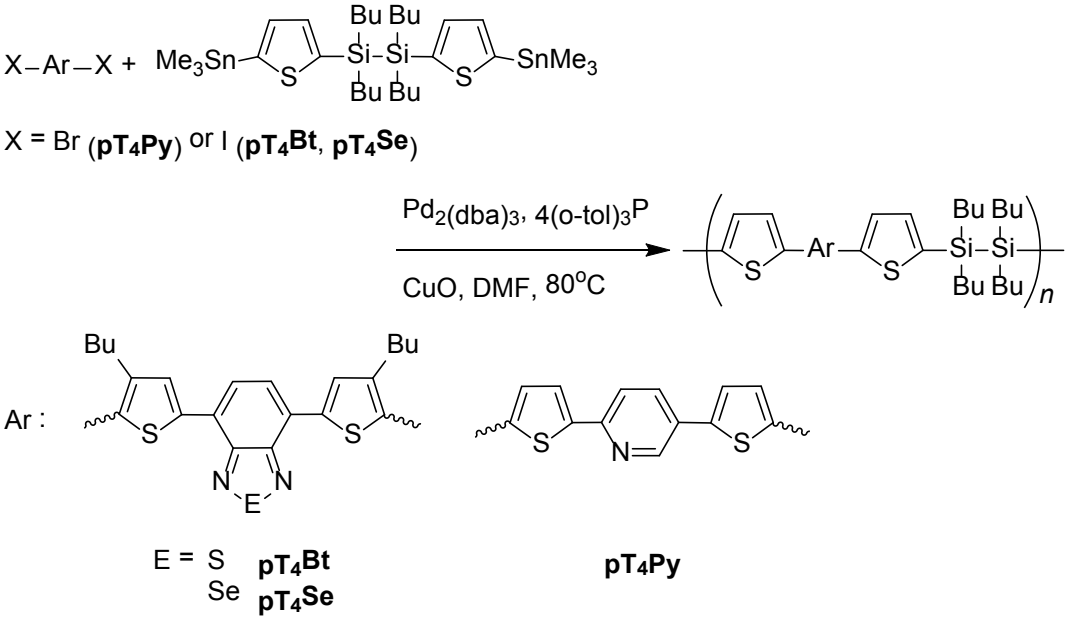

Scheme 1. Synthesis of D-A-type organosilicon polymers

Table 1. Synthesis and properties of D-A-type organosilicon polymers.

Polymer	M_n	M_w/M_n	yield/%	λ_{max}/nm[a]	λ_{em}/nm[b]
pT$_4$Bt	4400	1.7	16	330, 508	651
pT$_4$Se	5400	1.4	33	355, 546	716
pT$_4$Py	5500	1.4	24	416	474

[a] In chloroform; [b] Excited at the absorption maximum.

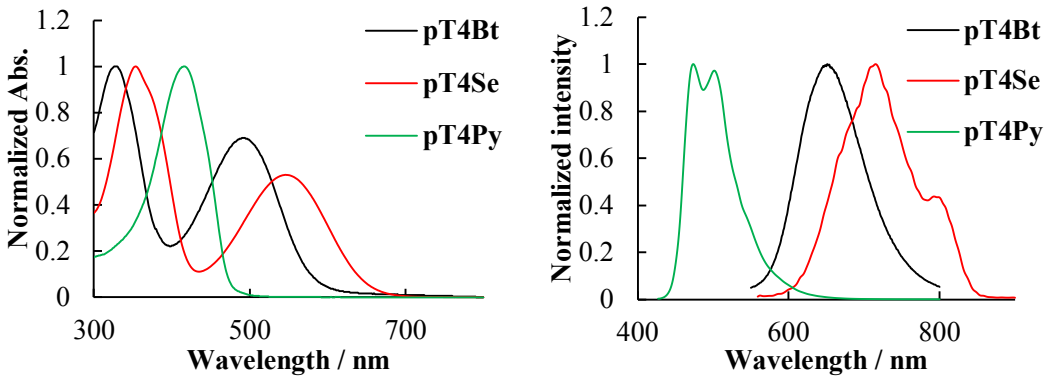

Figure 1. UV absorption (left) and photoluminescence (right) spectra of polymers **pT$_4$Bt**, **pT$_4$Se**, and **pT$_4$Py** in chloroform.

Applications of the polymers to DSSCs

As described in Chapter 1 and 2, irradiation of polymers bearing Si-Si bonds with TiO_2 produces polymer-modified TiO_2 by the photochemical reactions of the polymer Si-Si bonds with Ti-OH groups on the TiO_2 surface.[11] The present polymers were attached to TiO_2 electrodes under UV irradiation (method A, photochemical conditions), and the resulting polymer-modified TiO_2 electrodes were applied to DSSCs (FTO/polymer-TiO_2/I^-·I_3^-/Pt). The DSSC parameters are listed in Table 2, and the IPCE spectra and the *J*-*V* curves are shown in Figure 2. On the other hand, it has been reported that the coordination of pyridine units in sensitizing dyes with the TiO_2 Lewis acidic sites provides attachment of the dyes on the TiO_2 electrodes.[12] Similarly, pyridine-containing polymer **pT$_4$Py** was attached to the TiO_2 surface by simply dipping the TiO_2 electrode in the polymer solution in dark (method B, thermal conditions).

The IPCE spectrum profiles nearly overlapped with those of the UV absorptions. This indicated that the polymers attached on TiO_2 surface contributed to the photo-current generation. The PCE of the cell with the **pT$_4$Bt**-modified TiO_2 electrode is 0.28%, which is higher than that based on the **DS5T**-modified electrode (Chart 2).[11] This is likely due to the red-shifted broad

absorption band of **pT$_4$Bt**, as the result of the D-A structure in the polymer backbone. However, although **pT$_4$Se** shows a red-shifted broad absorption band and a high polymer amount adsorbed on **TiO$_2$** surface than those of **pT$_4$Bt**, the DSSC based on the **pT$_4$Se**-modified TiO_2 electrode exhibited the inferior performance with PCE of 0.11%. This result is most likely due to the higher magnitude of aggregation forming tendency of **pT$_4$Se** with heavier selenium atoms, leading to quenching of the photo-excited states of the polymer. Although the absorption band of **pT$_4$Bt** is broader than that of **pT$_2$Bt** reported previously,[10] the PCE of DSSC based on **pT$_4$Bt**-modified TiO_2 electrode (0.28%) is similar to **pT$_2$Bt** based one (0.25%), presumably due to that the π-π interactions between the polymer chains attached on the TiO_2 surface occur as the result of the more expanded π-conjugation of **pT$_4$Bt** than that of **pT$_2$Bt**, leading to also the concentration quenching. The highest PCE among the present DSSCs was 0.40% for the device using **pT$_4$Py** (method A). In the case of **pT$_4$Py**-based DSSC (method A), the polymer could be attached on both the Ti-OH sites and the Lewis acidic sites of TiO_2 to provide higher amount of the adsorbed polymer, thus leading to the high J_{sc}, realizing the highest PCE. High J_{sc} of the cell with the photochemically modified electrode by **pT$_4$Py** presumably originates from the efficient photoexcited electron injection provided by the pyridine-Ti coordination, as described in the previous literature.[6c] The DSSC using TiO_2 thermally modified by **pT$_4$Py** (method B), indeed, exhibits the activity, with a lower J_{sc}. This clearly indicates that both types of the dyes that attached on TiO_2 by the Si-O-Ti linkage and the N-Ti coordination exhibit the sensitizing effects.

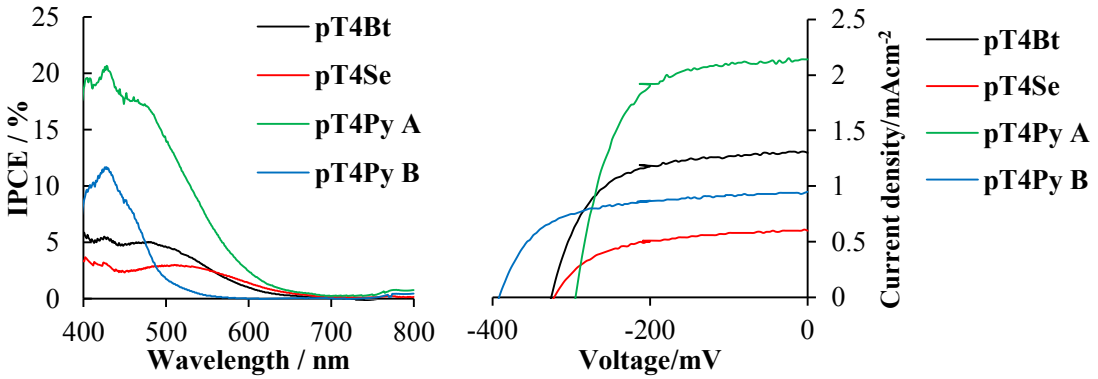

Figure 2. IPCE spectra (left) and *J-V* curves (right) of polymer-modified TiO_2 electrodes.

Table 2. DSSC performance of polymer-modified TiO_2 electrodes.

	method[a]	J_{sc}/mAcm^{-2}	V_{oc}/mV	FF	PCE/%	Adsorbed amt/μgcm^{-2} [b]
pT$_4$Bt	A	1.30	-324	0.63	0.28	29.6
pT$_4$Se	A	0.61	-324	0.57	0.11	38.0
pT$_4$Py	A	2.15	-296	0.63	0.40	18.4
pT$_4$Py	B	0.96	-396	0.61	0.23	15.9

[a] Polymers were attached by irradiation of polymer solutions with TiO_2 (method A) or dipping TiO_2 in polymer solution in dark (method B). [b] Amounts of the polymers adsorbed on the TiO_2 surface.

Conclusions

The author synthesized new D-A type organosilicon polymers that consisted of bithiophene as the donor and benzochalcogenadiazole or pyridine as the acceptor, and applied them as DSSC dye sensitizers. Polymers **pT$_4$Bt** and **pT$_4$Se** exhibit absorption maxima in low energy region as the result of the introduction of the D-A interaction. **pT$_4$Py** exhibits absorption maxima similar to **DS5T** which bears quinquethiophene as the π-conjugated unit since the steric repulsion of thiophene proton with pyridine proton suppressed the planarity of the π-conjugated system, which compensated with the effects of the pyridine acceptor. All the present polymers attached on TiO_2 photoelectrodes showed clear sensitizing effects in DSSCs. The highest PCE of the DSSCs achieved with the TiO_2 electrode based on the present polymers was 0.40% for **pT$_4$Py** (method A). This is presumably due to that **pT$_4$Py** can attach on TiO_2 surface by both of the Si-O-Ti bonds and the N-Ti coordination.

Experimental

General

All reactions were carried out under a dry argon atmosphere. THF and ether were dried over sodium/benzophenone and distilled immediately before use. DMF and triethylamine, and chloroform were distilled from calcium hydride and phosphorus (V) oxide, respectively, and were stored over activated molecular sieves 4 Å under an argon atmosphere until use. 1,1,2,2-Tetrabutyl-1,2-dichlorodisilane[12] and 4,7-bis(5-iodo-2-thienyl)-2,1,3-benzothiadiazole[10] were prepared by the procedure described in the literature. The usual work up described below involves separation of the organic layer, extraction of the aqueous layer with chloroform, drying the combined organic layer and the extracts over anhydrous magnesium sulfate, and evaporation of the solvent, in that order. Fabrication and evaluation of DSSCs were carried out in a fashion similar to Chapter 1.

Measurements

^{1}H and ^{13}C NMR spectra were recorded on Varian System500 and MR400 spectrometers. UV spectra were measured on a Hitachi U-3210 spectrophotometer. Emission spectra were measured on a Hitachi F-4500 spectrophotometer. Measurements of high resolution APCI and ESI mass spectra were carried out using a Thermo Fisher Scientific LTQ Orbitrap XL spectrometer at the Natural Science Center for Basic Research and Development (N-BARD), Hiroshima University.

Synthesis of 4,7-bis(4-butyl-2-thienyl)-2,1,3-benzoselenadiazole

In a 100 mL two necked flask fitted with a reflux condenser were placed 4,7-diiodo-2,1,3-benzoselenadiazole (1.83 g, 4.20 mmol), 4-butyl-2-tributylstannylthiophene (3.60 g, 8.40 mmol), $PdCl_2(PPh_3)_2$ (0.15 g, 0.21 mmol), CuI (0.040 g, 0.21 mmol), and THF (50 mL), and the

mixture was stirred at the reflux temperature for 2 days. After the usual work up, the residue was subjected to silica gel column chromatography with hexane/ethyl acetate = 20/1 as an eluent to give 1.29 g of the title compound (67% yield) as red solids: MS *m/z* = 460 [M^+]; ^{1}H NMR (δ in $CDCl_3$) 0.96 (t, 6H, *J* = 7.6 Hz, Bu), 1.42 (sext, 4H, *J* = 7.2 Hz, Bu), 1.68 (quin, 4H, *J* = 7.2 Hz, Bu), 2.69 (t, 4H, *J* = 8.0 Hz, Bu), 7.05 (d, 2H, *J* = 1.6 Hz, thiophene ring proton), 7.75 (s, 2H, benzene ring proton), 7.88 (d, 2H, *J* = 1.6 Hz, thiophene ring proton); ^{13}C NMR (δ in $CDCl_3$); 13.94, 22.43, 30.32, 32.65, 121.86, 125.83, 127.83, 128.93, 139.32, 143.99, 158.25; Anal. calcd for $C_{22}H_{24}N_2S_2Se$: C; 57.50, H; 5.26, N; 6.10. Found C; 57.49 H; 5.41 N; 6.20.

Synthesis of 4,7-bis(4-butyl-5-iodo-2-thienyl)-2,1,3-benzoselenadiazole

In a 100 mL two necked flask fitted with a reflux condenser were placed 4,7-bis(4-butyl-2-thienyl)-2,1,3-benzoselenadiazole (0.36 g, 0.78 mmol), chloroform (30 mL), and acetic acid (5 mL). The mixture was cooled down to 0 ^{o}C, and N-iodosuccinimide (0.350 g, 1.56 mmol) was slowly added to the mixture over 10 min at 0 ^{o}C. The mixture was further stirred for 6 h at room temperature. After the usual work up, the residue was subjected to silica gel column chromatography with hexane/ethyl acetate = 20/1 as an eluent to give 0.49 g the title compound (89% yield) as dark red solids: m.p. = 135.5 ^{o}C; MS *m/z* = 712 [M^+]; ^{1}H NMR (δ in $CDCl_3$) 0.97 (t, 6H, *J* = 7.2 Hz, Bu), 1.43 (sext, 4H, *J* = 7.2 Hz, Bu), 1.64 (quin, 4H, *J* = 7.2 Hz, Bu), 2.62 (t, 4H, *J* = 8.0 Hz, Bu), 7.60 (s, 2H, benzene ring proton), 7.71 (s, 2H, thiophene ring proton); ^{13}C NMR (δ in $CDCl_3$) 13.98, 22.38, 32.17, 32.24, 78.30, 125.11, 126.86, 127.86, 143.86, 147.76, 157.73, Anal. calcd for $C_{22}H_{22}N_2S_2SeI_2$: C; 37.15, H; 3.21, N; 3.94. Found C; 37.02, H; 2.97, N; 3.86.

Synthesis of 1,1,2,2,-tetrabulyl-1,2-bis(5-bromo-2-thienyl)disilane

In a 100 mL two necked flask fitted with a dropping funnel and a reflux condenser were placed

2,5-dibromothiophene (2.42 g, 10.0 mmol) and ether (100 mL). The mixture was cooled down to -78 ^{o}C and a 1.6 M *n*-butyllithium hexane solution (6.6 mL, 10 mmol) was slowly added to the mixture over 30 min at -78 ^{o}C. After the mixture was stirred for 1 h at -78 ^{o}C, 1,1,2,2-tetrabutyl-1,2-dichlorodisilane (1.78 g, 5.00 mmol) was added to the mixture at -78 ^{o}C and the mixture was further stirred overnight at room temperature. After the usual work up, the residue was subjected to silica gel column chromatography with hexane as an eluent to give 2.46 g of the title compound (81% yield) as colorless oil: ^{1}H NMR (δ in $CDCl_3$) 0.88 (m, 20H, Bu), 1.31 (m, 16H, Bu), 6.86 (d, 2H, J = 3.6 Hz, thiophene ring proton), 7.07 (d, 2H, J = 3.6 Hz, thiophene ring proton); ^{13}C NMR (δ in $CDCl_3$) 13.07, 13.62, 26.58, 26.61, 116.66, 131.23, 135.47, 139.25; ^{29}Si NMR (δ in $CDCl_3$) -20.867; High resolution APCI/MS calculated for $C_{24}H_{38}S_2Si_2Br_2$ *m/z* = 606.04712 ([M^+]), found *m/z* = 606.04822 ([M^+]).

Synthesis of 1,2-bis(5-trimethylstannyl-2-thienyl)-1,1,2,2-tetrabutyldisilane

In a 100 mL two necked flask fitted with a dropping funnel and a reflux condenser were placed 1,2-bis(5-bromo-2-thienyl)-1,1,2,2-tetrabutyldisilane (3.60 g, 5.00 mmol) and ether (50 mL). The mixture was cooled down to -78 ^{o}C, and a 1.6M *n*-butyllithium hexane solution (6.6 mL, 10 mmol) was slowly added to the mixture over 30 min at -78 ^{o}C and the mixture was further stirred for 1 h at -78 ^{o}C. Trimethylstannyl chloride (2.05 g, 10.0 mmol) was added to the mixture at -78 ^{o}C and the mixture was stirred overnight at room temperature. After the usual work up, volatile substances were removed from the residue by pumping at 50 ^{o}C to give colorless viscous oil (3.7 g, 94% yield), which was used for the following polymerization reactions without further purification: ^{1}H NMR (δ in $CDCl_3$) 0.36 (s, 18H, $SnMe_3$), 0.89 (m, 20H, Bu), 1.31 (m, 16H, Bu), 7.25 (d, 2H, J = 3.2 Hz, thiophene ring proton), 7.27 (d, 2H, J = 3.2 Hz, thiophene ring proton); ^{13}C NMR (δ in $CDCl_3$) -8.14, 13.60, 13.67, 26.71, 26.73, 135.65, 135.87, 142.40, 142.84; ^{29}Si NMR (δ in $CDCl_3$) -21.610; High

resolution ESI/MS calculated for $C_{24}H_{56}S_2Si_2Sn_2Na$ *m/z* = 801.14546 ($[M+Na]^+$), found *m/z* = 801.14557 ($[M+Na]^+$). No impurities were detected by the spectrometric analysis.

Polymer synthesis

In a 100 mL two necked flask fitted with a reflux condenser were placed 4,7-bis(4-butyl-5-iodo-2-thienyl)-2,1,3-benzothiadiazole (0.23 g, 0.34 mmol), 1,2-bis(5-trimethylstannyl-2-thienyl)-1,1,2,2-tetrabutyldisilane (0.27 g, 0.34 mmol), $Pd_2(dba)_3$ (8 mg, 0.009 mmol), (*o*-tol)$_3$P (21 mg, 0.070 mmol), CuO (27 mg, 0.34 mmol), and DMF (30 mL), and the mixture was stirred at 80 ^oC for 5 days. After the usual work up, the residue was reprecipitated from chloroform/hexane to give **pT$_4$Bt** in 47 mg (16% yield) as red purple solids: m.p. = 83.3 ^oC; M_n = 4400; M_w/M_n = 1.7; ^1H NMR (δ in $CDCl_3$) 0.88-1.03 (m, 30H, Bu proton), 1.33-1.56 (m, 16H, Bu proton), 2.86 (4H, m, Bu proton), 7.13 (m, 2H, thiophene proton), 7.31 (m, 2H, thiophene proton), 7.76 (m, 2H, phenylene proton), 7.96 (m, 2H, thiophene proton). Polymer **pT$_4$Se** was prepared in a fashion similar to that for **pT$_4$Bt** (*vide supra*): m.p. = 100.4 ^oC; M_n = 5400; M_w/M_n = 1.4; ^1H NMR (δ in $CDCl_3$) 0.91-1.02 (m, 25H, Bu proton), 1.22-1.72 (m, 25H, Bu proton), 2.85 (m, 4H, Bu proton), 7.13 (m, 2H, thiophene proton), 7.30 (m, 2H, thiophene proton), 7.68-7.76 (m, 2H, phenylene proton), 7.85-7.89 (m, 2H, thiophene proton). Polymer **pT$_4$Py** was prepared in a similar fashion to that for **pT$_4$Bt** (*vide supra*): m.p. = 107.3 ^oC; M_n = 5500; M_w/M_n = 1.4; ^1H NMR (δ in $CDCl_3$) 0.90-1.00 (m, 20H, Bu proton), 1.38 (m, 16H, Bu proton), 7.06 (m, 2H, thiophene proton), 7.16 (m, 2H, thiophene proton), 7.31 (m, 1H, thiophene proton), 7.43 (m, 1H, thiophene proton), 7.57 (m, 1H, pyridine proton), 7.78 (m, 1H, pyridine proton), 8.78 (m, 1H, pyridine proton on C6); ^{13}C NMR (δ in $CDCl_3$) 13.66, 13.70, 26.70, 26.72, 118.35, 124.55, 124.69, 125.27, 125.41, 128.11, 128.19, 130.59, 132.80, 134.98, 135.81, 135.94, 136.77, 137.88, 138.79, 139.61, 142.12, 142.56, 142.68, 146.10, 150.87.

Estimations of polymer amount adsorbed on TiO_2 surface

Polymer-modified TiO_2 electrodes were immersed in 3 mL of THF, and were added three drops of 1 M tetrabutylammonium fluoride THF solution in dark. After 1 day, UV absorption spectra of the resulting THF solutions were compared to that of 8×10^{-3} g/L pristine polymers solution treated by tetrabutylammonium fluoride. After fluoride treatment, the electrodes turned colorless, indicating that the polymers attached on TiO_2 were completely detached.

References

13 J. Tang, S. Qu, J. Hu, W. Wu, J. Hua, *Solar Energy*, **2012**, *86*, 2306.

14 (a) P. Péchy, F. P. Rotzinger, M. K. Nazeeruddin, O. Kohle, S. M. Zakeeruddin, R. Humphry-Baker, M. Gätzel, *J. Chem. Soc., Chem. Commun.*, *1995*, 65; (b) F. Odobel, E. Blart, M. Lagrée, M. Villieras, H. Boujtita, N. E. Murr, S. Caramori, C. A. Bignozzi, *J. Mater. Chem.*, **2003**, *13*, 502.

15 (a) Z.-S. Wang, F.-Y. Li, C.-H. Huang, L. Wang, M. Wei, L.-P. Jin, N.-Q. Li, *J. Phys. Chem. B*, **2000**, *104*, 9676; (b) Y.-S. Chen, C. Li, Z.-H. Zeng, W.-B. Wang, X.-S. Wang, B.-W. Zhang, *J. Mater. Chem.*, **2005**, *15*, 1654.

16 (a) E. L. Tae, S. H. Lee, J. K. Lee, S. S. Yoo, E. J. Kang, K. B. Yoon, *J. Phys. Chem. B*, **2005**, *109*, 22513; (b) R. Mosurkal, J.-A. He, K. Yang, L. A. Samuelson, J. Kumar, *J. Photochem. Photobiol. A*, **2004**, *168*, 191; (c) B.-K. An, W. Hu, P. L. Burn, P. Meredith, *J. Phys. Chem. C*, **2010**, *114*, 17964.

17 (a) K. Kakiage, M. Yamamura, E. Fujimura, T. Kyomen, M. Unno, M. Hanaya, *Chem. Lett.*, **2010**, *39*, 260; (b) M. Unno, K. Kakiage, M. Yamamura, T. Kogure, T. Kyomen, M. Hanaya, *Appl. Organometal. Chem.*, **2010**, *24*, 247; (c) C. Baik, D. Kim, M.-S. Kang, S. O. Kang, J. Ko, M. K. Nazeeruddin, M. Grätzel, *J. Photochem. Photobiol. A*, **2009**, *201*, 168.

18 (a) J. Mao, N. He, Z. Ning, Q. Zhang, F. Guo, L. Chen, W. Wu, J. Hua, H. Tian, *Angew. Chem.*, **2012**, *124*, 10011; (b) H. He, A. Gurung, L. Si, *Chem. Commun.*, **2012**, *48*, 5910; (c) Y. Ooyama, S. Inoue, T. Nagano, K. Kushimoto, J. Ohshita, I. Imae, K. Komaguchi, Y. Harima, *Angew. Chem. Int. Ed.*, **2011**, *50*, 7429.

19 (a) Y. Ooyama, Y. Harima, *Eur. J. Org. Chem.*, **2009**, *18*, 2903; (b) A. Hagfeldt, G. Boschloo, L. Sun, L. Kloo, H. Pettersson, *Chem. Rev.*, **2010**, *110*, 6595; (c) S. Ardo, G. J. Meyer, *Chem. Soc. Rev.*, **2009**, *38*, 115.

20 R. Jose, V. Thavasi, S. Ramakrishna, *J. Am. Ceram. Soc.*, **2009**, *92*, 289.

21 J. Ohshita, K. Yoshimoto, M. Hashimoto, D. Hamamoto, A. Kunai, Y. Harima, Y. Kunugi, K. Yamashita, M. Kakimoto, M. Ishikawa, *J. Organomet. Chem.*, **2003**, *665*, 29.

22 D. Tanaka, J. Ohshita, Y. Ooyama, T. Mizumo, Y. Harima, *J. Organomet. Chem.*, **2012**, *719*, 30.

23 J. Ohshita, J. Matsukawa, M. Hara, A. Kunai, S. Kawajima, Y. Ooyama, Y. Harima, M. Kakimoto, *Chem. Lett.*, **2008**, *37*, 316.

24 T. Iwahara, S. Hayase, R. West, *Macromolecules*, **1990**, *23*, 1298.

Chapter 4

Synthesis and Optical and Photovoltaic Properties of Dithienosilole-Dithienylpyridine and Dithienosilole-Pyridine Alternate Polymers and Polymer-$B(C_6F_5)_3$ Complexes

Introduction

In Chapter 1-3, synthesis, properties, and applications to DSSCs of organosilicon polymers were discussed and it was demonstrated that the DSSC performance could be improved by the polymer design. In Chapter 4, utility of organosilicon polymers as materials for a different type of organic photovoltaic cell, bulk heterojunction (BHJ)-type polymer solar cells (PSCs), is being described.

BHJ-type PSCs receive a great deal of attention because of their advantages, such as their low production cost, potential flexibility and tunable cell color, over conventional inorganic cells. Since photo-to-current conversion of BHJ-type PSCs arises in an active layer, that is a blend film of a π-conjugated polymer and a fullerene derivative, development of efficient polymer materials is essential for BHJ-type PSCs. Photocurrent of BHJ-type PSCs is mainly dependent on light harvesting property of the polymer in active layer. Thus, low energy and broad absorption band of the polymer is required, similarly to DSSCs. Voltage of BHJ-type PSCs, whereas, correlate to the energy gap between the polymer HOMO level and the fullerene derivative LUMO level. These indicate that D-A type polymers having the low-lying HOMO level are suitable for high voltage BHJ-type PSCs.

Silicon-bridged bithiophene, particularly dithienosilole (DTS), has been often employed as a building unit for π-conjugated functional materials.[4-8] DTS exhibits enhanced conjugation due to the orbital interaction between the silicon σ-bond and the bithiophene π-system, as well as a highly planar tricyclic structure.[9] Interestingly, DTS exhibits relatively low HOMO level than that of

carbon analogue, cyclopentadithiophene, which is suitable for BHJ-type PSC and likely due to that long bond length of C-Si-C bridge reduces an antibonding interaction between C(β) and C(β') in bithiophene fragment. Recently, several D-A-type compounds and polymers containing DTS units as the donor were prepared. They were shown to interact efficiently with acceptor groups, such as benzothiadiazole,[10] thiazolothiazole[11-13] and thienopyrrolodione,[14] and their applications to high-performance BHJ-type PSCs were explored.

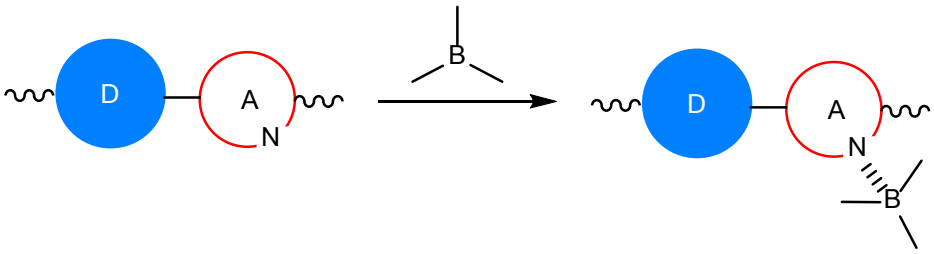

Scheme 1. Complex formation of D–A-type polymers with borane.

Recently, Bazan and coworkers found that a DTS-benzothiadiazole oligomer formed a complex with $B(C_6F_5)_3$ through N-B coordination to enhance the D-A interaction in the backbone, which shifted the absorption band significantly to a lower-energy region (Scheme 1).[15] Similar studies concerning complex formation with dithienocyclopentadiene–benzothiadiazole and dithieno-cyclopentadiene-pyridinothiadiazole oligomers and polymers have also been conducted.[16] Hayashi *et al.*[17,18] demonstrated formation of similar complex polymers as insoluble solid films from two routes, treatment of fluorine- and bithiophene-pyridine polymer films with BF_3-OEt_2 and oxidative electro-polymerization of a dithienylpyridine-BF_3 complex.

However, there have been no reports concerning the photovoltaic applications of such N-B complex polymers, despite the fact that complex formation can enhance the D-A interaction thus resulting in broad, red-shifted absorption peaks. To explore these photovoltaic applications, we prepared new soluble DTS-pyridine alternate polymers, with the hypothesis that the high Lewis

basicity of pyridine would induce a strong interaction between the polymers and $B(C_6F_5)_3$ molecules, thereby permitting the author to study applications of these complex polymers to BHJ-type PSCs. The author also examined the attachment of polymer to the TiO_2 surface due to the coordinative interaction between the polymer pyridine units and the Lewis acid sites of TiO_2, and the author subsequently used the resulting polymer-attached TiO_2 material in DSSCs.

Results and discussion

Polymer synthesis

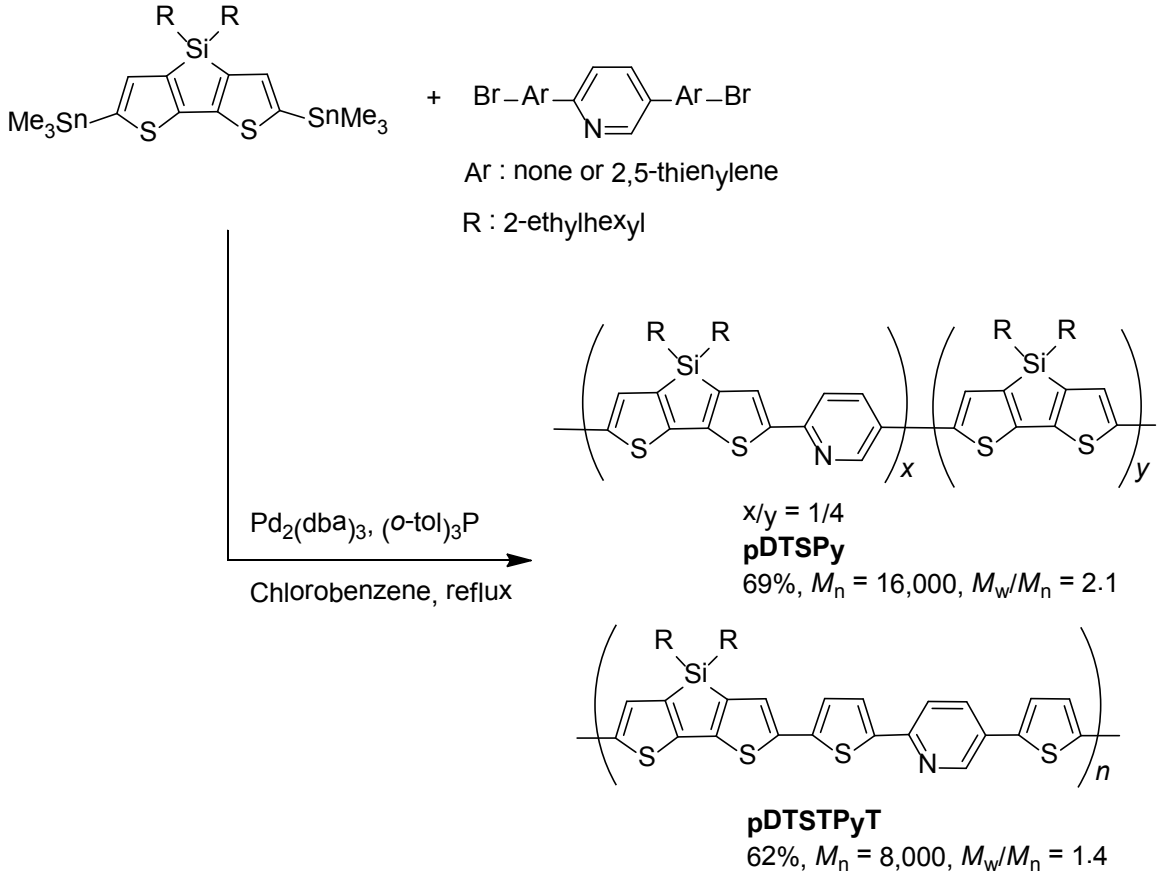

Scheme 2. Synthesis of DTS–pyridine polymers with yields and molecular weights following reprecipitation. Molecular weights were determined by GPC, relative to polystyrene standards.

Two D-A-type polymers with alternate dithienyldithienosilole-pyridine and DTS-pyridine units (**pDTSTPyT** and **pDTSPy**) were prepared via Stille coupling reactions, as shown in Scheme 2, and were subsequently purified by reprecipitation, followed by Soxhlet extraction, as red-purple and dark red solids. These purified polymers were soluble in chloroform, tetrahydrofuran and toluene but insoluble in hexane, methanol and ethanol. The ^{1}H NMR spectra of the polymers revealed broad peaks. The integration ratio of the ^{1}H signals of **pDTSTPyT** was consistent with the regular

structure shown in Scheme 2; however, **pDTSPy** possessed smaller integration ratios for the pyridine proton signals at 7.64, 7.84 and 8.84 ppm. than the theoretical ratios for the regularly arranged alternate DTS-pyridine structure, suggesting that homo-coupling of DTS units had occurred to some extent during polymerization. Similarly, competition between the homo-coupling of distannyl compounds and Stille cross-coupling has been previously reported.[21] The incorporation ratio of the homo-coupled units (DTS-DTS) was determined to be approximately x/y=4/1 (Scheme 2). The ^{1}H NMR spectrum of **pDTSPy** also possessed small signals at 8.00, 8.45 and 8.97 ppm., which were assigned to the terminal bromopyridyl groups. The molecular weight was determined to be 10 kDa based on the NMR integration of the terminal pyridine protons, which is comparable with the M_n determined by GPC relative to polystyrene standards. One might consider the possibility of preparing polymers using reverse-type coupling reactions of bis(stannyl)pyridine and dibromodithienosilole. However, it has already been reported that a similar reaction of mono(stannyl)pyridine with dibromodithienosilole provided the expected 2:1 coupling product, but only in low yield (12%).[6] Polymeric **pDTSPy** exhibited a monomodal GPC profile, whereas a bimodal distribution with peaks at M_n = 10,000 and 63,000 with an area ratio of ca. 10:1 was observed for **pDTSTPyT**; however, the reason for the bimodal profile is still unclear.

Optical properties

The prepared polymers possessed UV-Vis absorption maxima at approximately 520 nm in benzene, as shown in Figure 1 and Table 1. The absorption maxima were blue-shifted from those reported for DTS homopolymers (**pDTS**, λ_{max} = 533-561 nm),[22,23] DTS-bithiophene alternate polymers (**pDTS2T**, 544-558 nm)[22,23] and a DTS-pyridinothiadiazole alternate polymer (**pDTSPTA**, 732 nm)[20] (Scheme 3). The introduction of pyridine units into **pDTS2T** and **pDTS** appeared to hinder the planarity of the resulting π-conjugated systems due to steric repulsion between the C–H

bonds of the adjacent thiophene and pyridine rings. It is also likely that pyridine is less electron deficient than pyridinothiadiazole, and thus, it exhibited weaker D-A interactions with the dithienyl-DTS and DTS units in the polymers studied here. For the spin-coated films of **pDTSTPyT** and **pDTSPy**, shoulder peaks appeared at approximately 560 nm, as seen in Figure 1. This result is most likely due to stacking of the π-conjugated polymer chains, which indicates that there is an interchain interaction in the films, although the absorption maxima were affected slightly by the polymer state (that is, solution or film). Strong interchain interactions are important factors for BHJ-type PSC materials, because they accelerate carrier transport in the films.

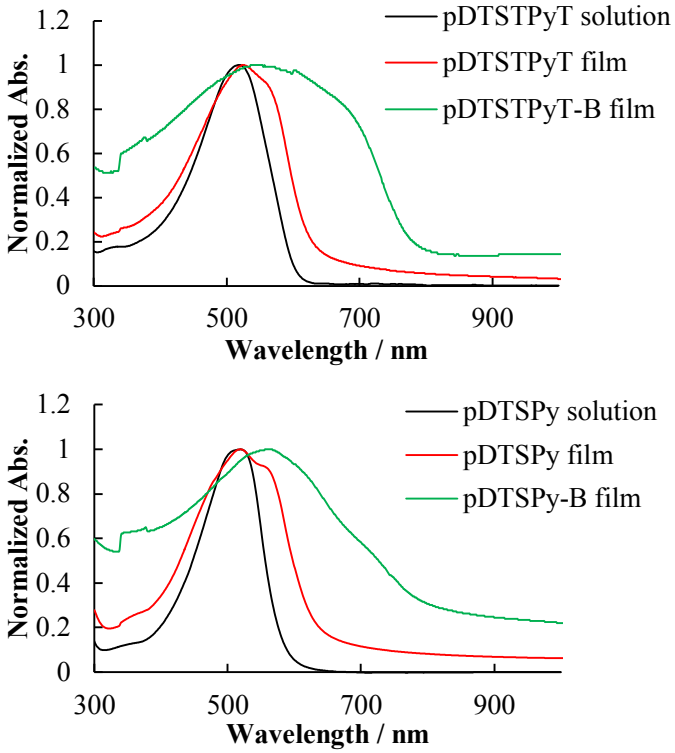

Figure 1. UV-vis absorption spectra of **pDTSTPyT** (top) and **pDTSPy** (bottom).

Table 1. Preparation and properties of DTS–pyridine-based polymers.

	UV-vis λ_{max} / nm	
Polymer	In benzene	As spin-coated film
pDTSTPyT	519	524, 564 (sh)[a]
pDTSPy	520	519, 558 (sh)[a]
pDTSTPyT-B	534, 666 (sh)[a]	546, 672 (sh)[a]
pDTSPy-B	564	559

[a]Shoulder.

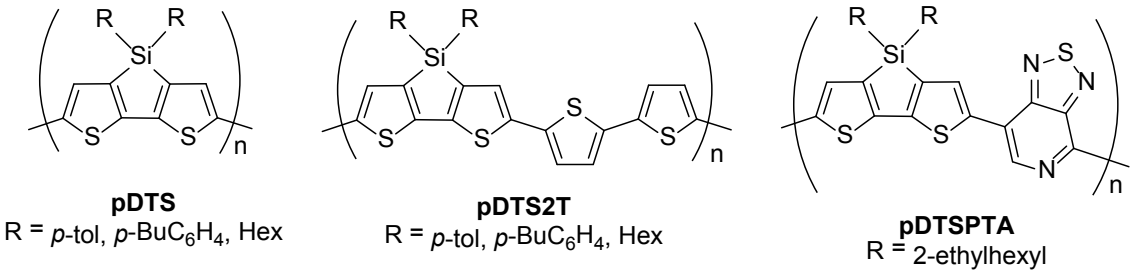

Scheme 3. DTS-containing conjugated polymers (refs 21–23)

Complex formation with $B(C_6F_5)_3$

Complex formation between the polymers and $B(C_6F_5)_3$ was monitored by UV-Vis absorption spectrophotometry, as shown in Figure 2. As $B(C_6F_5)_3$ was added to the solutions of **pDTSTPyT** and **pDTSPy** in benzene, the solution changed color from red to purple. Simultaneously, the absorbance of the UV-Vis bands of the parent polymers decreased, and new bands appeared at longer wavelengths, which became more intense with increasing concentration of $B(C_6F_5)_3$. This result is in good agreement with the previously reported[15–18] optical properties of similar complexes of pyridine-containing polymers with borane, and it clearly indicates that complex formation reduces

the polymer band gap, thereby potentially allowing for fine tuning of the electronic states. However, the changes were not completely saturated when one equivalent of $B(C_6F_5)_3$ was added, thus indicating that the coordinated and non-coordinated units were in equilibrium.

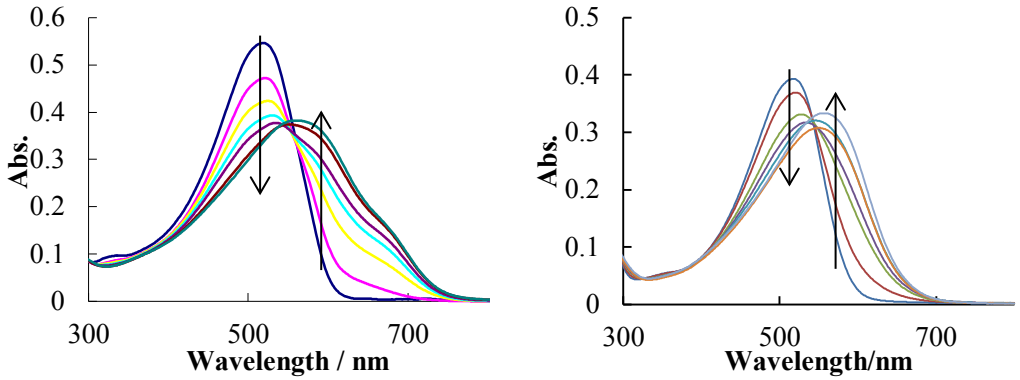

Figure 2. UV–Vis absorption spectra of polymers at (polymer) = 8 × 10^{-3} gL^{-1} in benzene for **pDTSTPyT** with $(B(C_6F_5)_3)$/(pyridine) = 0, 0.25, 0.5, 0.75, 1.0, 2.0, 3.0 (left) and **pDTSPy** with $(B(C_6F_5)_3)$/(pyridine) = 0, 0.15, 0.30, 0.45, 1.2, 1.8 (right).

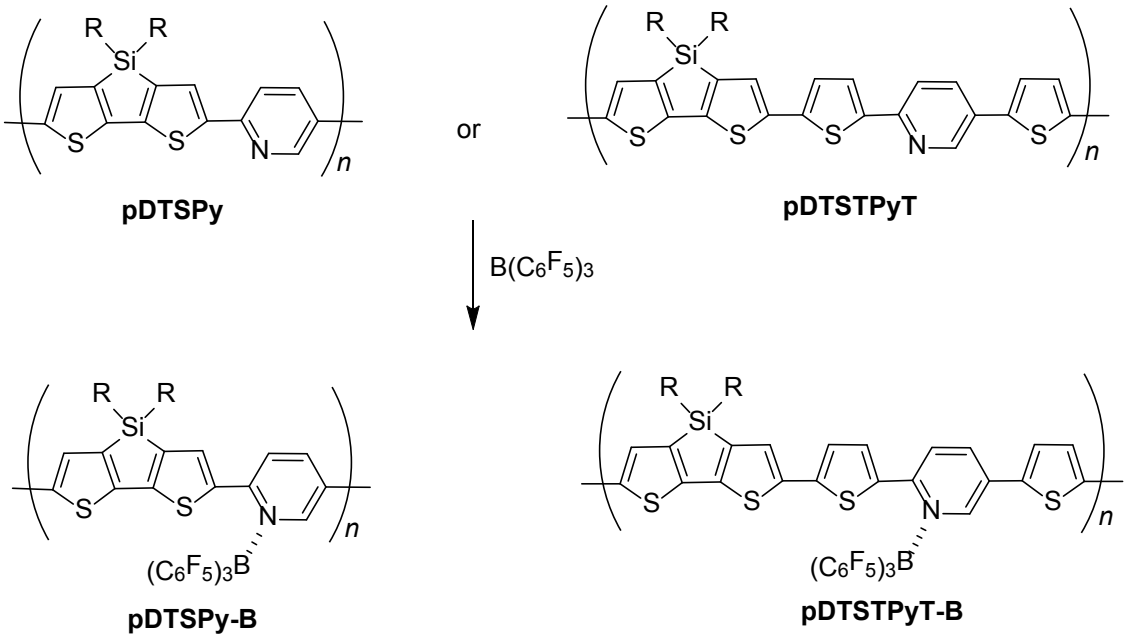

Scheme 4. Formation of the complex polymers.

To obtain more information about complex formation, **pDTSTPyT** was treated with $B(C_6F_5)_3$ (1.0 equiv for pyridine unit) on a preparative scale in chlorobenzene at room temperature. A similar experiment was also carried out for **pDTSPy** with a smaller ratio of $B(C_6F_5)_3$ (0.63 equiv), because **pDTSPy** had a more sensitive response than **pDTSTPyT** to $B(C_6F_5)_3$. At this loading ratio, **pDTSPy** was expected to exhibit a similar UV spectral profile to **pDTSTPyT**:$B(C_6F_5)_3$ = 1:1 (Figure 2). After the solvent had evaporated from the mixtures, the residues were analyzed by NMR and IR spectroscopies and were identified as being complex polymers **pDTSTPyT-B** and **pDTSPy-B** (Scheme 4). In the ^{1}H NMR spectra, the pyridine proton signals disappeared and decreased at 8.83 and 8.84 ppm for the **pDTSTPyT** and **pDTSPy** polymers, respectively. However, new broad signals attributable to the α-protons of the pyridine-boron complexes of **pDTSTPyT-B** and **pDTSPy-B** appeared at 8.28-8.51 and 8.33-8.50 ppm, respectively. For **pDTSPy-B**, signals ascribed to complex-free units were also observed in the ^{1}H NMR spectrum. However, the signals were too broad to determine the exact incorporation ratio of the complex units. The ^{11}B NMR spectra revealed signals at -4.06 and -4.00 ppm for **pDTSTPyT-B** and **pDTSPy-B**, respectively, which were high-field shifted relative to the complex-free $B(C_6F_5)_3$ signal. IR analysis also supports complex formation due to the characteristic N-B vibration signals at 1083 and 1085cm^{-1} for **pDTSTPyT-B** and **pDTSPy-B**, respectively.[24] The author also examined titration experiments of a 2,2':5',2''-terthiophene solution in benzene upon addition of $B(C_6F_5)_3$ via the UV-Vis absorption. However, no obvious spectral changes were found, thus indicating that the DTS units of the polymers in this study are not the coordination sites.

Upon spin-coating, the complex polymers **pDTSTPyT-B** and **pDTSPy-B** readily formed thin solid films for which the UV-Vis absorption spectra are presented in Figure 1. Although the absorption maxima were not significantly shifted from those of the corresponding complex-free parent polymers, the spectra exhibited broad bands with highly red-shifted absorption edges. The

ionization potentials that corresponded approximately to the HOMO (highest occupied molecular orbital) levels were measured in air for films of **pDTSPy** and **pDTSPy-B** via photoelectron yield spectroscopy to be -5.23 and -5.44 eV, respectively, which again indicates that complex formation decreased the HOMO levels. The LUMO (lowest unoccupied molecular orbital) energy levels of these films were then calculated to be -3.26 and -3.79 eV based on the ionization potentials and the optical band gaps of these films. These results are in good agreement with the electronic states of PEDOT:PSS (HOMO: -5.0 eV) and $PC_{71}BM$ (HOMO: -6.0 eV, LUMO: -4.3 eV).

Applications to OPV

To explore the utility of the polymers used in this study and their complexes as host materials for BHJ-type PSCs, cells were fabricated based on blend films of the polymers and $PC_{71}BM$ (ITO/PEDOT:PSS/polymer:$PC_{71}BM$ (1:2.0 wt)/LiF/Al), with an active area of 0.25 cm^2. The current density-voltage (*J-V*) curves and the incident photon-to-current conversion efficiency (IPCE) spectra of the cells are depicted in Figure 3, and the cell parameters are summarized in Table 2. The IPCE spectra are in agreement with the UV-vis absorption spectra of the polymer blend films and the polymer complexes with $PC_{71}BM$, although the IPCE edges of the cells with complex polymers were at approximately 750 nm, slightly shorter than the optical edges of the blend films (800 nm). The cell with **pDTSPy** exhibited a lower power-conversion efficiency (PCE) than the cell based on **pDTSTPyT** due to a lower open circuit voltage (V_{oc}). Although the reason for the different V_{oc} between these cells is still unclear, the lower degree of incorporation of pyridine units in **pDTSPy** seems to affect the V_{oc} to some extent. Interestingly, the use of complex polymeric **pDTSTPyT-B** and **pDTSPy-B** increased V_{oc}, although the close circuit current density (J_{sc}) was largely suppressed to lower the PCE. In the present study, the author found that annealing the active layers and the devices did not affect subsequent cell performance.

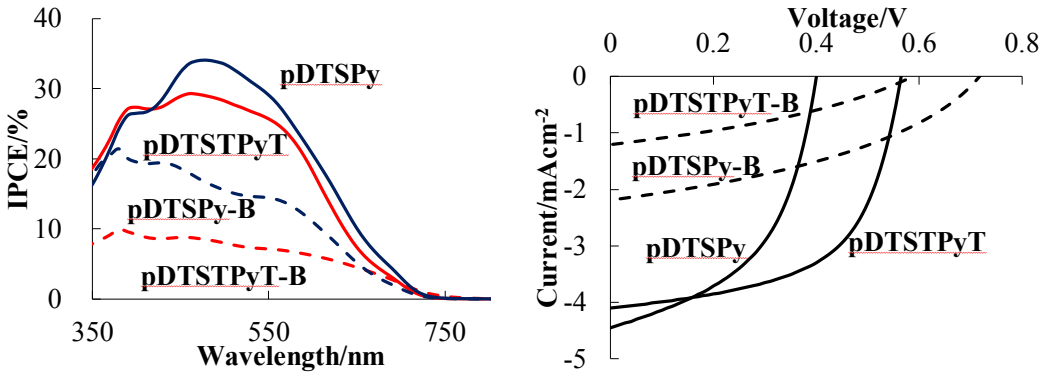

Figure 3. IPCE spectra (left) and IPCE *J-V* curves (right) of BHJ-type PSCs based on the DTS–pyridine polymers and their complexes.

Pyridine-containing D-A-type compounds have been recently studied as sensitizing dyes for DSSC.[25] In this case, pyridine functions not only as an acceptor unit but also as an anchoring unit that can coordinate with Lewis acid sites of TiO_2 to attach the dye to the TiO_2 surface; this pyridine-Ti anchor is known to facilitate electron injection from the photo-excited dye, compared with the conventional ester anchor. Based on this property, the author applied the **pDTSTPyT** and **pDTSPy** polymers to DSSC. TiO_2 electrodes were immersed in solutions of polymer in chloroform at room temperature to give polymer-attached TiO_2; DSSCs were fabricated with an FTO/polymer-attached TiO_2/LiI:I_2 in acetonitrile/Pt structure. As shown in Table 2 and Figure 4, the DSSCs formed using these polymers exhibited a clear response, with PCEs of 0.55% and 0.54% for the cells containing **pDTSTPyT** and **pDTSPy**, respectively.

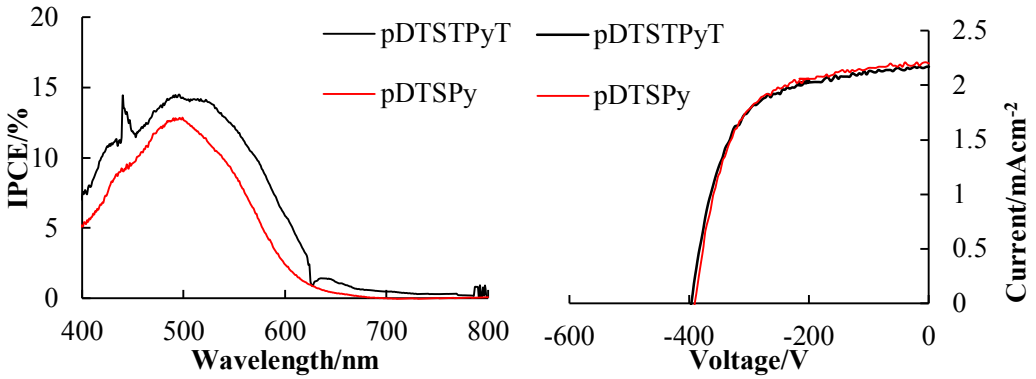

Figure 4. IPCE spectra (left) and *J-V* curves (right) of DSSCs based on the DTS–pyridine polymers.

Table 2. Photovoltaic properties of DTS–pyridine-based polymers

OPV	Polymer	J_{sc} / mAcm^{-2}	V_{oc} / V	FF	PCE / %
BHJ-PSC	**pDTSTPyT**	4.07	0.56	0.58	1.33
	pDTSTPyT-B	1.21	0.59	0.35	0.25
	pDTSPy	4.28	0.39	0.50	0.83
	pDTSPy-B	2.21	0.71	0.39	0.61
DSSC	**pDTSTPyT**	2.03	0.39	0.69	0.55
	pDTSPy	2.17	0.40	0.63	0.54

Conclusions

In conclusion, the author prepared new D-A-type polymers using dithienylDTS and DTS as the donors and pyridine as the acceptor. Although these polymers exhibited limited π-conjugation, likely due to their twisted structures and to the rather weak D-A interaction, potential applications of these polymers to BHJ-type PSCs and DSSCs were also explored. Interestingly, complex formation upon $B(C_6F_5)_3$ coordination enhanced the D-A interaction of the polymers. Furthermore, complex formation led to a higher V_{oc} of the BHJ-type PSCs compared with that of either **pDTSTPyT**- or **pDTSPy**-based PSCs. The present cells with complex polymers exhibited relatively low PCE, which was ascribed to the low J_{sc}, because the maximal PCE based on DTS-polymers was reported to be 7.3% for a DTS-thienopyrrolodione alternate polymer.[14] The increase in V_{oc} caused by complex formation provides useful information for the molecular design of efficient PSC materials.

Experimental

General

All reactions were carried out under dry argon. Chlorobenzene, which was used as the reaction solvent, was distilled from CaH_2 and stored over activated molecular sieves until use. The monomers, 2,6-bis(trimethylstannyl)-4,4-bis(2-ethylhexyl)dithienosilole[10] and 2,5-bis(5-bromo-2-thienyl)pyridine,[19] were prepared as reported in the literature. Fabrication and evaluation of DSSCs were carried out in a fashion similar to Chapter 1.

Measurements

^1H and ^{13}C NMR spectra were recorded on Varian System500 and MR400 spectrometers. UV spectra were measured on a Hitachi U-3210 spectrophotometer. GPC was carried out at ambient temperature using serially connected Shodex KF2001 and KF2002 columns with THF as the eluent.

Synthesis of DTS-pyridine alternate polymers

A mixture of 2,6-bis(trimethylstannyl)-4,4-bis(2-ethylhexyl)dithienosilole (0.39 g, 0.52 mmol), 2,5-bis(5-bromo-2-thienyl)pyridine (0.21 g, 0.52 mmol), $Pd_2(dba)_3$ (10 mg, 0.010 mmol), (*o*-tolyl)$_3$P (25 mg, 0.083 mmol) and chlorobenzene (30 mL) was placed in a 50 mL two-necked flask fitted with a reflux condenser, and the mixture was heated under reflux for 5 days (Scheme 2). The resulting mixture was allowed to cool to room temperature, and a 30 mL aqueous solution of sodium N,N-diethyldithiocarbamate trihydrate (3.1 g) was added; the mixture was then heated to 80 ^oC for 2 h. The organic layer was separated and washed in the following order: first water, followed by 3 vol% acetic acid aqueous solution, and finally water again. The organic layer was dried over anhydrous magnesium sulfate, and the solvent was removed under vacuum. Reprecipitation of the residue from chloroform/methanol gave polymeric substances, which were then placed in a Soxhlet

apparatus and washed with, in the following order: hot methanol, ethanol and hexane. Finally, the residue, which had remained insoluble in those hot solvents, was extracted using hot chloroform. The chloroform solution was then poured into hexane, and the precipitates were collected to provide **pDTSTPyT** (0.21 g, 62%) as red-purple solids: m.p. < 300 ^{o}C; M_n = 11,000, M_w/M_n = 2.1; ^{1}H NMR (δ in $CDCl_3$) 0.79-1.48 (br m, 34H, 2-ethylhexyl), 6.79-7.83 (br m, 8H, aromatic ring proton), 8.83 (br s, 1H, pyridylene proton on C6); ^{13}C NMR (δ in $CDCl_3$) 10.83, 14.29, 17.55, 23.01, 28.85, 35.16, 35.82. Sp^2 carbons could not be observed, likely due to signal broadening.

Polymer **pDTSPy** was synthesized as dark red solids using the Stille coupling reaction following a procedure similar to that described above for **pDTSTPyT**. Data for **pDTSPy**: 69% yield; m.p. < 300 ^{o}C; M_n = 16,000, M_w/M_n = 2.1; ^{1}H NMR (δ in $CDCl_3$) 0.83-1.51 (br m, 34H, 2-ethylhexyl), 7.14 (br s, 0.4H, homo-coupled DTS proton), 7.37 (br s, 0.8H, DTS proton), 7.59 (br s, 0.8H, DTS proton), 7.64 (br s, 0.8H, pyridylene proton), 7.84 (br s, 0.8H, pyridylene proton), 8.00 (br s, 0.1H, terminal Br-pyridyl proton), 8.45 (br s, 0.1H, terminal Br-pyridyl proton), 8.84 (br s, 0.8H, pyridylene proton on C6), 8.97 (br s, 0.1H, terminal Br-pyridyl proton on C6); ^{13}C NMR (δ in $CDCl_3$) 10.84, 14.18, 17.61, 17.65, 23.02, 28.89, 35.63, 35.65, 35.92. Sp^2 carbons could not be observed, likely due to signal broadening.

Preparation of polymer-borane complex

To a solution of 43mg of **pDTSTPyT** in 25 mL of chlorobenzene, a solution of 34 mg (1.0 equiv for pyridine unit) of tris(pentafluorophenyl)borane in 4 mL of chlorobenzene was added at room temperature (Scheme 4). The mixture was stirred for 1 day at room temperature, and the solvent was removed under vacuum to give **pDTSTPyT-B** as blue-purple solids: m.p. < 300 ^{o}C; ^{1}H NMR (δ in $CDCl_3$) 0.79-1.48 (br m, 34H, 2-ethylhexyl), 6.67-7.20 (br m, 3H, aromatic ring proton), 7.33-8.02 (br m, 5H, aromatic ring proton), 8.28-8.51 (br m, 1H, aromatic ring proton); ^{11}B NMR (δ

in C_6D_6) -4.06.

Polymer-borane complex **pDTSPy-B** was prepared by treating **pDTSPy** with tris(penta-fluorophenyl)borane (0.63 equiv for pyridine unit) and appeared as a purple solid, following a procedure similar to that described above for **pDTSTPyT-B**. In this experiment, a polymer containing non-coordinated pyridine units was obtained. Data for **pDTSPy-B**: m.p. < 300 ^{o}C; ^{1}H NMR (δ in $CDCl_3$) 0.71-1.56 (br m, 34H, 2-ethylhexyl), 7.42-7.52 (br m, 0.8H, DTS proton), 7.58-7.69 (br m, 0.4H, aromatic ring proton), 7.78-7.93 (br m, 0.8H, aromatic ring proton), 8.05-8.12 (br m, 0.8H, aromatic ring proton), 8.17-8.25 (br m, 0.8H, aromatic ring proton), 8.33-8.50 (br m, 0.8H, aromatic ring proton), 8.87 (br s, 0.18H, boron-free pyridylene proton on C6), 8.95 (br s, 0.02H, boron-free terminal Br-pyridyl proton on C6); the integrations could not be determined exactly due to signal broadening, and thus, approximate values are provided here; ^{11}B NMR (δ in C_6D_6) -4.00.

Fabrication of PSCs

Tin-doped indium oxide (ITO)-coated glass substrates were cleaned using a routine cleaning procedure, which included sonication in, in this order, detergent, distilled water, acetone and 2-propanol.[20] The ITO surface was cleaned further by exposure to ozone for 10min, and a layer of PEDOT:PSS with a thickness of 30 nm was spin-coated onto the cleaned ITO substrate immediately thereafter. The PEDOT:PSS-coated ITO substrate was heated at 150 ^{o}C for 10 min, onto which a solution of the polymer:$PC_{71}BM$ blend in *o*-dichlorobenzene containing diiodooctane (2.5 vol%) was spincoated after filtering through a 0.45-μm polytetrafluoroethylene syringe filter. Device fabrication was completed by depositing a LiF (0.5 nm) and Al (80 nm) cathode as the top electrode onto the polymer layer at 10^{-6} torr. After annealing of the PEDOT:PSS, all the handling was performed in a glove box equipped with a vacuum-deposition apparatus, and the devices were

evaluated in an inert atmosphere as follows.

The current density-voltage (*J-V*) characteristics of the PSCs were investigated under illumination with a 100mWcm^{-2} (AM 1.5 G) simulated solar light from a Peccell PEC-L11 solar simulator (Peccell Tecnologies, Inc., Kanagawa, Japan). The data were recorded with a Keithley 2400 source-measure unit (Keithley Instruments Inc., Cleveland, OH, USA). The incident photon-to-current conversion efficiency (IPCE) was measured as a function of wavelength from 300-900 nm with a halogen lamp as the light source, and calibration was performed with a silicon reference photodiode. The thickness of the thin film was measured with a Veeco Dektak 8 surface profilometer, with an accuracy of ±5nm.

References

1 C. J. Brabec, S. Gowrisanker, J. J. M. Halls, D. Laird, S. Jia, S. P. Williams, *Adv. Mater.*, **2012**, *22*, 3839.

2 J. Chen, Y. Cao, *Acc. Chem. Res.*, **2009**, *42*, 1709.

3 Y. Ooyama, Y. Harima, *Eur. J. Org. Chem.*, **2009**, 2903.

4 J. Chen, Y. Cao, *Macromol. Rapid Commun.*, **2007**, *28*, 1714.

5 J. Ohshita, *Macrmol. Chem. Phys.*, **2009**, *210*, 1360.

6 J. Ohshita, H. Kai, A. Takata, T. Iida, A. Kunai, N. Ohta, K. Komaguchi, M. Shiotani, A. Adachi, K. Sakamaki, K. Okita, *Organometallics*, **2001**, *20*, 4800.

7 D. -H. Kim, J. Ohshita, K. -H. Lee, Y. Kunugi, A. Kunai, *Organometallics*, **2006**, *25*, 1511.

8 W. Zeng, Y. Cao, Y. Bai, Y. Wang, Y. Shi, M. Zhang, F. Wang, C. Pan, C. Wang, *Chem. Mater.*, **2010**, *22*, 1915.

9 J. Ohshita, M. Nodono, H. Kai, T. Watanabe, A. Kunai, K. Komaguchi, A. Shiotani, K. Okita, Y. Harima, K. Yamashita, M. Ishikawa, *Organometallics*, **1999**, *18*, 1453.

10 J. Hou, H.-Y. Chen, S. Zhang, G. Li, Y. Yang, *J. Am. Chem. Soc.*, **2008**, *130*, 16144.

11 J. Peet, L. Wen, P. Byrne, S. Rodman, K. Forberich, Y. Shao, N. Drolet, R. Gaudiana, *Appl. Phys. Lett.*, **2011**, *98*, 043301.

12 S. Subramaniyan, H. Xin, F. S. Kim, S. Shoaee, J. R. Durrant, S. A. Jenekhe, *Adv. Energy Mater.*, **2011**, *1*, 854.

13 S. Subramaniyan, H. Xin, F. S. Kim, S. A. Jenekhe, *Macromolecules*, **2011**, *44*, 6245.

14 T.-Y. Chu, J. Lu, S. Beaupre, Y. Zhang, J.-R. Pouliot, S. Wakim, J. Zhou, M. Leclerc, Z. Li, J. Ding, Y. Tao, *J. Am. Chem. Soc.*, **2011**, *133*, 4250.

15 G. C. Welch, R. Coffin, J. Peet, G. C. Bazan, *J. Am. Chem. Soc.*, **2009**, *131*, 10802.

16 G. C. Welch, G. C. Bazan, *J. Am. Chem. Soc.*, **2011**, *133*, 4632.

17 S. Hayashi, A. Asano, T. Koizumi, *Polym. Chem.*, **2011**, *2*, 2764.

18 S, Hayashi, T. Koizumi, *Chem. Lett.*, **2012**, *41*, 979.

19 M. S. Khan, M. R. A. Al-Mandhary, M. K. Al-Suti, N. Feeder, S. Nahar, A. Köhler, R. H. Friend, P. J. Wilson, P. R. Raithby, *J. Chem. Soc. Dalton Trans.*, **2002**, 2441.

20 J. Ohshita, M. Miyazaki, F.-B. Zhang, D. Tanaka, M. Morihara, *Polymer J.*, **2013**, *45*, 979.

21 J. Ohshita, S. Kangai, H. Yoshida, A. Kunai, S. Kajiwara, Y. Ooyama, Y. Harima, *J. Organomet. Chem.*, **2007**, *692*, 801.

22 J. Ohshita, K. Kimura, K.-H. Lee, A. Kunai, Y.-W. Kwak, E.-C. Son, Y. Kunugi, *J. Polym. Sci. Part A, Polym. Chem.*, **2007**, *45*, 4588.

23 G. Lu, H. Usta, C. Risko, L. Wang, A. Facchetti, M. A. Ratner, T. J. Marks, *J. Am. Chem. Soc.*, **2008**, *130*, 7670.

24 N. Farfa´n, R. Contreras, *J. Chem. Soc. Perkin Trans. II*, **1987**, 771.

25 Y. Ooyama, T. Nagano, S. Inoue, I. Imae, K. Komaguchi, J. Ohshita, Y. Harima, *Chem. Eur. J.*, **2011**, *17*, 14837.

Chapter 5

Synthesis, Optical Properties, and Crystal Structure of Dithienostannole

Introduction

Heteroatom-bridged 2,2′-bithiophene derivatives have been extensively studied as functional materials, in which the highly planar tricyclic structure enhances π-conjugation.[1] In addition, electronic effects of the bridging heteroatom often provide the desirable manipulation of the bithiophene electronic state. Of those, group 14 dithienometalloles, dithienosilole (DTS)[2] is of particular interest, because of their unique electronic states (Chapter 4). In-phase interactions between the metal σ*- and bithiophene π*-orbitals lower the LUMO energy level to minimize the HOMO-LUMO energy gap.[2a,3a,4] Dithienogermole (DTG) has been also studied. Currently, DTS and DTG are widely used as the building units of functional π-conjugated polymers and oligomers that can be applied to the active materials of organic transistors[5] and photovoltaic cells.[3,6] Highly photo- and electroluminescent DTS compounds have also been developed to date.[7]

On the other hand, much less is known about tin-bridged bithiophene, namely dithienostannole (DTSn). Saito and coworkers have reported the synthesis of tin-bridged 3,3′-bithiophenes (Chart 1a).[8] For 2,2′-bithiophene derivatives, however, there has been only one report by Shimizu *et al.*[9] They prepared di(benzo[b]thieno)-1,1-dimethylstannole (Chart 1b) and demonstrated its potential utility as a starting material for polyannulated bithiophene derivatives, but no detailed properties of this DTSn were provided. In this chapter, the author describes the synthesis, optical properties, and crystal structures of two new DTSn compounds, 1,1-diphenyl-3,6-bis(trimethylsilyl)dithienostannole (**DTSn1**) and di(benzo[b]-thieno)-1,1-diphenylstannole (**DTSn2**) that exhibit σ*–π* conjugation, similarly to DTS and DTG. Crystallization-enhanced emission of **DTSn1** is also described.

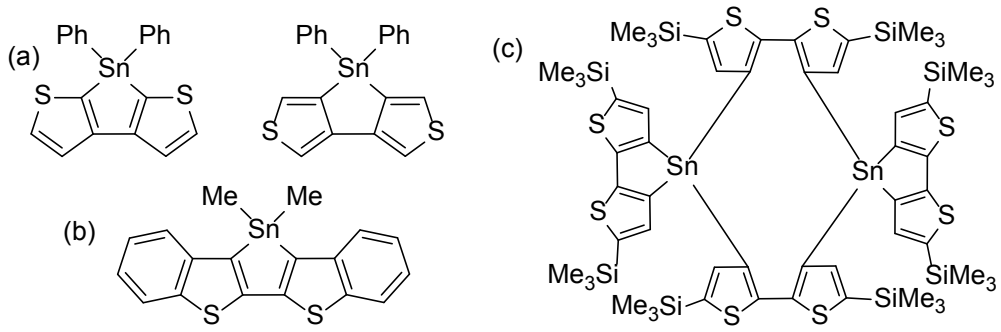

Chart 1. Dithienostannoles reported by Saito *et al* (a) (see reference 8), by Shimizu *et al* (b) (see reference 9), and by Ohshita *et al* (c) (see reference 10).

Results and discussion

Synthesis and stability of DTSn

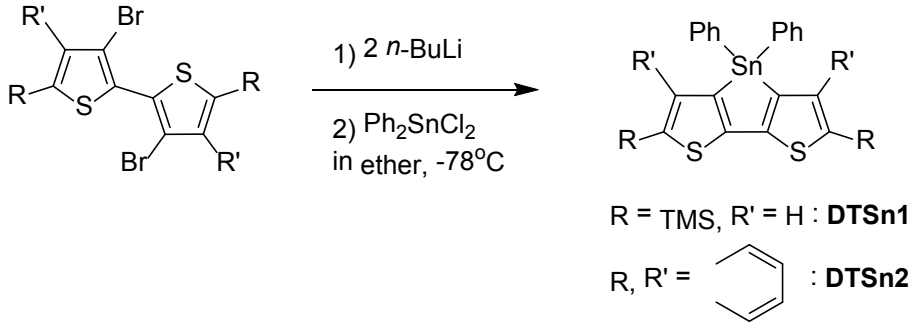

Scheme 1. Synthesis of **DTSn1** and **DTSn2**.

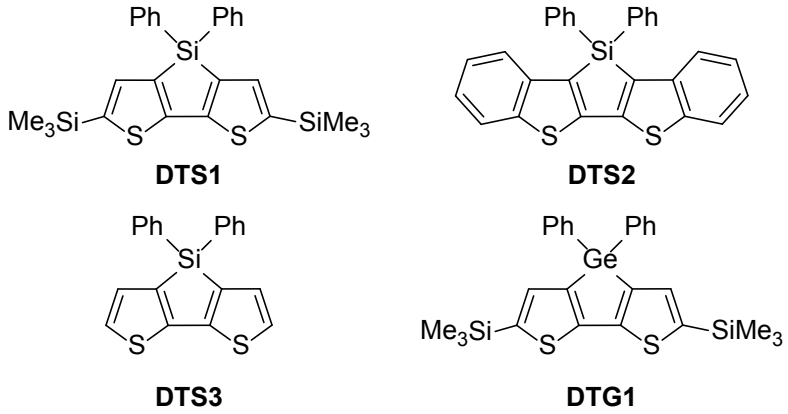

Chart 2. DTS and DTG derivatives.

Reactions of dichlorodiphenylstannane with 3,3′-dilithio-5,5′-bis(trimethylsilyl)-2,2′-bithiophene and 3,3′-dilithio-2,2′-bi-(benzo[b]thiophene) gave dithienostannoles **DTSn1** and **DTSn2**, respectively, as light yellow solids (Scheme 1). Ohshita *et. al.* recently demonstrated that spirobi-(dithienostannole) was thermally less stable than the dimer based on the DFT calculations, likely due to the ring strain of the spirobi(dithienostannole) system.[10] In fact, the attempted preparation of tetrakis(trimethylsilyl)spirobi(dithienostannole) by a 2:1 reaction of bis(trimethylsilyl)dilithio-bithiophene and tin tetrachloride provided no spiro compound but gave its macrocyclic dimer arising

from 4:2 coupling (Chart 1c), in contrast to similar reactions with silicon and germanium tetrachloride, which gave the corresponding spiro-condensed DTS and DTG derivatives in good yields. However, the present reaction proceeded cleanly to give **DTSn1** and **DTSn2** in 64% and 57% yields, respectively. They are stable enough to be handled without special care under ambient conditions. The author carried out DSC (differential scanning calorimetry) of **DTSn1** and **DTSn2** to investigate their thermal properties. They showed irreversible DSC profiles, and no evident peaks were observed in the cooling process after melting (Figure 1), indicative of the formation of the stable amorphous phase of **DTSn1** upon cooling. That no decomposition had occurred by melting **DTSn1** was confirmed by the UV-vis absorption spectrum of the sample after a cycle from room temperature to 160 °C (Figure 2). In contrast, the absorption spectrum of **DTSn2** once melted revealed a new broad band approximately at 540 nm, together with a major band ascribed to the original sample, indicating that **DTSn2** had undergone partial decomposition upon melting (Figure 3), although no DSC peaks were found up to the melting point.

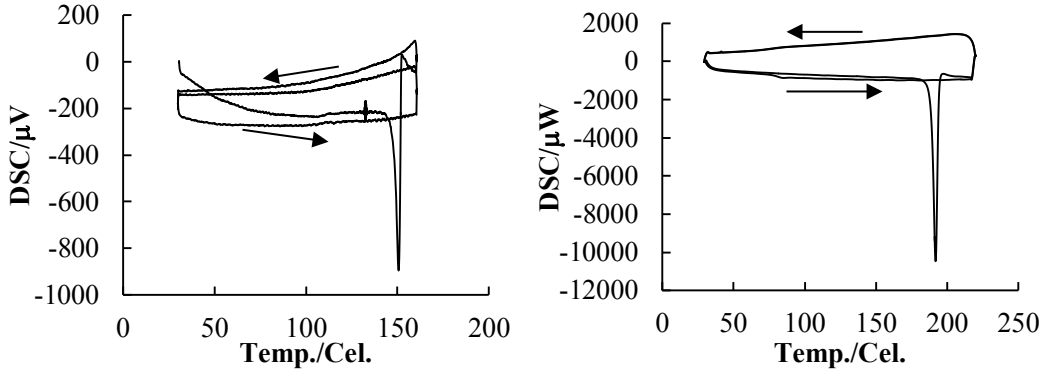

Figure 1. DSC curves of **DTSn1** (left) and **DTSn2** (right).

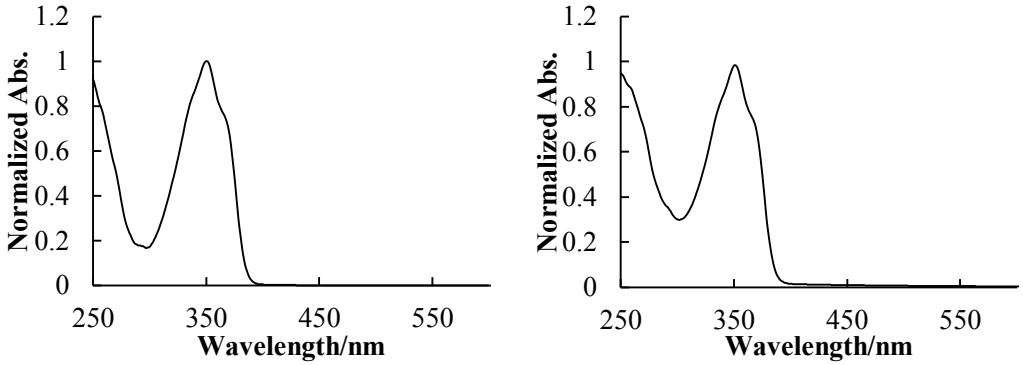

Figure 2. UV-vis absorption spectra of **DTSn1** in THF, before (left) and after (right) melting.

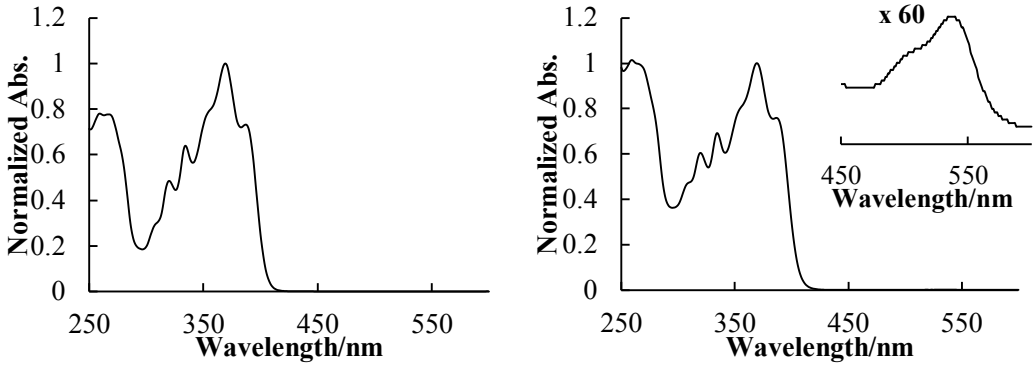

Figure 3. UV-vis absorption spectra of **DTSn2** in THF, before (top) and after (bottom) melting.

Optical properties and DFT calculations of DTSn

The optical properties of **DTSn1** and **DTSn2** were first examined in solution with respect to the UV absorption and photoluminescence (PL) spectra, and the data are summarized in Table 1. The absorption maximum of **DTSn1** in THF appeared at 350 nm (Figure 4), which was slightly blue-shifted from that of **DTS1** (λ_{max} 356 nm)[4] and nearly the same as that of **DTG1** (λ_{max} 350 nm),[10] reported previously (Chart 2), indicating the similarity of the electronic states of these group 14 dithienometalloles, regardless of the bridging element (i.e., metal = Si, Ge, Sn). **DTSn2** showed the maximum at 369 nm, again a wavelength slightly shorter than that of **DTS2** (λ_{max} 382 nm).[11] The quantum chemical calculations on model molecules (**BT**, **DTS0**, **DTG0**, and **DTSn0**) at the B3LYP/LanL2DZ level of theory suggested similar HOMO and LUMO energy levels of dithienometalloles, regardless of the bridging element (Figure 5 and Table 2),[3a] in accordance with the experimental observation. The σ^*-π^* interaction is clearly seen in the LUMO of **DTSn0**, similarly to **DTS0** and **DTG0**. All these dithienometalloles were predicted to possess band gaps smaller than that of nonbridged **BT**, as expected.

PL spectra of **DTSn1** and **DTSn2** in THF revealed maxima at 410 and 431 nm, respectively. Interestingly, **DTSn1** exhibited a much lower PL quantum yield in comparison to **DTS1** (λ_{em} 425 nm, Φ = 0.69) and **DTG1** (λ_{em} 409 nm, Φ = 0.71), which have the same substituents.[10] This is likely due to the long Sn-C bonds that promote molecular vibration, thus facilitating nonradiative decay processes. The heavy-atom effects of Sn may be also responsible for the lower Φ value of **DTSn1**. However, the author did not observe any phosphorescence from **DTSn1** and **DTSn2** and have no clear data to show how the heavy-atom effects affect the PL properties. A similar decrease of fluorescence quantum efficiencies of group 14 dibenzometallole derivatives on going from metal = Si to metal = Sn was reported previously.[12] The PL quantum yield of **DTSn1** was also lower than that of **DTSn2**, possibly due to the presence of two flexible trimethylsilyl groups, which provides a

path for nonradiative relaxation. It is also likely that the two benzo-annulated units in **DTSn2** hinder rotation of the phenyl groups on the stannole ring, thus suppressing nonradiative pathways in **DTSn2**. The PL spectra were measured also as crystals, revealing maxima slightly red-shifted from those in solution (Table 1 and Figure 4). The shift for **DTSn2** depending on the states (in solution or as crystal) was larger than that of **DTSn1**, presumably due to the higher degree of intermolecular interaction of **DTSn2** in the solid state, as indicated by its crystal structure analysis (vide infra). One might consider the possibility that conformational freezing in the solid states would change the electronic states of these dithienostannole derivatives. However, no significant changes of photo transition patterns depending on the geometry (crystal geometry or optimized gas-phase geometry) were provided by TD-DFT calculations on the real molecules of **DTSn1** and **DTSn2** (Table 3). No evident differences of HOMO and LUMO profiles are seen between them (Figure 6). In addition, major transitions that are ascribed to HOMO → LUMO for the crystal geometries of **DTSn1** and **DTSn2** are calculated to be blue-shifted from those in gas phase, respectively, in contrast to experimental observations that **DTSn1** and **DTSn2** showed higher energy absorption maxima in solution in comparison to those in crystals. These results clearly indicate that the dependence of optical properties of **DTSn1** and **DTSn2** on the state (solution, amorphous, or crystal) does not arise from changes in single molecular structures.

Table 1. Optical properties of **DTSn1** and **DTSn2**.

	UV abs λ_{max}/nm[a] (ε/Lmol^{-1}cm^{-1})	PL λ_{em}/nm (Φ_f)[a,b]	
DTSn1	350 (25846)	Solution	410 (0.009)
		Crystal	422 (0.556)
		Amorphous	411 (0.028)
DTSn2	369 (14600)	Solution	431 (0.296)
		Crystal	454 (0.214)

[a] In THF. [b] Excited at absorption maximum in solution.

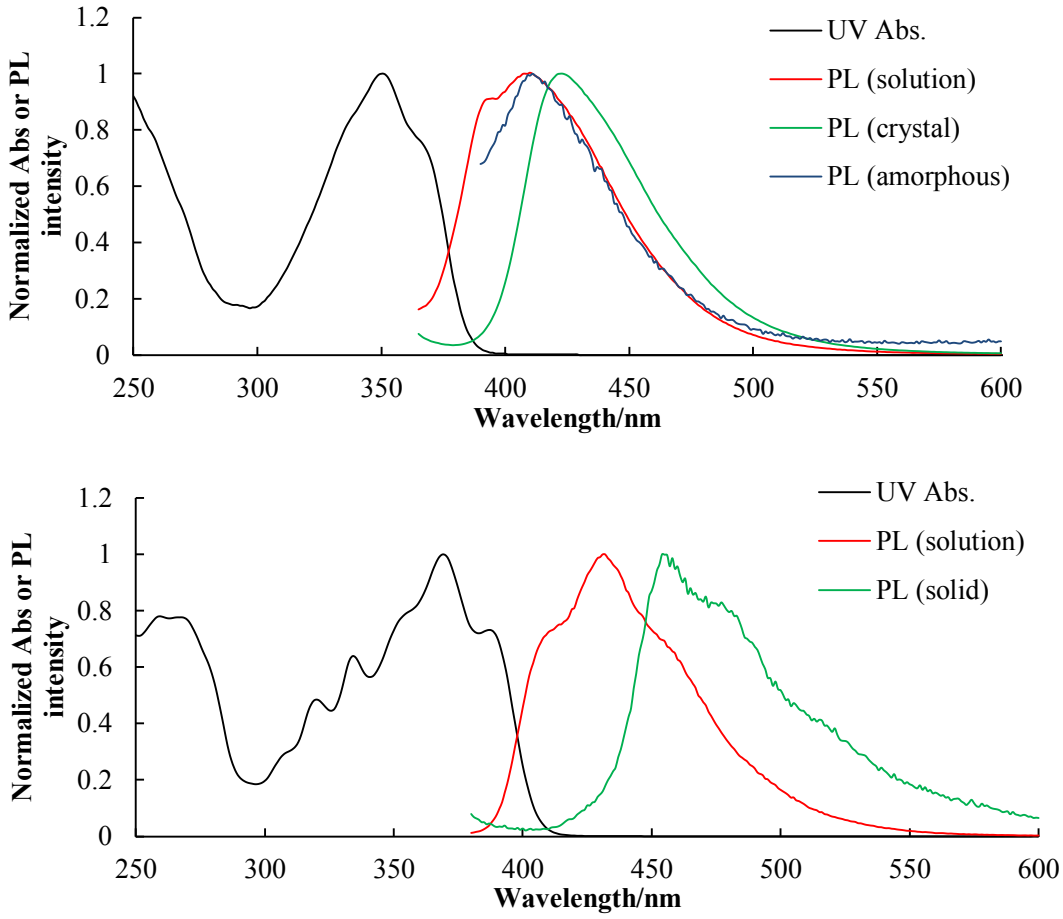

Figure 4. UV and PL spectra of **DTSn1** (top) and **DTSn2** (bottom). UV spectra are the same as presented in Figure 2 and 3.

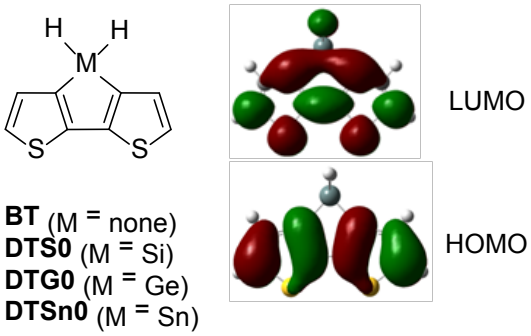

Figure 5. Structures of model compounds and HOMO and LUMO profiles of **DTSn0** based on DFT calculations at B3LYP/LanL2DZ.

Table 2. HOMO and LUMO energy levels of dithienometalloles derived from DFT calculations at B3LYP/LanL2DZ.

	BT	**DTS0**[a]	**DTG0**[a]	**DTSn0**[b]
HOMO/eV	-5.81	-5.74	-5.74	-5.72
LUMO/eV	-1.72	-1.83	-1.81	-1.80
Δ(LUMO-HOMO)/eV	4.09	3.91	3.93	3.92

[a] See reference 3(a). [b] Present work, see Figure 1.

Table 3. TD-DFT calculations on **DTSn1** and **DTSn2** at the B3LYP/LanL2DZ level[a]

	Crystal[b]		Optimized[b]	
	Transition energy / eV (Wavelength / nm)	Oscillator strength	Transition energy / eV (Wavelength / nm)	Oscillator strength
DTSn1	3.68 (336)	0.4036	3.62 (342)	0.3699
	4.19 (296)	0.0225	4.19 (296)	0.0523
	4.54 (273)	0.0249	4.49 (276)	0.0019
	4.59 (270)	0.0022	4.64 (267)	0.0000
	4.71 (263)	0.0019	4.65 (267)	0.0152
DTSn2	3.40 (364)	0.3726	3.21 (386)	0.4152
	4.05 (306)	0.1221	3.86 (322)	0.0901
	4.08 (304)	0.1028	3.89 (319)	0.0820
	4.22 (294)	0.0357	3.96 (313)	0.0523
	4.48 (277)	0.0088	4.28 (290)	0.0012

[a]Five low-energy transitions were calculated. [b]Definitions: crystal, calculated on the crystal structure determined by X-ray diffraction analysis; optimized, calculated on optimized geometry at the B3LYP/LanL2DZ level.

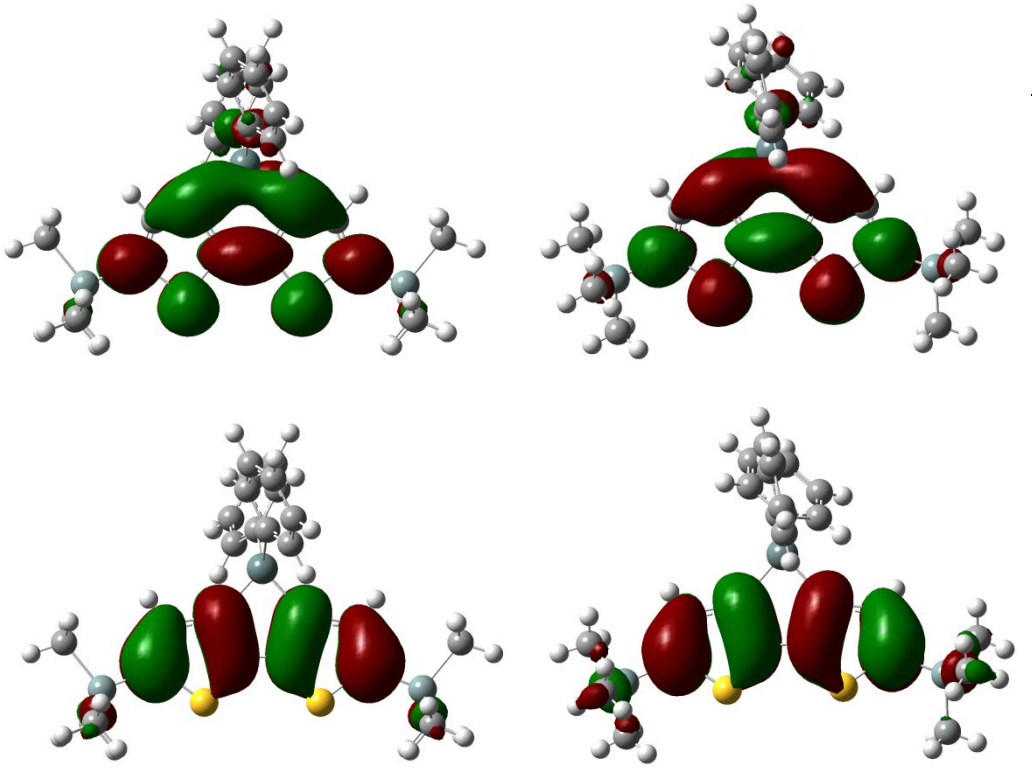

Figure 6. HOMO and LUMO profiles of **DTSn1** based on optimized (left) and crystal structures (right) derived from DFT calculations at the B3LYP/LanL2DZ level.

Crystallization induced emission enhancement characteristics of DTSn

To our surprise, the PL quantum yield of the crystals of **DTSn1** was approximately 20 times higher than that in solution. In the amorphous phase, **DTSn1** exhibited weak emission with Φ = 0.028, similar to that in solution, as presented in Figure 7. Thus, reversible crystallization enhanced emission was readily performed by melting/cooling of the crystal sample to form the amorphous state, followed by its recrystallization to recover the crystals. **DTSn2** showed moderate quantum efficiencies, regardless of the states (in solution or as crystal). The emission lifetime of **DTSn2** as crystals was also measured to be 2.6 ns, which was shorter than but at the same order as that of **DTS1** (4.5 ns). The lifetime of **DTSn1** could not be determined exactly, because the lifetime was shorter than the pulse width, but it was estimated to be approximately 0.35 ns. Although the reason

for the relatively short lifetimes of **DTSn1** and **DTSn2** is still unclear, this clearly indicates that the dithienostannole emission is based on fluorescence, but not phosphorescence.

Figure 8 and Figure 9 depict the crystal structures of **DTSn1** and **DTSn2**, and Table 4 summarizes the selected bond distances and angles. Tables 5 and 7 summarize crystal data, experimental conditions, and summary of structural refinement of **DTSn1** and **DTSn2**, respectively. Table 6 and 8 summarize all bond distances and angles, except for hydrogen atom. They show similar structural parameters for the dithienostannole core fragments with Sn-C(Ph) and Sn-C(stannole) bond distances between 2.128(3) and 2.144(3) Å, which are in the standard range for Sn-C(sp^2) bonds[13] and are similar to those reported for 3,3′-dithienostannole.[8] The endocyclic C-Sn-C angles are 84.08(9) and 83.6(4)°, respectively, smaller than the C-Si-C angle reported for a dithienosilole **DTS3** (Chart 2),[4b] reflecting the longer Sn-C bond distances relative to Si-C bonds. These acute angles may be indicative of ring strain in the dithienostannole system. Figures 8 and 9 also represent the molecular packing of the dithienostannoles. For **DTSn1**, the dithienostannole fluorophores are efficiently separated by phenyl and trimethylsilyl groups, thus preventing aggregation-induced quenching of the fluorophore, a phenomenon often observed for organic PL materials in the solid state. π-π Stacking contacts between phenyl rings are the only intermolecular interactions observed in this structure. These interactions suppress motion of the phenyl rings but do not seem to have an influence on the electronic states of **DTSn1**, as no significant electron density is localized on the phenyl substituents in the frontier orbitals (Figure 6). In contrast, **DTSn2** showed intermolecular face-to-face π-π contacts between the dithienostannole core fragments, with the shortest interplane distance being only 3.8 Å. These short contacts most certainly provide a pathway for at least nonradiative quenching of the excited state to enhance the nonradiative decay. Thus, somewhat serendipitously, **DTSn2** has the same PL efficiency in the solid state and in solution.

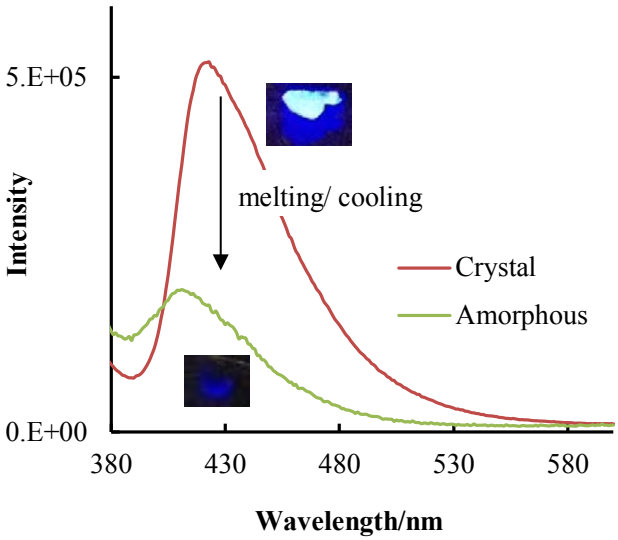

Figure 7. PL spectra of **DTSn1**. Insets are photos of **DTSn1** as crystals and amorphous under UV-irradiation (365 nm).

Table 4. Selected bond distances and angles of **DTS3**, **DTSn1**, and **DTSn2**.

	Bond distance/Å		Bond angle/deg	
	C(metallole)-M	C(Ph)-M	Inner ring C-M-C	C (Ph)-M-C(Ph)
DTSn1	2.135(3), 2.143(3)	2.128(3), 2.136(3)	84.08(9)	110.65(9)
DTSn2	2.144(9), 2.131(9)	2.137(9), 2.118(9)	83.6(4)	105.9(4)
DTS3[a]	1.868(3), 1.875(3)	1.859(3), 1.865(3)	92.0(1)	112.5(1)

[a] See reference 4b.

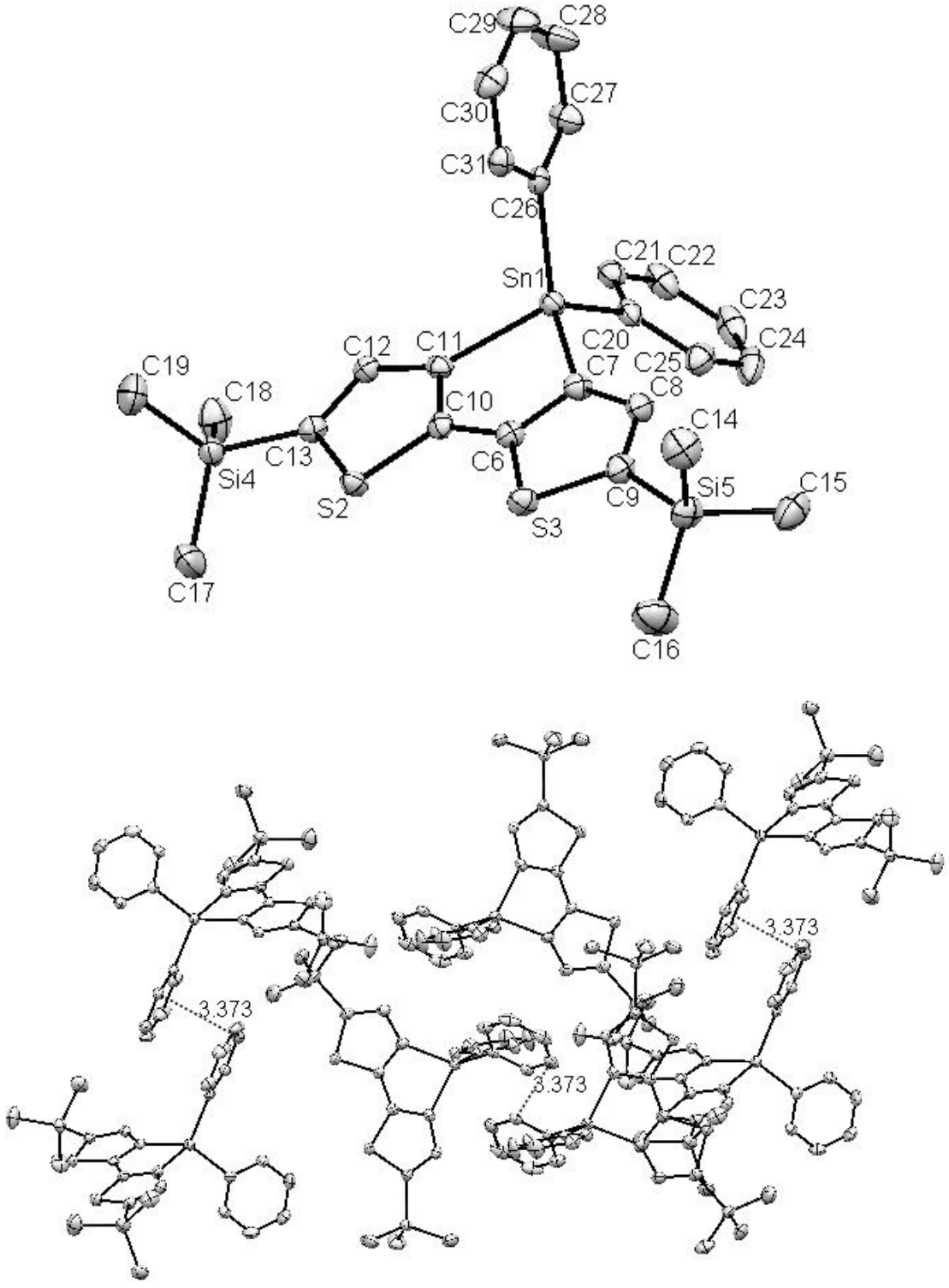

Figure 8. Crystal structures (top) and molecular packing (bottom) of **DTSn1**.

Table 5. Crystal data, experimental conditions, and summary of structural refinement for **DTSn1**

Molecular formula	C26 H30 S2 Si2 Sn
Molecular weight	581.50
Crystal style	Monoclinic
Space group	P 1 21/c 1
Cell dimens	
a, Å	12.3622(13)
b, Å	9.7428(9)
c, Å	23.458(3)
α, deg	90.0000
β, deg	92.106(3)
γ, deg	90.0000
V, $Å^3$	2823.4(5)
Z	4
D_{calcd}, g/cm^3	1.368
F_{000}	1184.00
cryst size, mm^3	0.20×0.10×0.10
cryst color	Pale yellow
μ, cm^{-1}	1.149
Diffractometer	Rigaku RAXIS-RAPID
temp, °C	-150 °C
Wavelength, Å	0.71075 (MoKα)
Monochromator	Graphite
no. of obsd rflns (I> 3δ(I))	26562
R	0.0317
R_w	0.0706

Table 6. Selected distances (Å) and angles (deg) for **DTSn1** with their Esd's in parentheses

distance / Å					
Sn(1)- C(7)	2.135(3)	Si(5)-C(9)	1.869(3)	C(20)-C(25)	1.392(4)
Sn(1)- C(11)	2.143(3)	Si(5)-C(14)	1.866(4)	C(21)-C(22)	1.384(4)
Sn(1)-C(20)	2.128(3)	Si(5)-C(15)	1.863(4)	C(22)-C(23)	1.369(5)
Sn(1)-C(26)	2.136(3)	Si(5)-C(16)	1.854(4)	C(23)-C(24)	1.375(5)
S(2)-C(10)	1.720(3)	C(6)-C(7)	1.379(4)	C(24)-C(25)	1.388(5)
S(2)-C(13)	1.735(3)	C(6)-C(10)	1.461(4)	C(26)-C(27)	1.387(4)
S(3)-C(6)	1.723(3)	C(7)-C(8)	1.424(4)	C(26)-C(31)	1.390(4)
S(3)-C(9)	1.732(3)	C(8)-C(9)	1.372(4)	C(27)-C(28)	1.383(5)
Si(4)-C(13)	1.868(3)	C(10)-C(11)	1.385(4)	C(28)-C(29)	1.380(5)
Si(4)-C(17)	1.853(4)	C(11)-C(12)	1.421(4)	C(29)-C(30)	1.386(4)
Si(4)-C(18)	1.851(4)	C(12)-C(13)	1.378(4)	C(30)-C(31)	1.383(4)
Si(4)-C(19)	1.862(4)	C(20)-C(21)	1.395(4)		
angle / deg					
C(7)-Sn(1)-C(11)	84.08(9)	C(14)-Si(5)-C(16)	110.52(18)	S(2)-C(13)-Si(4)	123.00(13)
C(7)-Sn(1)-C(20)	114.88(10)	C(15)-Si(5)-C(16)	110.55(19)	S(2)-C(13)-C(12)	109.22(18)
C(7)-Sn(1)-C(26)	115.55(10)	S(3)-C(6)-C(7)	111.54(18)	Si(4)-C(13)-C(12)	127.78(18)
C(11)-Sn(1)-C(20)	116.67(10)	S(3)-C(6)-C(10)	127.86(19)	Sn(1)-C(20)-C(21)	121.40 (19)
C(11)-Sn(1)-C(26)	112.88(9)	C(7)-C(6)-C(10)	120.6(3)	Sn(1)-C(20)-C(25)	120.17(19)
C(20)-Sn(1)-C(26)	110.65(9)	Sn(1)-C(7)-C(6)	107.56(17)	C(21)-C(20)-C(25)	118.4(3)
C(10)-S(2)-C(13)	92.93(12)	Sn(1)-C(7)-C(8)	141.04(19)	C(20)-C(21)-C(22)	120.6(3)
C(6)-S(3)-C(9)	92.69(12)	C(6)-C(7)-C(8)	111.4(3)	C(21)-C(22)-C(23)	120.1(3)
C(13)-Si(4)-C(17)	109.83(15)	C(7)-C(8)-C(9)	114.6(3)	C(22)-C(23)-C(24)	120.4(3)
C(13)-Si(4)-C(18)	107.04(14)	S(3)-C(9)-Si(5)	123.72(15)	C(23)-C(24)-C(25)	120.0(3)
C(13)-Si(4)-C(19)	109.50(15)	S(3)-C(9)-C(8)	109.7(2)	C(20)-C(25)-C(24)	120.4(3)
C(17)-Si(4)-C(18)	110.92(17)	Si(5)-C(9)-C(8)	126.6(2)	Sn(1)-C(26)-C(27)	120.72(19)
C(17)-Si(4)-C(19)	108.70(18)	S(2)-C(10)-C(6)	127.92(18)	Sn(1)-C(26)-C(31)	120.52(18)
C(18)-Si(4)-C(19)	110.84(17)	S(2)-C(10)-C(11)	111.63(18)	C(27)-C(26)-C(31)	118.7(3)
C(9)-Si(5)-C(14)	109.31(14)	C(6)-C(10)-C(11)	120.4(3)	C(26)-C(27)-C(28)	120.6(3)
C(9)-Si(5)-C(15)	106.77(15)	Sn(1)-C(11)-C(10)	107.25(17)	C(27)-C(28)-C(29)	120.4(3)
C(9)-Si(5)-C(16)	110.22(16)	Sn(1)-C(11)-C(12)	141.61(17)	C(28)-C(29)-C(30)	119.5(3)
C(14)-Si(5)-C(15)	109.38(16)	C(10)-C(11)-C(12)	111.1(2)	C(29)-C(30)-C(31)	120.1(3)
C(26)C(31)-C(30)	120.7(3)	C(11)-C(12)-C(13)	115.1(2)		

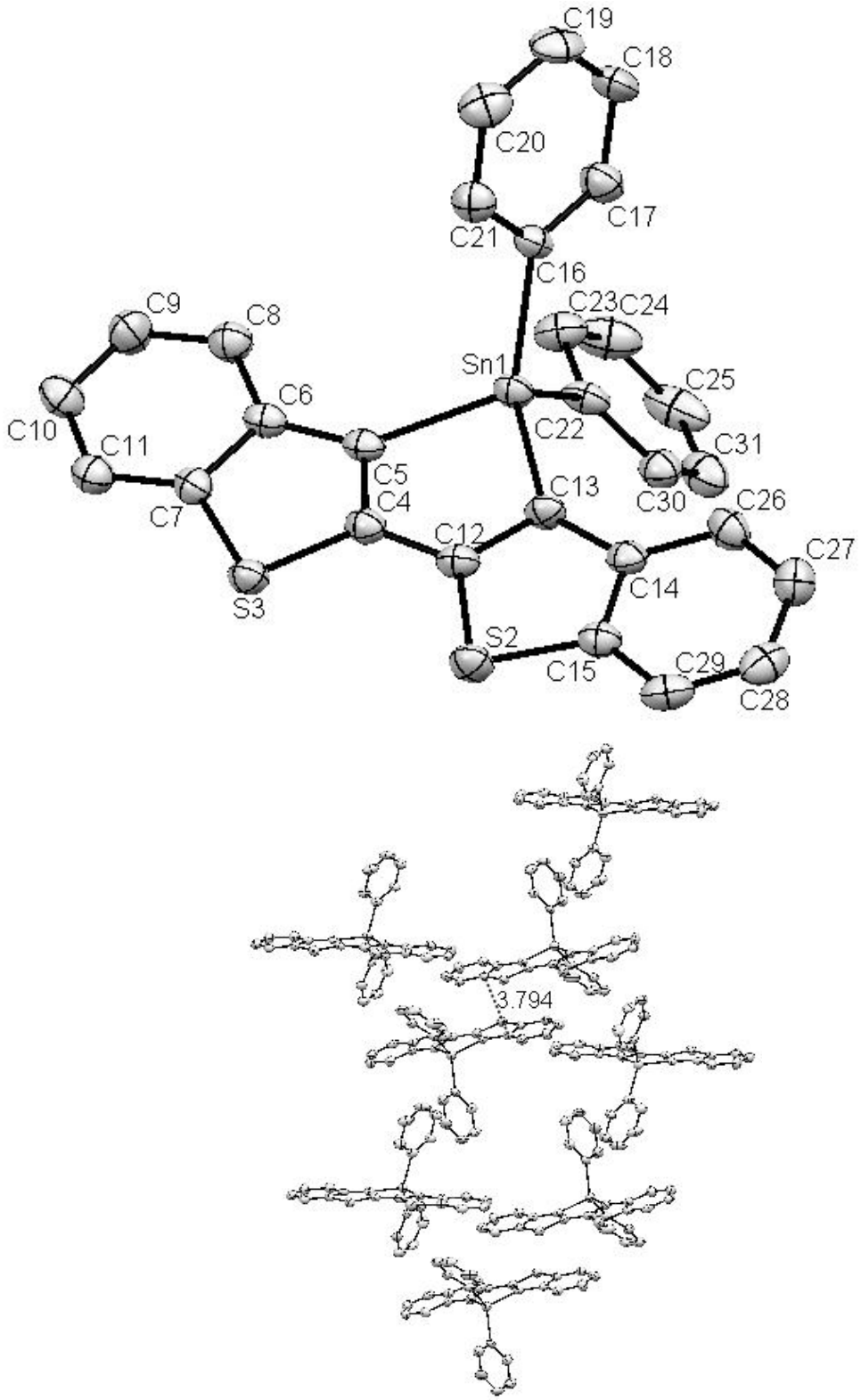

Figure 9. Crystal structures (top) and molecular packing (bottom) of **DTSn2**.

Table 7. Crystal data, experimental conditions, and summary of structural refinement for **DTSn2**

Molecular formula	C28 H18 S2 Sn
Molecular weight	537.26
Crystal style	Monoclinic
Space group	P 1 21/n 1
Cell dimens	
a, Å	9.8322(19)
b, Å	14.341(3)
c, Å	18.363(3)
α, deg	90.0000
β, deg	93.380(5)
γ, deg	90.0000
V, $Å^3$	2584.8(8)
Z	4
D_{calcd}, g/cm^3	1.381
F_{000}	1072.00
cryst size, mm^3	0.25×0.10×0.10
cryst color	greenish-yellow
μ, cm^{-1}	1.162
Diffractometer	Rigaku RAXIS-RAPID
temp, °C	-150 °C
Wavelength, Å	0.71075 (MoKα)
Monochromator	Graphite
no. of obsd rflns (I> 3δ(I))	24579
R	0.0781
R_w	0.2567

Table 8. Selected distances (Å) and angles (deg) for **DTSn2** with their Esd's in parentheses

distance / Å					
Sn(1)-C(5)	2.144(9)	C(4)-C(12)	1.447(13)	C(13)-C(14)	1.436(13)
Sn(1)-C(13)	2.131(9)	C(5)-C(6)	1.425(13)	C(14)-C(15)	1.391(13)
Sn(1)-C(16)	2.137(9)	C(6)-C(7)	1.410(12)	C(14)-C(26)	1.419(13)
Sn(1)-C(22)	2.118(9)	C(6)-C(8)	1.405(14)	C(15)-C(29)	1.391(14)
S(2)-C(12)	1.742(10)	C(7)-C(11)	1.378(13)	C(16)-C(17)	1.358(13)
S(2)-C(15)	1.757(10)	C(8)-C(9)	1.381(14)	C(16)-C(21)	1.401(13)
S(3)-C(4)	1.742(9)	C(9)-C(10)	1.367(15)	C(17)-C(18)	1.393(15)
S(3)-C(7)	1.751(10)	C(10)-C(11)	1.385(15)	C(18)-C(19)	1.377(15)
C(4)-C(5)	1.368(13)	C(12)-C(13)	1.365(12)	C(19)-C(20)	1.399(16)
C(20)-C(21)	1.366(15)	C(22)-C(23)	1.397(15)	C(22)-C(30)	1.404(14)
C(23)-C(24)	1.399(16)	C(24)-C(25)	1.343(19)	C(25)-C(31)	1.380(17)
C(26)-C(27)	1.375(15)	C(27)-C(28)	1.392(15)	C(28)-C(29)	1.352(15)
C(30)-C(31)	1.380(14)				
angle / deg					
C(5)-Sn(1)-C(13)	83.6(4)	S(3)-C(7)-C(11)	126.2(7)	Sn(1)-C(16)-C(17)	119.4(7)
C(5)-Sn(1)-C(16)	114.6(4)	C(6)-C(7)-C(11)	122.7(9)	Sn(1)-C(16)-C(21)	121.7(7)
C(5)-Sn(1)-C(22)	118.4(4)	C(6)-C(8)-C(9)	119.8(9)	C(17)-C(16)-C(21)	118.8(9)
C(13)-Sn(1)-C(16)	119.6(4)	C(8)-C(9)-C(10)	121.6(10)	C(16)-C(17)-C(18)	121.7(10)
C(13)-Sn(1)-C(22)	114.3(4)	C(9)-C(10)-C(11)	120.6(10)	C(17)-C(18)-C(19)	119.2(10)
C(16)-Sn(1)-C(22)	105.9(4)	C(7)-C(11)-C(10)	118.3(9)	C(18)-C(19)-C(20)	119.8(10)
C(12)-S(2)-C(15)	90.8(5)	S(2)-C(12)-C(4)	126.0(7)	C(19)-C(20)-C(21)	119.8(10)
C(4)-S(3)-C(7)	90.7(5)	S(2)-C(12)-C(13)	113.4(7)	C(16)-C(21)-C(20)	120.7(9)
S(3)-C(4)-C(5)	113.4(7)	C(4)-C(12)-C(13)	120.6(9)	Sn(1)-C(22)-C(23)	120.2(7)
S(3)-C(4)-C(12)	125.6(7)	Sn(1)-C(13)-C(12)	107.7(7)	Sn(1)-C(22)-C(30)	121.9(7)
C(5)-C(4)-C(12)	121.0(8)	Sn(1)-C(13)-C(14)	140.6(7)	C(23)-C(22)-C(30)	117.9(9)
Sn(1)-C(5)-C(4)	107.0(7)	C(12)-C(13)-C(14)	111.7(8)	C(22)-C(23)-C(24)	119.7(10)
Sn(1)-C(5)-C(6)	140.5(7)	C(13)-C(14)-C(15)	113.2(8)	C(23)-C(24)-C(25)	121.0(12)
C(4)-C(5)-C(6)	112.2(8)	C(13)-C(14)-C(26)	129.0(9)	C(24)-C(25)-C(31)	120.8(11)
C(5)-C(6)-C(7)	112.6(8)	C(15)-C(14)-C(26)	117.8(9)	C(14)-C(26)-C(27)	119.0(9)
C(5)-C(6)-C(8)	130.3(8)	S(2)-C(15)-C(14)	110.9(7)	C(26)-C(27)-C(28)	121.3(9)
C(7)-C(6)-C(8)	117.1(9)	S(2)-C(15)-C(29)	126.9(8)	C(27)-C(28)-C(29)	120.6(10)
S(3)-C(7)-C(6)	111.1(7)	C(14)-C(15)-C29)	122.2(9)	C(15)-C(29)-C(28)	119.0(10)
C(22)-C(30)-C(31)	121.0(10)	C(25)-C(31)-C(30)	119.5(11)		

Conclusions

In summary, the author prepared two new dithienostannoles **DTSn1** and **DTSn2** and studied their optical properties and crystal structures. Interestingly, clear and reversible crystallization-enhanced emission was observed for **DTSn1**. There has been only a limited number of reports about compounds that show crystallization-enhanced emission,[14] and this is the first example of a thiophene-based compound.

Experimental

General

All reactions were carried out under a dry argon atmosphere. THF and ether used as the reaction solvents were dried over calcium hydride and were stored over activated molecular sieves 4A under an argon atmosphere until use. The starting compounds 5,5′-bis(trimethylsilyl)-3,3′-dibromo-2,2′-bithiophene[4a] and 3,3′-dibromo-2,2′-bibenzo[b]thiophene[11] were prepared as reported in the literature. ^{1}H and ^{13}C NMR spectra were recorded on Varian System500 and MR400 spectrometers. UV and PL spectra were measured on Hitachi U-3210 and F-4500 spectrophotometers, respectively. Measurements of high-resolution APCI and ESI mass spectra were carried out using a Thermo Fisher Scientific LTQ Orbitrap XL instrument at the Natural Science Center for Basic Research and Development (N-BARD), Hiroshima University. Emission life times were measured on a Spec Fluorolog-3 ps instrument with a nanoLED 370 nm light source, (pulse width 1.5 ns).

Synthesis of DTSn1

In a 100 mL two-necked flask fitted with a 10 mL dropping funnel were placed 5,5′-bis(trimethylsilyl)-3,3′-dibromo-2,2′-bithiophene (2.20 g, 4.70 mmol) and ether (80 mL). To this was added dropwise a solution of 1.64 M *n*-BuLi/hexane (5.70 mL, 9.40 mmol) at −78 °C over a period of 1 h. After the mixture was stirred at this temperature for 30 min, 1.61 g (4.70 mmol) of diphenyltin dichloride in 10 mL of ether for 10 min was slowly added to the mixture. The mixture was further stirred at -78 °C for 1 h and warmed to room temperature. To the resulting mixture was added 50 mL of hexane to precipitate inorganic salts, which were removed by filtration. After evaporation of the solvent from the filtrate, the residue was subjected to preparative gel permeation chromatography (GPC) with toluene as eluent to give 1.75 g (64% yield) of **DTSn1** as a colorless

solid: ^{1}H NMR (δ in $CDCl_3$) 0.33 (s, 18H, Me_3Si), 7.25 (s, 2H, thiophene ring protons), 7.38−7.41 (m, 6H, m- and p-phenyl protons), 7.61−7.62 (m, 4H, o-phenyl protons); ^{13}C NMR (δ in $CDCl_3$) 0.08, 128.84, 129.67, 136.63, 137.13, 138.70, 139.71, 141.44, 154.84; ^{119}Sn NMR (δ in $CDCl_3$ from $SnMe_4$) −153.50; highresolution ESI/MS calcd for $C_{24}H_{30}S_2Si_2Sn$ *m/z* 583.04222 ([M^+]), found *m/z* 606.04822 ([M^+]). Single crystals of **DTSn1** suitable for the X-ray diffraction study were obtained by solvent diffusion crystallization from toluene/methanol.

Synthesis of DTSn2

In a 50 mL two-necked flask fitted with a 10 mL dropping funnel were placed 3,3′-dibromo-2,2′-bibenzo[b]-thiophene (0.70 g, 1.70 mmol), ether (30 mL), and THF (5 mL). To this was added dropwise a 1.64 M solution of *n*-BuLi/hexane (2.00 mL, 3.40 mmol) at −78 °C over a period of 30 min. After the mixture was stirred at this temperature for 30 min, 0.64 g (1.80 mmol) of diphenyltin dichloride in 5 mL of ether was slowly added to the mixture. The mixture was further stirred at −78 °C for 1 h and warmed to room temperature. To the resulting mixture was added 20 mL of hexane to precipitate inorganic salts, which were removed by filtration. After evaporation of the solvent from the filtrate, the residue was subjected to preparative GPC with toluene as eluent to give 0.52 g (57% yield) of **DTSn2** as a light yellow solid: ^{1}H NMR (δ in $CDCl_3$) 7.29−7.43 (m, 10H, benzothiophene, m- and p-phenyl protons), 7.66−7.69 (m, 4H, o-phenyl protons), 7.77−7.79 (m, 2H, benzothiophene protons), 7.91−7.93 (m, 2H, benzothiophene); ^{13}C NMR (δ in $CDCl_3$) 122.99, 124.18, 124.79, 125.17, 129.15, 130.01, 135.68, 136.56, 137.08, 142.99, 143.51, 149.21; ^{119}Sn NMR (δ in $CDCl_3$ from $SnMe_4$) −145.72; high-resolution APCI/MS calcd for $C_{28}H_{19}S_2Sn$ *m/z* 538.99447 ([M + H^+]) found *m/z* 538.99430 ([M + H^+]). Single crystals of **DTSn1** suitable for the X-ray diffraction study were obtained by solvent diffusion crystallization from toluene/methanol.

References

1 (a) A. Mishra, C.-Q. Ma, P. Bäuerie, *Chem. Rev.*, **2009**, *109*, 1141; (b) I. Osaka, R. D. McCullough, *Acc. Chem. Res.*, **2008**, *41*, 1202.

2 (a) J. Ohshita, *Macromol. Chem. Phys.*, **2009**, *210*, 1360; (b) J. Chen, Y. Cao, *Macromol. Rapid Commun.*, **2007**, *28*, 1714.

3 (a) J. Ohshita, Y.-M. Hwang, T. Mizumo, H. Yoshida, Y. Ooyama, Y. Harima, Y. Kunugi, *Organometallics*, **2011**, *30*, 3233; (b) Y.-M. Hwang, J. Ohshita, T. Mizumo, H. Yoshida, Y. Kunugi, *Polymer*, **2011**, *52*, 1360; (c) D. Gendron, P. O. Morin, P. Berrouard, N. Allard, B. R. Aich, C. N. Garon, Y. Tao, M. Leclerc, *Macromolecules*, **2011**, *44*, 7188; (d) C. M. Amb, S. Chen, K. R. Graham, J. Subbiah, C. E. Small, F. So, J. R. Reynolds, *J. Am. Chem. Soc.*, **2011**, *133*, 10062; (e) C. E. Small, S. Chen, J. Subbiah, C. M. Amb, S. W. Tsang, T. H. Lai, J. R. Reynolds, F. So, *Nat. Photonics*, **2012**, *6*, 115.

4 (a) J. Ohshita, M. Nodono, H. Kai, T. Watanabe, A. Kunai, K. Komaguchi, M. Shiotani, A. Adachi, K. Okita, Y. Harima, K. Yamashita, M. Ishikawa, *Organometallics*, **1999**, *18*, 1453; (b) J. Ohshita, M. Nodono, T. Watanabe, Y. Ueno, A. Kunai, Y. Harima, K. Yamashita, M. Ishikawa, *J. Organomet. Chem.*, **1998**, *553*, 487; (c) G. Lu, H. Usta, C. Risko, L. Wang, A. Facchetti, M. A. Ratner, T. J. Marks, *J. Am. Chem. Soc.*, **2008**, *130*, 7670.

6 (a) L. Liao, L. Dai, A. Smith, M. Durstock, J. Lu, J. Ding, Y. Tao, *Macromolecules*, **2007**, *40*, 9406; (b) L. Huo, H.-Y. Chen, J. Hou, T. L. Chen, Y. Yang, *Chem. Commun.*, **2009**, 5570; (c) M. Zhang, H. Fan, X. Guo, Y. He, Z. Zhang, J. Min, J. Zhang, G. Zhao, X. Zhan, Y. Li, *Macromolecules*, **2010**, *43*, 5706; (d) J. Ding, N. Song, Z. Li, *Chem. Commun.*, **2010**, *46*, 8668; (e) J. S. Moon, C. J. Takacs, S. Cho, R. C. Coffin, H. Kim, G. C. Bazan, A. J. Heeger, *Nano Lett.*, **2010**, *10*, 4005; (f) M. C. Scharber, M. Koppe, J. Gao, F. Cordella, M. A. Loi, P. Denk, M. Morana, H.-J. Egelhaaf, K. Forberich, G. Dennler, R. Gaudiana, D. Waller, Z. Zhu, X. Shi, C. J.

Brabec, *Adv. Mater.*, **2010**, *22*, 367; (g) J. Hou, H.-Y. Chen, S. Zhang, G. Li, Y. Yang, *J. Am. Chem. Soc.*, **2008**, *130*, 16144; (h) H.-Y. Chen, J. Hou, A. E. Hayden, H. Yang, K. N. Houk, Y. Yang, *Adv. Mater.*, **2010**, *22*, 371.

7 (a) J. Ohshita, Y. Kurushima, K.-H. Lee, Y. Ooyama, Y. Harima, *Organometallics*, **2007**, *26*, 6591; (b) J. Ohshita, Y. Tominaga, T. Mizumo, Y. Kuramochi, H. Higashimura, *Heteroat. Chem.*, **2011**, *22*, 514; (c) J. Ohshita, Y. Tominaga, D. Tanaka, Y. Ooyama, T. Mizumo, N. Kobayashi, H. Higashimura, *Dalton Trans.*, **2013**, *42*, 3646; (d) J. Ohshita, K. Kimura, K.-H. Lee, A. Kunai, Y.-W. Kwak, E.-C. Son, Y. Kunugi, *J. Polym. Sci., Part A, Polym. Chem.*, **2007**, *45*, 4588.

8 M. Saito, M. Shiratake, T. Tajima, J.-D. Guo, S. Nagase, *J. Organomet. Chem.*, **2009**, *694*, 4056.

9 I. Nagao, M. Shimizu, T. Hiyama, *Angew. Chem., Int. Ed.*, **2009**, *48*, 7573.

10 K.-H. Lee, J. Ohshita, D. Tanaka, Y. Tominaga, A. Kunai, *J. Organomet. Chem.*, **2012**, *710*, 53.

11 J. Ohshita, K.-H. Lee, K. Kimura, A. Kunai, *Organometallics*, **2004**, *24*, 5622.

12 K. Geramita, J. MaBee, T. D. Tilley, *J. Org. Chem.*, **2009**, *74*, 820.

13 K. M. Mackey, In The Chemistry of Organic Germanium, Tin, and Lead Compounds; Patai, S., Ed.; Wiley: Chichester, U.K., **1995**.

14 (a) Y. Dong, J. W. Y. Lam, A. Qin, J. Sun, J. Liu, Z. Li, J. Sun, H. H. Y. Sung, I. D. Williams, H.-H.S. Kwok, B. Z. Tang, *Chem. Commun.*, **2007**, 3255; (b) Y. Dong, J. W. Y. Lam, A. Qin, Z. Li, J. Sun, H. H.-Y. Sung, I. D. Williams, B. Z. Tang, *Chem. Commun.*, **2007**, 40; (c) L. Qian, B. Tong, J. Shen, J. Shi, J. Zhi, Y. Dong, F. Yang, Y. Dong, J. W. Y. Lam, Y. Liu, B. Z. Tang, *J. Phys. Chem. B*, **2009**, *113*, 9098.

Summary

The author prepared new organosilicon polymers and Sn-containing π-conjugated compounds. In Chart 1, improvement of PCE of DSSCs based on organosilicon polymers are depicted. The author employed two approaches to develop efficient dye sensitizer. As one of the approaches for development of efficient dye sensitizer described in Chapter 1, the author employed hybridization of organosilicon polymer with SWNT, which led to higher PCE than the pristine polymer-based DSSC, originated from improvement of J_{sc}. This resulted from good electron transporting property of SWNT. As another approach for development of dye sensitizer, structure modifications of organosilicon polymers are also employed as described in Chapter 2-4. Introduction of D-A structure to organosilicon polymers can improve PCE as the results of red-shifted broad absorption as described in Chapter 2. DSSCs based on Lewis basic acceptor-containing organosilicon polymer exhibit further improvement of PCE due to the large amount of the adsorbed polymer and efficient photo-excited electron injection through Ti-N coordination as described in Chapter 3. The author prepared organosilicon polymers with well-expanded π-conjugation consisted of dithienosilole and pyridine as described in Chapter 4. Since these organosilicon polymers have broad low energy absorption and efficient anchor units, DSSCs based on these polymers show the highest PCE in this thesis work.

The author also describes development of high voltage BHJ solar cell materials based on complexes of dithienosilole-pyridine alternate polymers with organoboron compound in Chapter 4. Low-lying HOMO energy level of polymer-borane complex leading to high voltage BHJ solar cell material is achieved by not only relatively low-lying HOMO energy level of dithienosilole, but also reduced HOMO level of pyridine-borane complex units (Chart 2).

As a new group 14 element-containing system, the author describes synthesis of dithienostannole and dibenzothienostannole, and their unique optical property. Dithienostannole shows

crystallization induced emission enhancement (CIEE) although electronic state of dithienostannole is quite similar to the silicon- and germanium-bridged analogues. The CIEE behavior of dithienostannole originated from long bond length of bridging tin atom which leads non-radiative decay by vibration of phenyl group on tin atom in solution and the amorphous phase (Chart 3).

On the basis of these studies, group 14 element-containing π-conjugated polymers and compounds that have a great potential for their applications to organic photovoltaics and unique luminescent materials were developed. The introductions of element characteristics are useful concept for functional material designs.

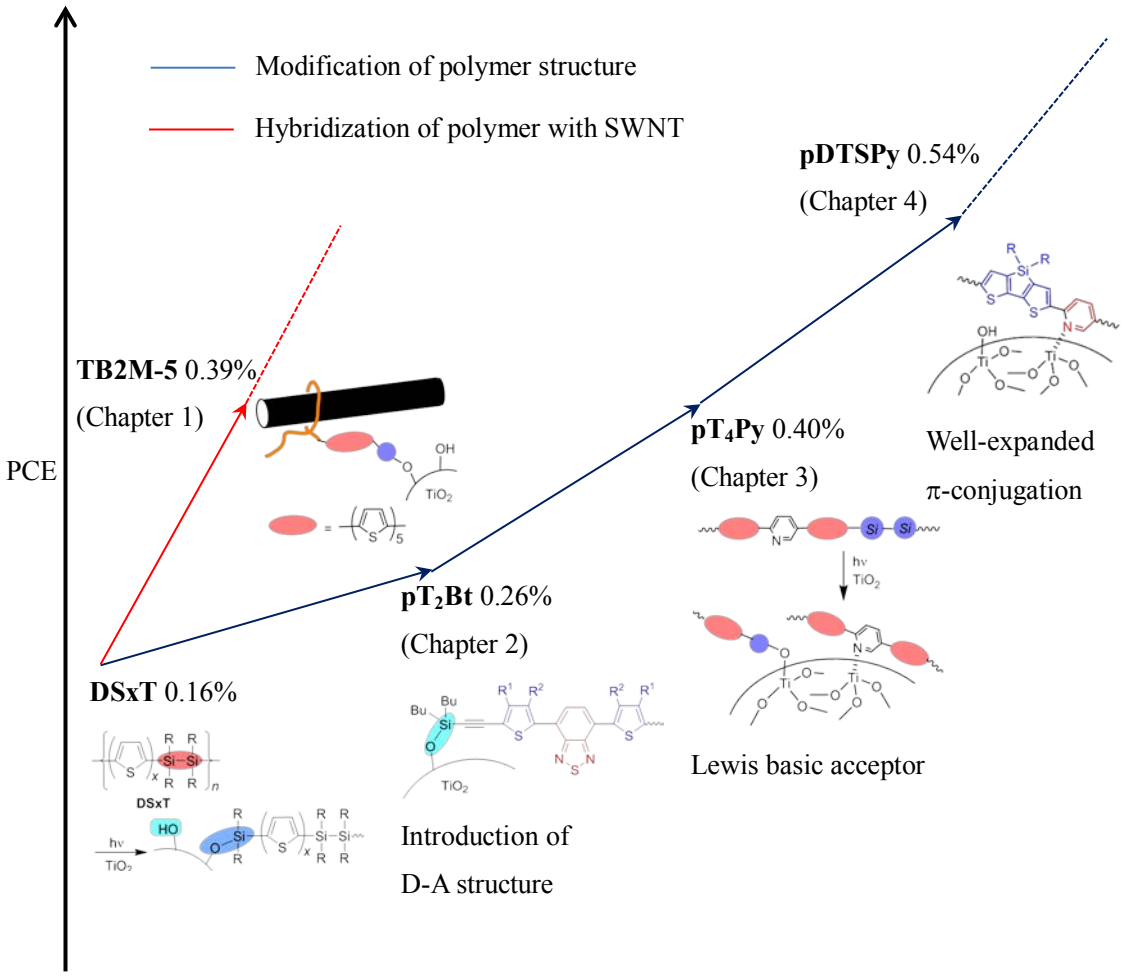

Chart 1. Development of organosilicon polymers for DSSCs dye sensitizer.

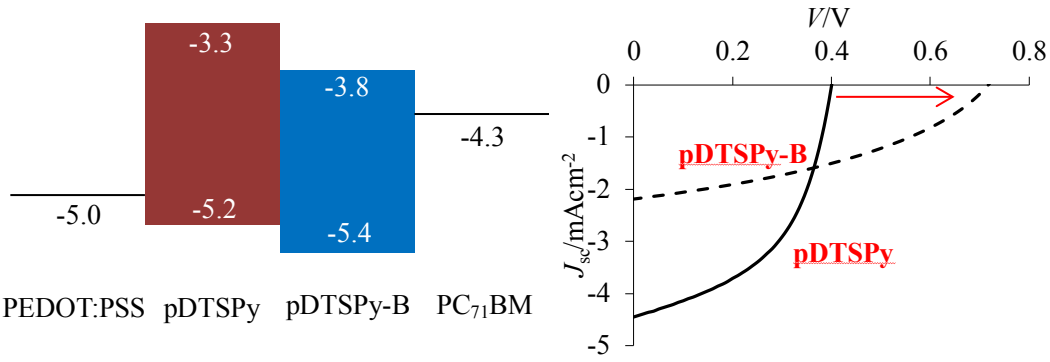

Chart 2. Dithienosilole-based high voltage BHJ solar cell material.

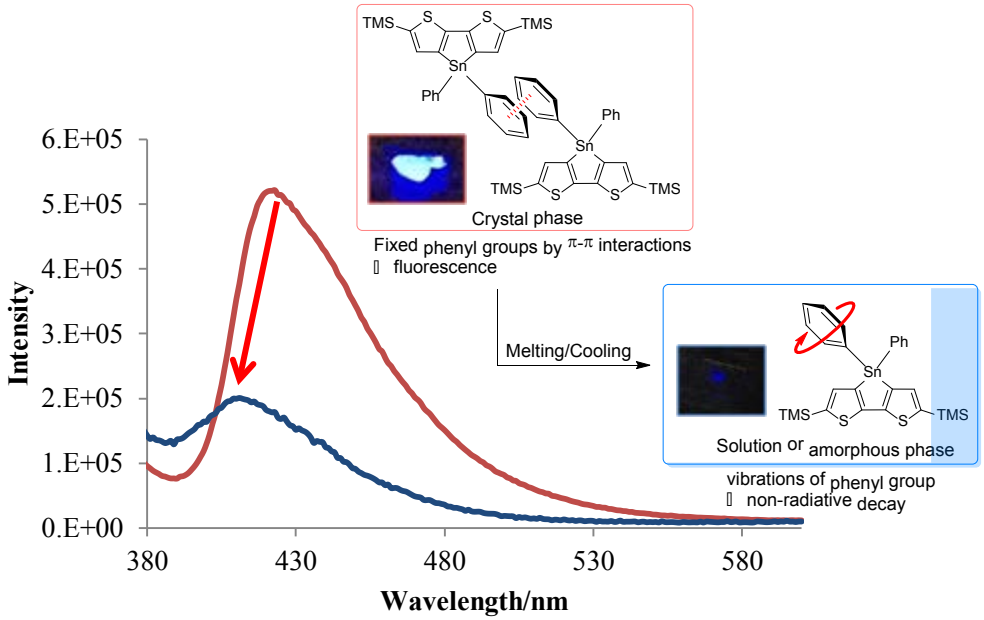

Chart 3. Crystallization-induced emission enhancement behavior of DTSn.

List of publications

Chapter 1. Hybridization of Carbon Nanotubes with Si–π Polymers and Attachment of Resulting Hybrids to TiO_2 Surface

Joji Ohshita, Daiki Tanaka, Junya Matsukawa, Tomonobu Mizumo, Hiroto Yoshida, Yousuke Ooyama, and Yutaka Harima

Chemistry Letters, **2011**, *40*, 87.

Chapter 2. Synthesis of Disilanylene Polymers with Donor-Acceptor-Type π-Conjugated Units and Applications to Dye-Sensitized Solar Cells

Daiki Tanaka, Joji Ohshita, Yousuke Ooyama, Tomonobu Mizumo, and Yutaka Harima

Journal of Organometallic Chemistry, **2012**, *719*, 30.

Chapter 3. Synthesis of Donor-Acceptor Type New Organosilicon Polymers and Their Applications to Dye-Sensitized Solar Cells

Daiki Tanaka, Joji Ohshita, Tomonobu Mizumo, Yousuke Ooyama, and Yutaka Harima

Journal of Organometallic Chemistry, **2013**, *741-742*, 97.

Chapter 4. Synthesis and Optical and Photovoltaic Properties of Dithienosilole-Dithienylpyridine and Dithienosilole-Pyridine Alternate Polymers and Polymer-$B(C_6F_5)_3$ Complexes

Daiki Tanaka, Joji Ohshita, Yousuke Ooyama, and Yasushi Morihara

Polymer Journal, **2013**, *45*, 1153.

Chapter 5. Synthesis, Optical Properties, and Crystal Structure of Dithienostannole

Daiki Tanaka, Joji Ohshita, Yousuke Ooyama, Norufumi Kobayashi, Hideyuki Higashimura, Takayuki Nakanishi, and Yasuchika Hasegawa

Organometallics, **2013**, *32*, 4136.

Other papers not included in this thesis

Preparation of Poly(disilanylenetetracyanobutadienyleneoligothienylene)s as New Donor-Acceptor type Organosilicon Polymers

Joji Ohshita, Tomonari Kajihara, Daiki Tanaka, Yousuke Ooyama

Journal of. Organometallic Chemistry, **2014**, *749*, 255.

Synthesis and Properties of Dithienometallole-Pyridinochalcogenadiazole Alternate Polymers

Joji Ohshita, Masayuki Miyazaki, Fei-Bao Zhang, Daiki Tanaka, Yasushi Morihara,

Polymer Journal, **2013**, *45*, 979.

Synthesis and Optical Properties of Organosilicon-Oligothiophene Branched Polymers

Joji Ohshita, Yuta Tominaga, Daiki Tanaka, Tomonobu Mizumo, Yuki Fujita, Yoshihito Kunugi

Journal of Organometallic Chemistry, **2013**, *736*, 50.

Synthesis of Oligo(dimethylsiloxane)-Oligothiophene Alternate Polymers from Alpha,Omega-Dibromooligo(dimethylsiloxane)

Zhou Lu, Joji Ohshita, Daiki Tanaka, Tomonobu Mizumo, Yuki Fujita, Yoshihito Kunugi

Journal of Organometallic Chemistry, **2013**, *731*, 73.

Synthesis of Poly(dithienogermole-2,6-diyl)s

Joji Ohshita, Masayuki Miyazaki, Daiki Tanaka, Yasushi Morihara, Yuki Fujita, Yoshihito Kunugi

Polymer Chemistry., **2013**, *4*, 3116.

Synthesis of Dithienosilole-Based Highly Photoluminescent Donor-Acceptor Type Compounds

Joji Ohshita, Yuta Tominaga, Daiki Tanaka, Yousuke Ooyama, Tomonobu Mizumo, Norufumi Kobayashi, Hideyuki Higashimura

Dalton Transactions, **2013**, *42*, 3646.

Synthesis and Reactions of Silicon-Bridged Dithienylbiphenyls. Fine Tuning of Electronic States by Bridging Silicon Chain Lengths

Joji Ohshita, Kazuya Murakami, Daiki Tanaka, Hiroto Yoshida

Heterocycles, **2012**, *86*, 1167.

Preparation, Hybrid Formation with Single-Walled Carbon Nanotube, and Film Morphology of Pyrene-Containing Polysiloxanes

Zhou Lu, Joji Ohshita, Daiki Tanaka, Tomonobu Mizumo, Yuki Fujita, Yoshihito Kunugi

Composit Interfaces, **2012**, *19*, 573.

Synthesis and Optical Properties of Dithienostiboles

Joji Ohshita, Risa Fujita, Daiki Tanaka, Yousuke Ooyama, Norifumi Kobayashi, Hideyuki Higashimura, Yohsuke Yamamoto

Chemistry Letters, **2012**, *41*, 1002.

Synthesis and Optical Properties of Spirobi(dithienometallole)s and Spirobi(dithienothiametalline)s

Kwang-Hoi Lee, Joji Ohshita, Daiki Tanaka, Yuta Tominaga, Atsutaka, Kunai

Journal of Organometallic Chemistry, **2012**, *710*, 53.

Preparation of Alkyl-Modified Silicon Nanosheets by Hydrosilylation of Layered Polysilane (Si_6H_6)

Hideyuki Nakano, Mitsuru Nakano, Koji Nakanishi, Daiki Tanaka, Yusuke Sugiyama, Takashi Ikuno, Hirotaka Okamoto, Toshiaki Ohta

Journal of the American Chemical Society, **2012**, *134*, 5452.

Synthesis and Chromic Behaviors of Dithienosiloles with Push-Pull Substituents Toward VOC Detection

Joji Ohshita, Daiki Tanaka, Kwang-Hoi Lee, Yasunori Kurushima, Shotaro Kawajima, Yousuke Ooyama, Yutaka Harima, Atsutaka Kunai, Yoshihito Kunugi

Molecular Crystals and Liquid Crystals, **2010**, *529*, 1.

Acknowledgement

The thesis is a summary of my studies from 2011 to 2014 under the direction of Professor Joji Ohshita at the Hiroshima University.

I wish to express my sincerest gratitude to Professor Joji Ohshita for his constant guidance, helpful comments, and wholehearted encouragement throughout this work. I am also deeply grateful to Associate Professor Yousuke Ooyama for his constant advice, and helpful discussion. I wish to acknowledge the suggestion of Associate Professor Hiroto Yoshida and Dr. Tomonobu Mizumo.

I would like to thank Mr. Junya Matsukawa, Mr. Hiroshi Hashimoto, Mr. Yunito Yoshikawa, Dr. Takami Morishita, Mr. Yousuke Hatanaka, Mr. Masashi Mukae, Mr. Shigenori Matsui, Mr. Masakazu Arita, Mr. Shota Kawashima, Mr. Yuji Asatsu, Mr. Qin Yi, Dr. Yong Mook Hwang, Ms. Risa Fujita, Mr. Yuta Tominaga, Mr. Yousuke Kawano, Mr. Ryuma Yoshida, Mr. Roh Yamamoto, Mr. Masayuki Miyazaki, Mr. Yuichiro Oda, Mr. Yuta Hagiwara, Mr. Yuki Takemoto, Mr. Yu Ito, Mr. Tomonari Kajihara, Dr. Zhou Lu, Mr. Kazuki Yamamoto, Mr. Kazuya Murakami, Mr. Fumiya Kaneko, Mr. Makoto Nakashima, Mr. Takehiro Yamada, Ms. Ayaka Terada, Mr. Tetsuya Sugiyama, Mr. Kazuaki Yamamoto, Mr. Koji Uenaka, Mr. Takafumi Sato, Ms. Haruna Muragishi, Mr. Yohei Adachi, Mr. Masashi Nakamura, Mr. Toshiaki Enoki, Mr. Kenji Tsuchida, Mr. Kensuke Furue, Mr. Keishi Matsuo, Ms. Sayako Koge for their kind collaboration.

Finally, I am particularly grateful to my family for their encouragement and support.